



MURI Center for Dynamic Magneto-Optics (DYNAMO)

**Stephen Rand
REGENTS OF THE UNIVERSITY OF MICHIGAN**

**05/08/2020
Final Report**

DISTRIBUTION A: Distribution approved for public release.

**Air Force Research Laboratory
AF Office Of Scientific Research (AFOSR)/ RTB1
Arlington, Virginia 22203
Air Force Materiel Command**

DISTRIBUTION A: Distribution approved for public release.

REPORT DOCUMENTATION PAGE		<i>Form Approved</i> <i>OMB No. 0704-0188</i>	
<p>The public reporting burden for this collection of information is estimated to average 1 hour per response, including the time for reviewing instructions, searching existing data sources, gathering and maintaining the data needed, and completing and reviewing the collection of information. Send comments regarding this burden estimate or any other aspect of this collection of information, including suggestions for reducing the burden, to Department of Defense, Executive Services, Directorate (0704-0188). Respondents should be aware that notwithstanding any other provision of law, no person shall be subject to any penalty for failing to comply with a collection of information if it does not display a currently valid OMB control number.</p> <p>PLEASE DO NOT RETURN YOUR FORM TO THE ABOVE ORGANIZATION.</p>			
1. REPORT DATE (DD-MM-YYYY) 15-06-2020	2. REPORT TYPE Final Performance	3. DATES COVERED (From - To) 15 Feb 2014 to 14 Feb 2020	
4. TITLE AND SUBTITLE MURI Center for Dynamic Magneto-Optics (DYNAMO)		5a. CONTRACT NUMBER	
		5b. GRANT NUMBER FA9550-14-1-0040	
		5c. PROGRAM ELEMENT NUMBER 61102F	
6. AUTHOR(S) Stephen Rand, TOBIN MARKS		5d. PROJECT NUMBER	
		5e. TASK NUMBER	
		5f. WORK UNIT NUMBER	
7. PERFORMING ORGANIZATION NAME(S) AND ADDRESS(ES) REGENTS OF THE UNIVERSITY OF MICHIGAN 503 THOMPSON ST ANN ARBOR, MI 48109-1340 US		8. PERFORMING ORGANIZATION REPORT NUMBER	
9. SPONSORING/MONITORING AGENCY NAME(S) AND ADDRESS(ES) AF Office of Scientific Research 875 N. Randolph St. Room 3112 Arlington, VA 22203		10. SPONSOR/MONITOR'S ACRONYM(S) AFRL/AFOSR RTB1	
		11. SPONSOR/MONITOR'S REPORT NUMBER(S) AFRL-AFOSR-VA-TR-2020-0002	
12. DISTRIBUTION/AVAILABILITY STATEMENT A DISTRIBUTION UNLIMITED: PB Public Release			
13. SUPPLEMENTARY NOTES			
14. ABSTRACT The MURI Center for Dynamic Magneto-Optics (DYNAMO) was established to investigate magneto-electric phenomena at the molecular level and to evaluate their possible utility for energy conversion. While M-E processes are well-known in bulk magnetic material, and have been studied for energy conversion and sensor technology, magneto-electric rectification, magnetization and harmonic generation at the molecular level in non-magnetic materials have not previously been investigated in any detail. The three nonlinear optical phenomena at the core of this program depend uniquely on the magnetic (Lorentz) force of light under non-relativistic conditions (i.e. at intensities < 1018 W/cm ²). Dynamic magneto-optic effects are expected to be negligible at low intensities, but it was found that parametric resonance and the exchange of orbital and rotational angular momenta can intensify nonlinearities mediated by the optical Lorentz force at non-relativistic intensities. Torque enhancement was confirmed experimentally in spectra of magneto-electrically scattered light that contained rotational features, confirming the importance of librational motion and low libration frequencies in magneto-electric transitions at the molecular level. The program also developed three different analytic approaches to understand charge separation, magnetization, and harmonic generation: a classical torque model, an exact dressed state analysis, and a density matrix treatment which displayed the dependences of M-E processes on transition moments, detuning, relaxation rates, intensity, and polarization.			
15. SUBJECT TERMS magnetolectric, point symmetry, inverse symmetry, optical capacitor, optomagnetic, relativistic, non-relativistic, spin, quantum information, spintronics, transformation optic, nanotechnology			
16. SECURITY CLASSIFICATION OF:			

Standard Form 298 (Rev. 8/98)
Prescribed by ANSI Std. Z39.18

DISTRIBUTION A: Distribution approved for public release.

a. REPORT Unclassified	b. ABSTRACT Unclassified	c. THIS PAGE Unclassified	17. LIMITATION OF ABSTRACT UU	18. NUMBER OF PAGES	19a. NAME OF RESPONSIBLE PERSON SAYIR, ALI
					19b. TELEPHONE NUMBER <i>(Include area code)</i> 703-696-7236

Final Report
(February 15, 2014-February 14, 2020)

of the

MURI Center
for
Dynamic Magneto-Optics
(DYNAMO)

Principal Investigator

Professor Stephen C. Rand
Optics & Photonics Laboratory
EECS Department, University of Michigan
2200 Bonisteel Blvd., Ann Arbor, MI 48109-2099
Tel: 734-763-6810; FAX: 734-647-2718; scr@umich.edu
DOD Grantee: AFOSR FA9550-14-1-0040 POC Ali Sayir 703-696-7236
& ARO-MRI POC Richard Hammond 919-549-4357

Funded Collaborators: Northwestern University, Stanford University,
and University of Central Florida

2013 MURI Topic #14
ONR-BAA12-020

"Magneto-electric Energy Conversion Materials:
Terahertz Emission and Efficient Energy Conversion in Unbiased Dielectrics"

Table of Contents

Section	Page
1. Introduction	
1.1. Vision of the Research Program	3
1.2. Research Thrusts and Tasks	3
1.3. Scope and Synergy of the MURI Effort	3
2. Summary of Research Results by Task	4
2.1. Research Highlights	4
2.2. Charge Separation	5
2.2.1. Theory of Magneto-electric Charge Separation	5
2.2.2. Estimation of Magneto-electric Energy Conversion	10
2.2.3. First Observation of M-E Charge Separation	11
2.2.4. M-E Rectification Materials	14
2.2.5. Experimental M-E THz Generation	17
2.3. Optical Magnetization	21
2.3.1. Magnetic Light Scattering in Small Molecules	21
2.3.2. Magnetic Light Scattering in Macromolecules	25
2.3.3. Magnetic Light Scattering in Solids	28
2.4. Magneto-electric Second Harmonic Generation	30
2.4.1. Observation of M-E SHG in Graphene	30
2.4.2. Experiments on Magnetic Effects in 2-D Materials	31
2.5. Rational Design & Characterization of M-E Materials	34
2.5.1. A Link between Conventional and M-E NLO Materials	35
2.5.2. Design Guidelines for M-E Magnetization Materials	35
2.5.3. Design Guidelines for M-E Rectification Materials	36
2.5.4. Measurements of M-E Susceptibilities	37
2.6. Angular Momentum Theory and Dual Field Interactions	40
2.7. Summary	43
3. Cumulative List of MURI Awards & Honors	44
4. Cumulative List of MURI Publications	46
4.1. Journal Articles	46
4.2. Conference Presentations	57
4.3. Seminars & Colloquia	68
5. People Supported	72
6. Visitors & Collaborators	72

1. Introduction

1.1. Vision of the Research Program

In the past decade homogeneous dielectrics have been found to display magnetic dipole (MD) scattering comparable to electric dipole (ED) scattering in structureless, "non-magnetic" materials. This development has prompted widespread interest in dynamic magneto-optic interactions occurring at the molecular level for the first time. These effects reportedly have unprecedented strengths and potential applications to dielectric metamaterials, non-equilibrium magnetic materials, and energy conversion. Consequently this new family of optical nonlinearities potentially presents new prospects for scientific and defense applications such as power beaming to sustain air and space missions, conversion of sunlight to electricity with near-unit efficiency on satellites and on the ground, generation of large magnetic fields and negative permeability in uniform dielectrics at light frequencies.

The MURI Center for Dynamic Magneto-Optics (DYNAMO) at the University of Michigan (UM) was established to investigate the fundamental science of magneto-electric interactions at the molecular level for the first time. At its conclusion, this research program can be said to have succeeded in this goal. It has elucidated the physics, chemistry, mathematics and materials science required (i) to convert coherent or incoherent light energy to electricity without the thermodynamic constraints that limit traditional processes, (ii) to create intense optical magnetization in bulk centro-symmetric media where quadratic nonlinearities are normally forbidden. Research under this program has analyzed the dynamics and technological implications of novel magneto-optic phenomena. A foundation has been established for this topic through a combination of theoretical and experimental firsts. This final report summarizes the six year research program that has allowed us to measure, understand, and harness these nonlinear optical phenomena, and to optimize materials suitable for novel technology and capabilities based on magneto-electric photonics and energy conversion.

1.2. Research Thrusts and Tasks

Research at DYNAMO consisted of four main experimental tasks, with corresponding theoretical efforts. The experimental tasks can be described as (Task 1) magneto-electric (M-E) charge separation (at UM), (Task 2) optical magnetism (at UM), (Task 3) M-E harmonic generation (at Stanford) and (Task 4) materials synthesis and characterization (at NW & UM). Since the project began, the characterization effort was expanded to include UCF to explore the connections between M-E nonlinearities and traditional all-electric nonlinear optical processes. On the theoretical side, a significant effort (Task 5) was directed to develop insights and computer codes simulating transient response, as well as to distinguish between magneto-electric effects and the existing constellation of electromagnetic phenomena (UM, Riken). Results from all task areas are summarized in Section 2 of this report, following the order of tasks above.

1.3. Scope & Synergy of the MURI Effort

A key objective of research at DYNAMO was evaluation of the potential of M-E charge separation to support radiant power conversion or light-by-light switching. Team members also investigated induced magnetization in nominally non-magnetic host media to determine if very large (oscillatory) induced magnetic fields could be generated with light. Optically-generated magnetic fields could help preserve spin orientation for improved spintronics, or provide direct read/write capabilities for magnetic information storage, magnetic sensor technology, or

quantum computing. Additional aspects of the research program examined new mechanisms for optical rectification and second harmonic generation in centrosymmetric media. A broad range of materials was evaluated for these purposes, guided by density matrix calculations of magneto-electric susceptibilities.

As a multi-university collaboration, this project trained undergraduate, graduate and postdoctoral fellows in tabletop methodologies of ultrafast optical science, materials chemistry, and mathematics. The inter-disciplinary character of the proposed research was ideal for preparing next generation researchers to undertake the scientific challenges of the future in an environmentally-responsible manner. To enhance scientific exchanges with institutions outside the MURI collaboration, the Dynamo Center actively sponsored many visitors (see appended lists), and collaborations with international researchers. The Principal Investigators and their students also engaged in regular meetings following the inception of the project. These forums brought together the chemists and materials science teams from Northwestern University and the University of Michigan, as well as the optics researchers from UM and Stanford and UCF, for day long exchanges that served to focus the research and avoid duplication of effort. Graduates and postdocs of the Center have since gone on to teaching or research positions at universities, the Air Force Institute of Technology, Jet Propulsion lab, and companies like Northrop-Grumman and Intel. Activities and accomplishments related to Dynamo research are detailed on a publicly-accessible website created by Amy Brooks (<http://dynamo.engin.umich.edu/>).

2. Summary of Research Results by Task

This report summarizes the results of the six-year MURI research program that explored magneto-electric (M-E) phenomena at the molecular level for the first time. The M-E phenomena that were investigated comprised (a) rectification, (b) optically-induced magnetization, and (c) M-E second harmonic generation. Sections 2.1-2.3, respectively, summarize results of investigations on these topics.

The very first measurements undertaken in this program were light scattering experiments to observe optically-induced magnetization in simple liquids, as described in Section 2.2.1. These results were important because they permitted a benchmark comparison of experiment and theory which showed that our theoretical analysis of M-E interactions was sound. However after that it became possible to investigate more complex materials, as outlined in Section 2.1.3, as well as to turn to the detection of magneto-electric (ME) charge separation which was arguably the genesis of the MURI program. We begin this report by focusing on the charge separation phenomenon because of its prominent role in our original proposal centered on energy conversion. However this research program investigated the entire family of magneto-electric nonlinearities that take place at the atomic scale, predicted over a century ago but never observed until now. Hence the report has been prepared in a comprehensive way to include results obtained by the research team on magnetization and harmonic generation in later sections.

2.1. Research Highlights

- First observation of magneto-electric charge separation
- First observation of magneto-electric second harmonic generation
- First observation of optically-induced magnetization resulting in magnetic scattering as intense as Rayleigh scattering
- Derivation of equivalences between M-E and all-electric susceptibility tensor elements

- Formulation of material design rules for energy conversion and magnetization
- Demonstration of non-reciprocal transmission in coupled micro-cavities
- Classical and exact quantum theories of M-E interactions at the molecular level
- Development of classical torque model to predict evolution of M-E response vs. time
- Successful quantitative confirmation of quantum theory of M-E magnetization by systematic light scattering experiments in a series of tetrahalide liquids
- Experimental confirmation of the magnetic torque mechanism in tetrahalide liquids
- Discovery of the quantum spin Hall effect of light

2.2. Charge Separation (Magneto-electric Rectification)

The next four sub-sections summarize results on M-E rectification developed during this research program (Sec. 2.2.1). A theoretical torque model is outlined first, to anticipate the outcomes of experiments. Then experimental evidence is presented to reveal when and how M-E rectification, a previously unknown optical nonlinearity, takes place. A novel experimental setup is described in Section 2.2.2 that detects second harmonic generation (SHG) induced in a centrosymmetric medium by applying intense laser pulses. SHG is normally forbidden in the presence of inversion symmetry, but during M-E rectification the pump field breaks this symmetry thereby permitting harmonic generation. In the third sub-section, the materials synthesis effort dedicated to the study of the rectification nonlinearity is described. Finally experiments to detect Terahertz radiation arising from M-E rectification are summarized.

The observation of dynamic symmetry-breaking by the M-E interaction, and other results presented in later sections of this report, confirm that ultrafast magneto-electric interactions take place under non-relativistic conditions and hold promise for new scientific and mission capabilities. A particularly intriguing aspect of these interactions is that they can take place in all dielectrics regardless of symmetry and unlike previously known nonlinearities do not require coherent light. As hoped, this program has therefore paved the way to enabling light-by-light switching at right angles, the generation of intense magnetic fields at optical frequencies, and the direct conversion of light to electricity or THz radiation in homogeneous insulators. Indeed the findings may launch an entirely new field, namely magneto-photonics.

2.2.1. Theory of Magneto-electric Charge Separation University of Michigan (A. Fisher, E. Cloos, G. Smail)

Even in moderate light fields on the order of $E_0=10^9$ (V/m), which is far below the value required to accelerate electrons to light speed during an optical cycle, electrons in atoms or molecules undergo motion in which the optical magnetic field can exert an important role. This can be confirmed with a simple harmonic oscillator model that includes Lorentz forces. Trajectories in real space resemble those in Figure 1, which are clearly nonlinear and break inversion symmetry with respect to the origin on the left of each figure. The loss of inversion symmetry points to the involvement of the optical magnetic field.

To account for the appearance of magnetic response at low intensities, our research program identified two sources of enhancement. The first was due to parametric resonance and the second was due to magnetic torque. Models that include the Lorentz force are implicitly subject to parametric resonance and we showed that it was important to incorporate torque dynamics into the model as well when molecules were considered. Our analyses have been published (see Publications List) but the basic approach and results will be reviewed below to provide perspective on the experimental advances presented throughout this report.

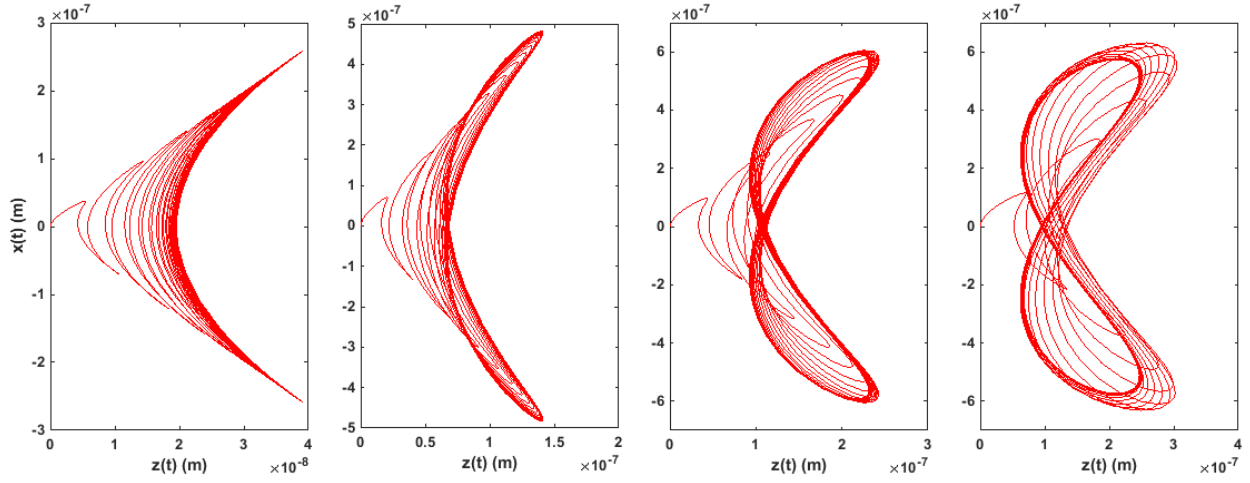


Figure 1. Classical trajectories of an electron driven simultaneously by the electric and magnetic field components of linearly-polarized light incident from the right. The light frequency is tuned to match the atomic resonance, thereby exciting a primary parametric resonance which boosts the electron response to the relativistic range. The electric field strengths used in this simulation were $E_0=10^8$, $E_0=2 \times 10^8$, $E_0=3 \times 10^8$, and $E_0=4 \times 10^8$ (V/m), from left to right. The corresponding intensities are eight orders of magnitude below the relativistic threshold.

An important detail of the modelling is that when Lorentz forces are included, the equilibrium point of the electron in the intra-molecular potential well cannot be used as a fixed point of reference because the molecule must be free to rotate. Instead, the origin of the coordinate system must coincide with the center-of-mass. This choice encompasses an extra degree of freedom, namely rotation about the center-of mass, which permits the exertion of torque by the optical magnetic field on the molecular charge system. Following the published analyses, the displacement of the electron from equilibrium is taken to be $\bar{r} = \bar{\xi} - \bar{r}_A$, where \bar{r}_A specifies the point of equilibrium in the absence of light and $\bar{\xi}$ specifies electron position with respect to the center-of-mass. The equation of motion with respect to the center-of-mass in a fixed molecular frame of reference is

$$\frac{d^2 \bar{\xi}(t)}{dt^2} + \gamma \frac{d \bar{\xi}(t)}{dt} + \omega_0^2 (\bar{\xi}(t) - \bar{r}_A) = \frac{\bar{F}(t)}{m}, \quad (2.2.1)$$

where γ is the damping constant and ω_0 the resonant frequency of the oscillator. m is the reduced mass. $\bar{F}(t)$ is the external force acting on the oscillator, comprised of electric and magnetic fields \bar{E} and \bar{B} are chosen to lie along x and y respectively. The direction of propagation is along z .

Electron in this model experience a Hooke's Law restoring force of the form $\bar{F}_i(t) = -k\bar{r}(t)$. When the electron is out of equilibrium, the molecule also experiences an equal but opposite reaction force $\bar{F}_r = -\bar{F}_i$ that causes a torque on the molecule.

$$\bar{T} = \bar{r}_A \times \bar{F}_r = m\omega_0^2 \bar{r}_A \times \bar{\xi}. \quad (2.2.2)$$

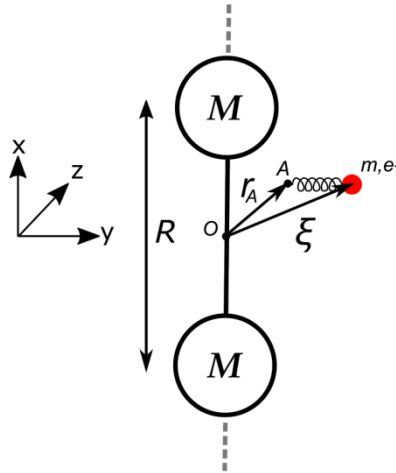


Fig. 2. Model of a homonuclear diatomic molecule oriented along x , the assumed direction of the incident E field that propagates along the z -axis, together with the coordinate system and position vectors $\bar{\xi}$ and \bar{r}_A specifying electron position and the point of equilibrium.

Assuming the electron starts from rest, its position $\bar{\xi}(t)$ and velocity $\partial\bar{\xi}(t)/\partial t$ can be calculated after a first time step from the equation of motion. Then, the angular velocities can be computed and the position of the equilibrium or “attachment” point updated with the solution to the equation

$$\frac{d\bar{r}_A(t)}{dt} = \bar{\Omega}(t) \times \bar{r}_A(t), \quad (2.2.3)$$

where $\bar{\Omega}(t)$ is the angular velocity of the molecule. With the new value of \bar{r}_A , one can find $\bar{\xi}(t)$ and $\partial\bar{\xi}(t)/\partial t$ after a second time step, and iterate this procedure to find the induced electric polarization $\bar{P}(t)$ or magnetization $\bar{M}(t)$ according to

$$\bar{P}(t) = e\bar{\xi}(t), \quad (2.2.4)$$

and

$$\bar{M}(t) = -\left(\frac{e}{2m}\right)\bar{L} = -\left(\frac{e}{2}\right)\bar{\xi}(t) \times \frac{d\bar{\xi}(t)}{dt}. \quad (2.2.5)$$

Results of this torque model are reproduced in Figs. 3 and 4 to illustrate key features of a *molecular*, as opposed to an *atomic*, treatment of charge dynamics. By comparing left and right figures it can be ascertained that for molecules with a ratio of optical to rotational frequencies of 1000 or more (i.e. all molecules), $P(t)$ and $M(t)$ are enhanced by a similar factor.

Figure 5 reveals that while torque and parametric resonance both enhance charge motions originating from the Lorentz force of light near electronic resonance, torque is more effective in generating relativistic-like response under non-relativistic conditions. By solving the extended simple harmonic oscillator model for incident fields in the form of Gaussian pulses, simulations can also be performed to predict transient charge separation signals. With parameter values appropriate to pentacene and excitation with 200 fs pulses at 800 nm, the simulation predicts the dynamics of the M-E rectification field shown in Figure 6.

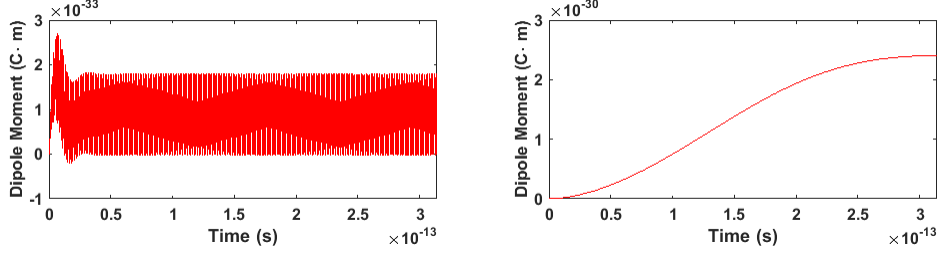


Fig. 3. Evolution of charge separation, $P_z(0)$, of the test charge versus time for $I_{\perp} / I_{\parallel} = 1$ (left) and $I_{\perp} / I_{\parallel} = 1000$ (right). Other fixed parameters were $\omega_0 = 1.63 \times 10^{16}$ rad/s, $I_{\parallel} = \hbar / \omega_0$, $\omega = 0.9\omega_0$, $E = 1 \times 10^9$ V/m and $\gamma = 0.1\omega_0$.

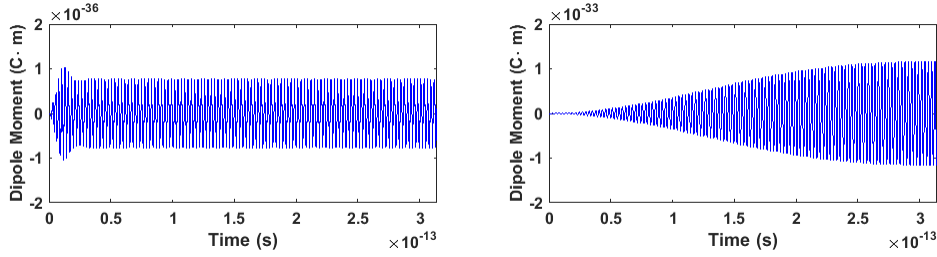


Fig. 4. Evolution of the magnetic moment (divided by c) versus time for $I_{\perp} / I_{\parallel} = 1$ (left) and $I_{\perp} / I_{\parallel} = 1000$ (right). Other fixed parameters were $\omega_0 = 1.63 \times 10^{16}$ rad/s, $I_{\parallel} = \hbar / \omega_0$, $\omega = 0.9\omega_0$, $E = 1 \times 10^9$ V/m and $\gamma = 0.1\omega_0$.

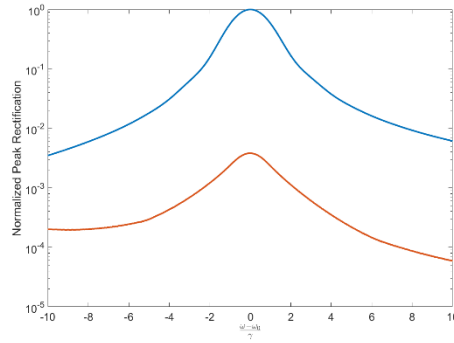


Figure 5. Amplitude of M-E rectification calculated with (upper trace) and without (lower trace) magnetic torque. The parametric resonance centered about the optical frequency is present in both traces but the upper trace has much higher amplitude over a broad range of detuning, due to torque enhancement. Fixed parameter values were $I_{\perp} / I_{\parallel} = 1000$, $\omega_0 = 1.63 \times 10^{16}$ rad/s and $\gamma = 0.1\omega_0$.

The dependences of M-E rectification and magnetization on pump intensity are given by the theoretical traces in Figure 6. (Quantum mechanical analyses are very similar when magnetic torque by the optical magnetic field is taken into account. Hence the reader is referred to the publication list for extensive treatments on this topic.) The trends emphasize the importance of using materials with low libration frequency (ω_{ϕ}) to enhance magneto-electric response. In the third year of the MURI program, important molecular design criteria began to emerge from analyses like these for the optimization of magneto-electric materials. Such findings provided

guidance to chemical synthesis efforts by the MURI team, since libration frequency directly reflected desirable structural details of molecules, such as high moments of inertia.

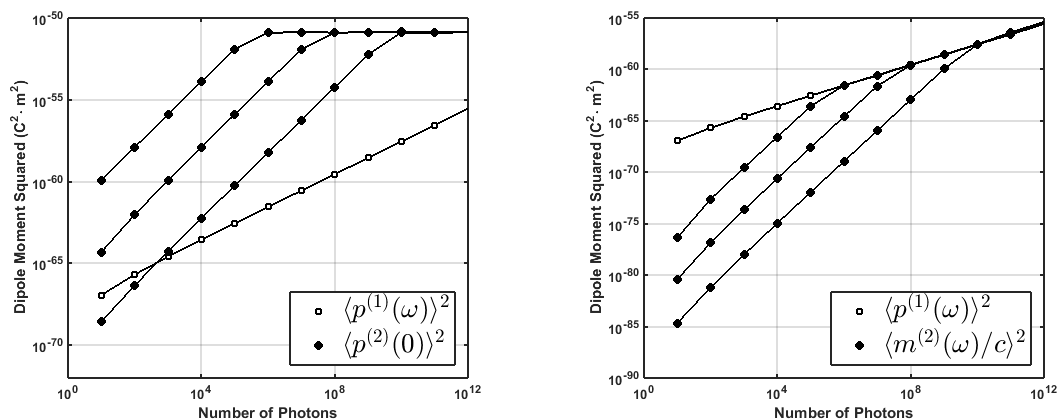


Fig. 6. (Left) Squared values of magneto-electric rectification dipole moments (filled circles) compared to the first-order, all-electric dipole moment (open circles). The all-electric response is proportional to Rayleigh scattering intensity which has a linear dependence on input intensity. The filled circles were computed for libration frequencies given by $\omega_\phi / \omega_0 = 10^{-7}, 10^{-5}, 10^{-3}$. (Right) Squared magnitudes of the induced magnetic moment versus number of photons (intensity) for libration frequencies of $\omega_\phi / \omega_0 = 10^{-7}, 10^{-5}, 10^{-3}$ from left to right. Open circles are again proportional to Rayleigh scattering intensity whereas closed circles are proportional to the nonlinear magnetic dipole scattering intensity.

A clear conclusion from the earlier Figures 3 and 5 was that magnetic torque enhances charge separation and magnetization. Yet during the course of this research an answer was sought to the question of how this occurs mechanistically. How is it that a normally relativistic effect can take place under non-relativistic conditions?

This question was answered by showing that a transfer of orbital angular momentum to rotational angular momentum in a molecule alters the area associated with circular charge motion. The idea is illustrated schematically in Figure 8. Since the value of a magnetic moment m depends on the area enclosed by an orbiting charge according to $m=IA$, any increase of area at constant current I enhances the moment. The velocity of the electron does not change during this process because magnetic fields can do no work. Surprisingly, the degree of enhancement that takes place during the transfer of orbital to rotational momentum easily makes up for the normally large difference between (weak) induced magnetic dipole moments and (strong) electric dipole moments. Contrary to expectations based on the multipole expansion, this explains how intense magneto-electric nonlinearities can be induced in virtually all (non-magnetic) dielectric materials. The comparison of M-E response with and without torque in Figures 3 and 5 shows the importance of this mechanism. Experimental results on the mechanism of magnetization described in Section 2.3 also directly reveal the presence of torque-induced rotations in M-E light scattering processes.

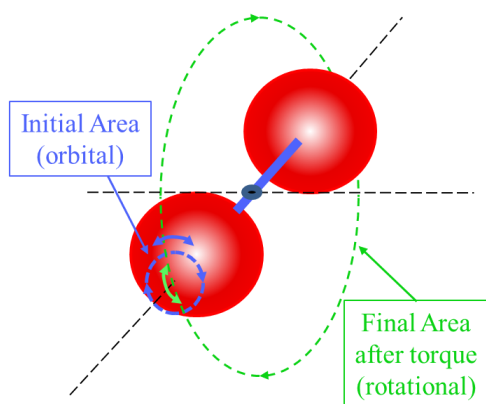


Figure 7. Magnetic torque mediates a rotation of the axis about which there is orbital angular momentum of an electron in the excited state. In a diatomic molecule, the axis about which orbital motion takes place is the internuclear axis, which is also the quantization axis for angular momentum. The inverse ratio of optical to rotational frequencies in virtually all molecules is small, reflecting a large difference in radii of orbital versus rotational motion. Hence the action of magnetic torque of the light field on the internal angular momentum of the excited state transfers orbital kinetic energy to rotation (libration) and enlarges the area enclosed by electron motion. This in turn enhances the magnetic moment and the M-E rectification electric dipole moment.

2.2.2. Estimation of Magneto-electric Energy Conversion

The torque model provides reliable predictions of the internal electric fields formed during M-E rectification, and is therefore useful for estimating the efficiency of M-E energy conversion. In M-E energy conversion at the molecular level, light power is theoretically convertible directly to electric power. The process can be pictured as optical charging of a capacitor followed by discharge into a storage circuit. Conversion efficiency was originally estimated by W.M. Fisher et al., J.A.P. 109, 064903(2011), at a time when torque enhancement of M-E processes was unknown. Based on results of this research program, it is now possible to make more realistic estimates of energy conversion, especially for off-resonant conditions.

As indicated by the torque model simulation in Figure 8, electric fields in the range of

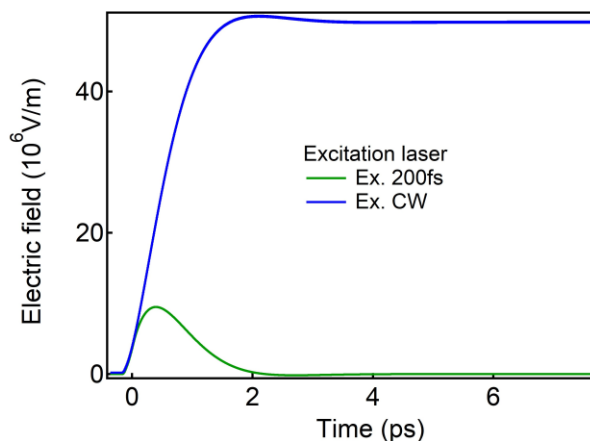


Figure 8. Temporal development of the internal electric field of magneto-electric rectification in pentacene for continuous-wave (CW, blue) or 200 fs pulsed laser excitation (green) at 800 nm. Average pump power was 1 Watt at 10 kHz. The response timescale exceeds the laser pulsewidth because of magnetic torque-initiated electron motion within the molecule. The CW curve has been magnified to permit comparison of temporal behavior.

10 MV/m form in pentacene during irradiation with 200 fs pulses. Fields of this magnitude are also expected for longer, Q-switched pulses which one can imagine being focused into a waveguide. To estimate the efficiency of a magneto-electric "optical capacitor", consider an optical fiber with the properties of pentacene to be a M-E conversion medium in the following example. The incident laser is assumed to operate at 800 nm near the resonance of pentacene with an average power of 300 Watts, emitting 30 ns pulses at a rate of 10 kHz in a beam of area $A=1 \text{ cm}^2$. With pulses of this power focused into a fiber of cross-sectional area $A = 10^{-6} \text{ m}^2$ and length $d=10$ meters, an internal electric field of strength $E=10^7 \text{ V/m}$ is predicted between the two ends of the fiber. With (100%) efficient energy harvesting electronics, following the estimation procedure of Fisher (2011), the extractable energy per pulse should be

$$\frac{\text{Energy}}{\text{pulse}} = \frac{1}{2}(\epsilon_0 A d)E^2 \cong 4.4 \times 10^{-3} (J) \quad (2.2.6)$$

At the stated repetition rate, the extractable power would therefore be 44.3 Watts. Thus the conversion efficiency could be as high as

$$\eta \equiv \frac{P_{out}}{P_{in}} \cong \frac{44.3}{300} = 14.7\% . \quad (2.2.7)$$

This performance is comparable to solar cells. While admittedly unimpressive in this context, it should be noted that magneto-electric conversion works equally well with high power monochromatic lasers or broadband incoherent light and generates a negligible amount of heat. Based on the quantum theory briefly described in Section 2.3, the relative amount of heat energy deposited in the medium per photon pair, which we represent here as $\Delta H/H$, is only

$$\frac{\Delta H}{H} = \frac{\hbar\omega_\phi}{2\hbar\omega} < 5 \times 10^{-4} . \quad (2.2.8)$$

Given its low heat production and insensitivity to the exact wavelength or coherence of incident light, M-E energy conversion is attractive for some applications currently served by photovoltaic technology. The estimate above affirms the potential of M-E processes for broadband energy conversion in space where thermal loads from solar converters normally lower efficiency and cause undesirable mechanical distortions of the apparatus. Efficiencies approaching unity should be possible for M-E conversion of monochromatic electromagnetic beams to stored electrical energy at wavelengths near optical resonances.

2.2.3. First Observation of M-E Charge Separation

University of Michigan (M.T. Trinh & K. Makhal)

In the fifth year of research two new methods became available to compute charge separation fields. These approaches augmented the torque model and facilitated the design of a successful experiment to observe charge separation, which is summarized in this section.

One of the new theoretical methods derived the internal rectification field based on an equivalent field argument (see Lou et al. 2019 Supplement). This advance linked the macroscopic susceptibilities of magneto-electric processes with the all-electric susceptibilities of conventional nonlinear optics. This is discussed further in Section 2.5. The result was that the charge separation field could be expressed as

$$(P)_k^{(2)}(0) = \chi_{klm}^{(2)}(0; \omega, -\omega) H_l^* E_m , \quad (2.2.9)$$

where the M-E susceptibility obeyed a numerical equivalence relation $\chi_{klm}^{(eme)} = -\eta_0 \chi_{kknm}^{(3)}$.

The second result was a quantum mechanical derivation of the rectification field,

$$P^{(2)}(0) = \mu_0^{(e)} \left\{ \frac{1}{\sqrt{2}} \right\} \left(\frac{(\Omega_{21}/2)(\Omega_{23}^*/2)}{(\Delta_{12} - i\Gamma_{12})(\Delta_{13} - i\Gamma_{13})} \right) + c.c., \quad (2.2.10)$$

where Ω_{21} and Ω_{23}^* are the Rabi frequencies of the first and second photon transitions that comprise the M-E interaction. (The quantum picture of M-E interactions is presented in figures of Section 2.3.) These new expressions permitted quantitative predictions of signal strengths for the first time, guiding MURI investigators to the selection of a suitable sample and experimental approach for the first *observation* of M-E charge separation in pentacene thin films grown by Prof. Kim's group at the University of Michigan (See Sec. 2.2.3).

Charge separation experiments were performed using a time-resolved second harmonic generation technique, as shown in Figure 9. A femtosecond laser beam acted as an optical pump with photon energy well below the bandgap of the material to induce M-E charge separation in the sample. The internal, quasi-static electric field associated with ME charge separation introduced uniaxial symmetry into the film during - and for a short time after - the pump pulse. In turn this dynamic symmetry-breaking interaction, which eliminated inversion symmetry in the films, permitted second harmonic (M-EFISH) generation of the probe beam. The second

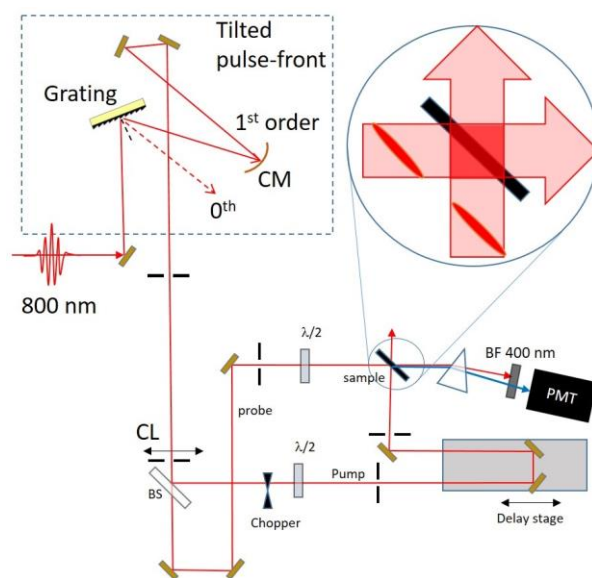


Figure 9. Schematic of the crossed-beam pump-probe experiment. The pump beam generates a M-E charge separation field (E_{dc}) in the pentacene sample. The detected probe signal is at twice the optical frequency (2ω).

harmonic signal therefore emerged from the sample as a signature of the internal field induced by M-E charge separation. Its evolution in time could then be followed by varying the pump-probe delay time. To preserve temporal resolution on the order of the incident pulsewidths - despite having pump and probe beams at right angles to one another - a novel tilted pulse-front technique devised. The best arrangement for preservation of temporal resolution with orthogonal beams and pulses tilted to 45° is shown schematically in the red enlargement of Fig. 9.

By monitoring the M-EFISH signal while varying the pump-probe delay, we were able to study charge separation dynamics for the first time (Figure 10 (a)). The internal electric field that accompanies charge separation initiates second harmonic generation of the probe beam with a

decay time of roughly 500 fs. The induced probe harmonic signal follows a quadratic dependence on pump intensity (Fig. 10(b)). Signal strength was boosted by choosing polycrystalline pentacene as the sample. This material is centrosymmetric, so SHG is forbidden in the bulk of the sample, although harmonic radiation can still take place at the input and output surfaces. This minimized the "noise" by limiting background harmonic generation to sample interfaces. Surface-induced SHG was easily distinguished from the M-EFISH signal because it was independent of pump-probe delay (as in Fig. 10(a)). The study of pentacene samples also provided resonant enhancement of the signal by virtue of the small detuning of the first pentacene resonance at 680 nm from the laser wavelength of 800 nm (Figure 10 (c)).

To ascertain the origin of the constant background in M-EFISH signals, a careful study of probe polarization dependence was performed. The results are shown in Figure 11. Based on the geometry sketched in Fig. 11(a), and the orientation of the magneto-electric rectification field along the pump axis, surface SHG (SSHG) should follow a $\sin^4\alpha$ dependence on polarization angle α , whereas a M-EFISH signal should vary as $\sin^2\alpha$. The fitted curves in Fig. 11(b) therefore provide compelling evidence that the pump-induced signals (in red) arise from a M-EFISH interaction and the background (in blue) arises from surface harmonic generation.

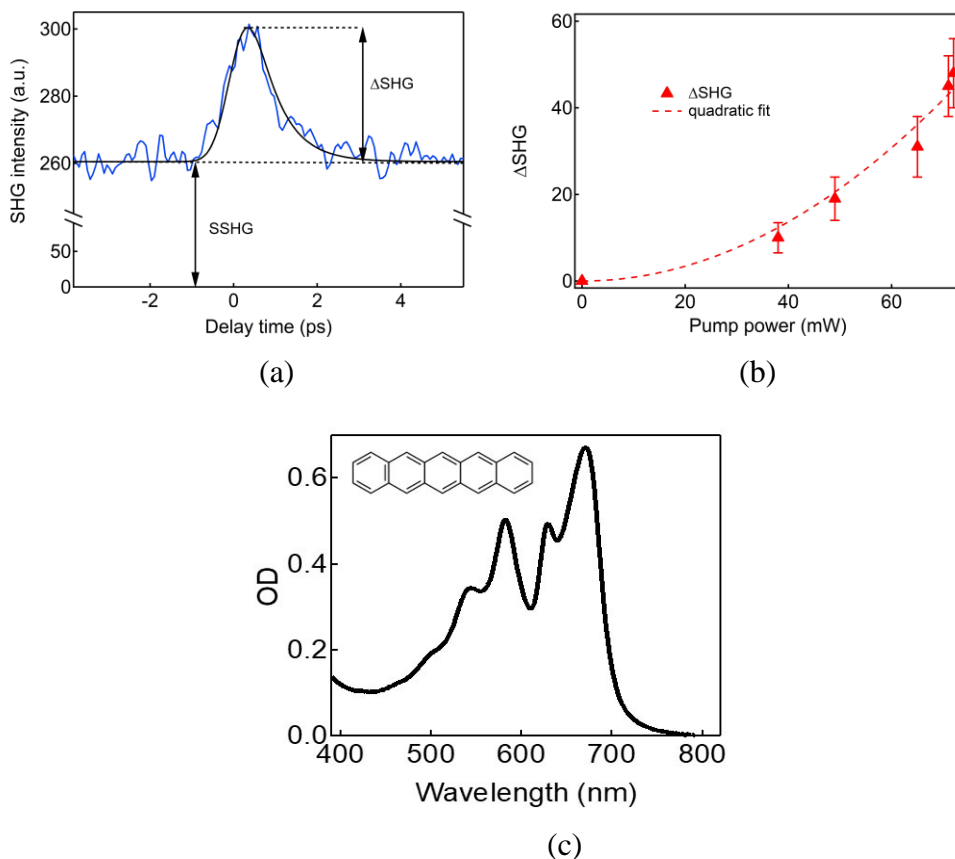


Figure 10. (a) Pump-induced M-EFISH signal observed in a polycrystalline pentacene using 100 fs pulses from an amplified mode-locked Ti:Al₂O₃ laser with a repetition rate of 10 KHz. The black curve is a convolution of instrumental response and a torque model simulation with a signal decay time of ~0.5 ps. The flat background was determined to be surface SHG (see below). (b) The induced (Δ SHG) signal intensity varied quadratically with pump power as expected. (c) The absorption spectrum of pentacene shows the longest wavelength transition at 680 nm which provided modest resonant enhancement of the M-EFISH signal due to its proximity to the laser wavelength (800 nm). Inset: The molecular structure of pentacene.

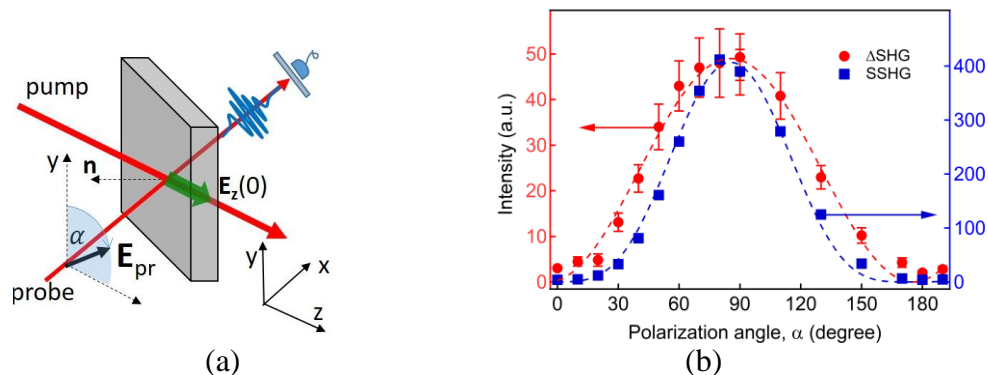


Figure 11. Dependence of the background SHG (blue) and pump-induced SHG (red) signals on probe polarization. The background SHG obeys $\sin^4 \alpha$ where α is probe polarization angle while the pump-induced SHG obeys $\sin^2 \alpha$.

Confirmation of the existence of M-E rectification, and the unusual orientation of the induced electric field, prompted the idea of investigating light-by-light switching between beams propagating at right angles. The possibility of controlling the transmission of a signal beam with a control beam at 90° would be unprecedented in nonlinear optics. For this reason a follow-on proposal on magneto-electric photonics submitted by PI Professor Rand was funded by the National Science Foundation in 2020.

2.2.4. M-E Rectification Materials

University of Michigan (J. Kim)

One of the primary objectives of the materials research effort for this project was to build understanding on how molecular structure affects the magnetoelectric properties of organic materials and to synthesize liquid, crystal, and thin film samples appropriate for rectification and magnetization experiments. Following the successful establishment of material design rules by the Northwestern team in 2017, this effort became more focused. For rectification experiments thin film samples of oriented polymers and the organic crystal pentacene became a priority for synthesis at the University of Michigan. For experiments on magnetization, high purity liquids comprising a series of tetrahedral molecules with a wide range of moments of inertia were prepared at Northwestern University. Together, these two sets of samples permitted advances on both the theoretical and experimental fronts of both topics. The gradual systematization of the materials effort led to breakthroughs in the comparison of magneto-electric scattering results with theory and the successful pump-probe experiment described in the previous section, which revealed the existence of M-E charge separation for the first time.

A series of conjugated polymers (NCP1 - NCP8 - see Figure 12) were synthesized to investigate the validity of design rules based on small molecules to macromolecules and simultaneously to try to orient polymer samples. In the first two years of the project, magnetic scattering experiments in simple molecular liquids identified the desirability of conjugated structures, large ratios of optical to libration frequencies and large transition dipole moments (See Sec. 2.3). Our objective in this task was to combine these properties with emerging techniques from Prof. Kim's lab which could align certain polymers, a finding that was deemed very desirable for rectification, since aligned molecules would allow for extension of charge

separation along the axis of oriented samples. Additionally, polymers offered the possibility of positioning absorptive resonances close to the laser wavelength for resonant enhancement and ensuring transparency at THz frequencies which were pursued as an alternative approach to observe transient rectification effects (see Sec. 2.2.5).

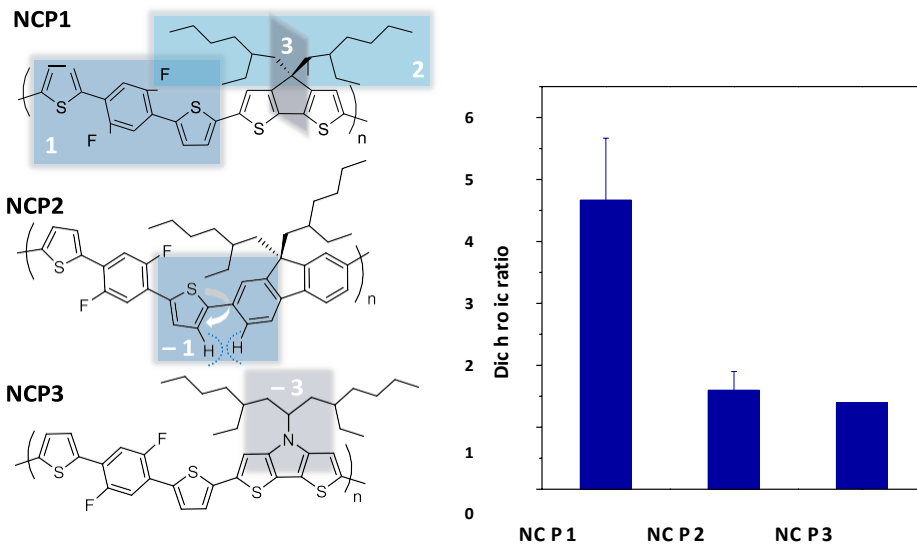


Figure 12. (a) Representative conjugated polymer (CP) structures and (b) alignment properties showing the need for three design features for directed alignment possessed only by NCP1: (1) concentration-induced planarization, and (2) bulky side chains linked to (3) a tetrahedral carbon.

The first polymer, NCP1, was found to meet all three design factors and could be synthesized with directed alignment using an appropriate building block. After full characterization, two other polymers NCP2 and NCP3 were found to resist alignment and did not satisfy other design requirements (Figure 12). In an attempt to make synthesis more versatile and extend it to more compounds, the effect of three separate factors on conjugation and aggregation was therefore investigated systematically. Additional conjugated polymers were prepared to study the effects of (1) the influence of the branching position of the side chains, (2) introducing an intrinsically planar unit in the polymer backbone instead of the concentration-induced planarization via intramolecular S \cdots F interaction, and (3) incorporation of S \cdots O interactions as an alternative to S \cdots F interaction.

When NCP4 was synthesized with a 5-methylhexyl side chain having a branch point away from the co-polymer backbone, it aggregated in solution whereas no aggregation was observed in the NCP1 solution. Regarding Factor 1 above, this permitted the conclusion to be drawn that only if the branching point was sufficiently close to the polymer backbone would the side chains provide adequate steric hindrance to prevent the aggregation caused by strong intermolecular π - π interactions. So while conjugation was inherently advantageous in providing quasi-free electrons to undergo magneto-electric processes, it could cause troublesome aggregation.

Regarding Factor 2, a distinctive aggregation band was observed at 580 nm from the absorption spectra of NCP5 and NCP6 in the solution state (Figs. 13(a) and 13(b)). The absorption spectra of the solution and its spin cast film are similar for NCP5 and NCP6, implying that the intrinsically planar multi-thiophene unit makes the polymer backbone planar, causing it

to aggregate even in solution. Consequently, these two CPs do not exhibit satisfactory self-alignment properties, supporting the conclusion that a concentration-induced planarization unit is important for alignment.

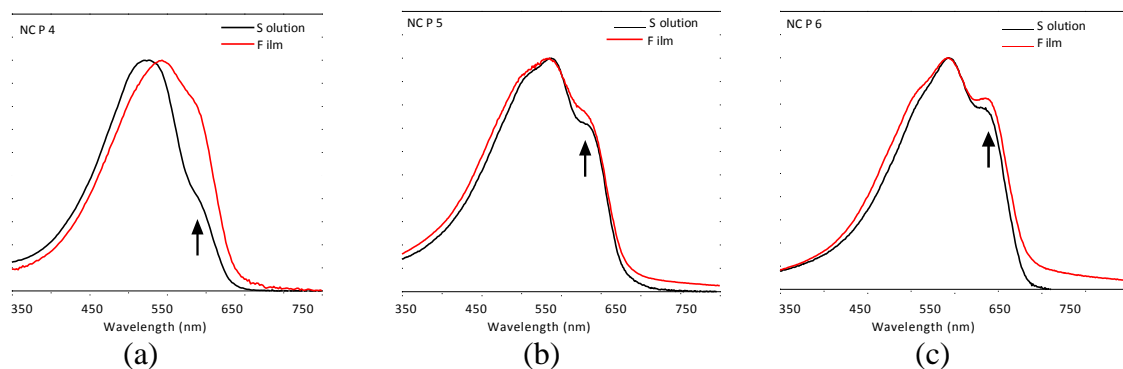


Figure 13. UV-VIS absorption spectra of (a) NCP4, (b) NCP5, and (c) NCP6

To investigate the design factor 3), we synthesized NCP7 (Figure 14). We found that even though the S...O interaction can achieve the required concentration-induced chain planarization, NCP7 did not show alignment capability. We postulated that the fluorine atom in the polymer backbone largely affects the alignment capability of CPs by changing the surface energy and wettability of CPs on a solid substrate. To exam this hypothesis we synthesized NCP8. Although NCP8 has a more torsionally twisted structure compared to NCP7 (Figure 14), the additionally added fluorine substitutions in main chains enables NCP8 to have the alignment properties (Table 1).

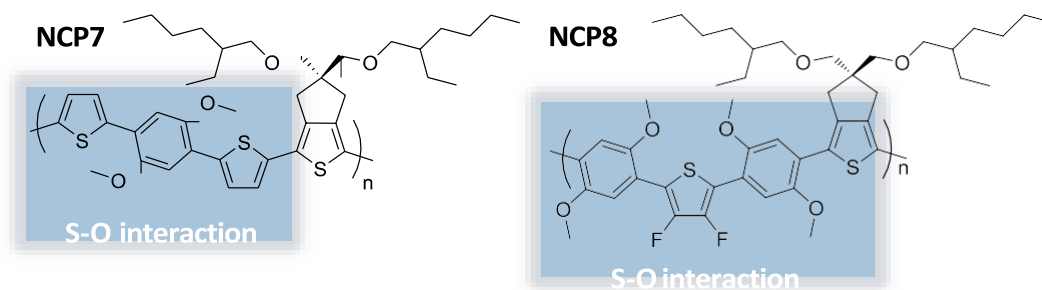


Figure 14. Chemical structures of NCP7 and NCP8.

Polymer Name	Conformation Lock	#F atoms/repeat unit	Dichroic Ratio
NCP1	S...F	2	4.67
NCP7	S...O	None	0.98
NCP8	S...O	2	1.51

Table 1. Structural properties of NCP1, NCP7, and NCP8.

For pump-probe experiments to observe M-E rectification, thin films of poly-crystalline pentacene were also prepared. Free-standing thin films of centrosymmetric or amorphous solids

were needed to allow short pulse experiments that did not compromise temporal resolution. So while samples could not exceed a thickness of 100 microns, resonant absorption near 750 nm was needed to enhance the magneto-electric response at the wavelength of our laser source, centered at 800 nm.

2.2.5. Experimental M-E THz Generation

University of Michigan (J. Whitaker)

As an alternative approach in the quest to observe magneto-electric charge separation at the molecular level, the MURI team searched for the generation of THz radiation in unbiased dielectric samples illuminated with intense laser pulses. While this objective proved elusive, this effort played an important role in developing a tilted wave technique that ultimately enabled success in the experiments on rectification (Sec. 2.2.2). It also contributed the only patent awarded for DYNAMO research by inventing a new method of steering THz radiation.

Magneto-electric charge separation (or rectification) is theoretically capable of converting optical power directly to electrical field energy via the “optical capacitor” effect (W.M. Fisher, J.A.P. 109, 064903(2011)). In so doing, THz radiation polarized along the direction of propagation of incident light can be produced in ultrafast magneto-electric interactions. However the forward direction of the rectification field forces the THz emission to emerge in a Cerenkov cone, which makes it awkward to detect experimentally and difficult to concentrate into a beam (Figure 15). As a consequence the experimental setup became unconventional and challenging, necessitating the use of tilted optical wavefronts to match the Cerenkov cone angle and optimize the theoretical power radiated in any specific direction. While M-E THz generation was not observed in the course of this project, the tilted wave technique did develop into a method to generate steerable THz radiation from thin, biased emitters. Consequently this section focuses on a summary of the methodology and application of this tilted pulse-front technology.

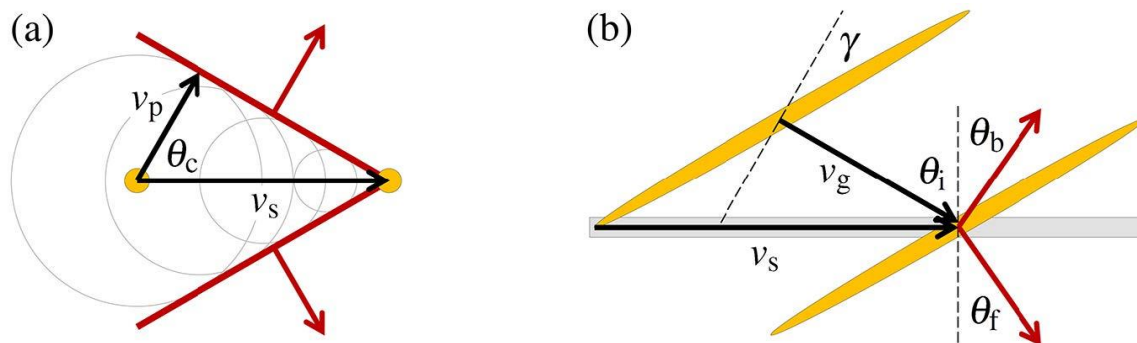


Figure 15. The generation of coherent THz radiation. (a) A small area optical pulse travelling through a THz-emitting material, and (b) a large area optical pulse impinging on a thin THz-emitting material (shown in gray). The gold ellipses are cross-sectional snapshots of the propagating optical pulse, and the dark red lines and arrows depict the THz wavefronts and direction of propagation, respectively.

The development of the tilted pulse-front technique proceeded as follows. Optically generated THz pulses in a bulk material were first studied experimentally using an ultrafast pulses in a beam of width $w \ll \lambda_{thz}$, where λ_{thz} is the central wavelength of the broad THz-pulse spectrum in the material. This spot-size condition permits the use of a model that treats the

focused pump pulse as a point source of THz radiation traveling at a speed $v_s = v_g$, where v_g is the group velocity of the pump. Following Huygens' Principle, the THz point source will emit outgoing spherical THz waves that propagate with phase velocity v_p and coherently form a cone of radiation, as depicted in Fig. 15(a). Basic trigonometry then reveals that

$$\cos \theta_c = \frac{v_p}{v_s}, \quad (2.2.11)$$

where θ_c is the so-called Cherenkov cone angle. Clearly this geometry only produces coherent radiation in the superluminal regime defined by $v_s > v_p$.

Next we analyzed the direction of THz emission with wide beams incident on a flat surface. Instead of generating a traveling THz point source, the THz radiation in the thin emitter geometry of Fig. 15(b) is now produced from an infinite series of stationary point sources distributed throughout the generation region - each one of which begins to radiate once the optical pulse-front reaches it. Since the pulse-front is flat, the series of phased stationary point sources is directly analogous to a single point source traveling at a speed v_s which is in general no longer equal to v_g . More trigonometry reveals that the speed of the analogous point source is

$$v_s = \frac{v_g \cos \gamma}{\sin(\theta_i - \gamma)}. \quad (2.2.12)$$

Thus, the direction of coherent THz emission can be determined by substituting Eq. (2.2.12) into Eq. (2.2.11) to yield

$$\sin \theta_f = \frac{v_p \sin(\theta_i - \gamma)}{v_g \cos \gamma} \quad (2.2.13)$$

where θ_f and θ_b are the forward and backward THz-emission angles, respectively, relative to the surface normal (Fig. 15(b)).

From Eq. (2.2.13) it is clear that a THz pulse may be steered by controlling the tilt angle of the pulse-front of the optical pump beam. This is in contrast to the THz pulses generated in bulk media using tilted pulse-fronts, which cannot be steered and are velocity-matched for only a small range of pulse-front tilt angles. Hence we investigated this new feature of THz generation using the tilted-wavefront apparatus depicted in Figure 16.

Although the tilt angle of the pulse wavefront was adjusted mechanically by rotating the sample, such an adjustment could potentially be done electronically to facilitate rapid steering of the output. Alternatively, steering could also be achieved by manipulating either the THz phase velocity or optical group velocity of the surrounding material. Or, both the forward and backward emission could be steered by rotating the thin emitter to change the angle of incidence. However directional steering was not the main interest of this work. Instead, basic confirmation of the analysis of output direction was sought. Hence systematic measurements of output beam patterns were made in the forward and backward directions for ten different angles of incidence as a check on the method. The results are shown in the intensity profiles of Figs. 17(a), (c) and the comparison with theory appears in Figs. 17(b), (d).

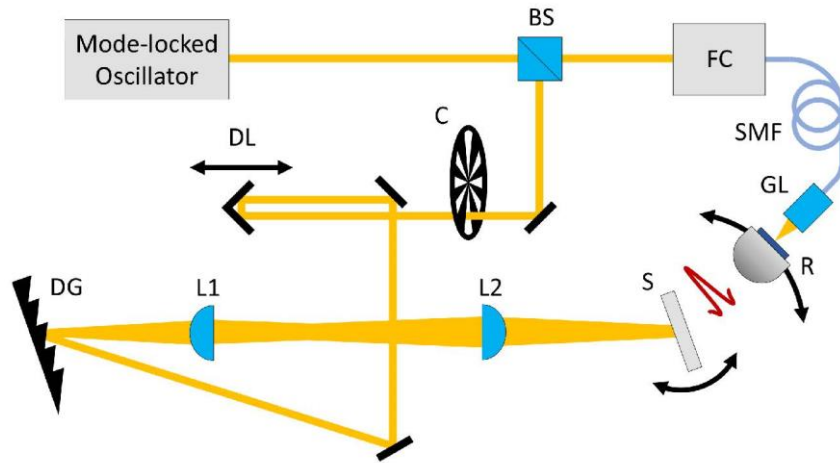


Figure 16. Apparatus for measurements of tilted wavefront THz generation.

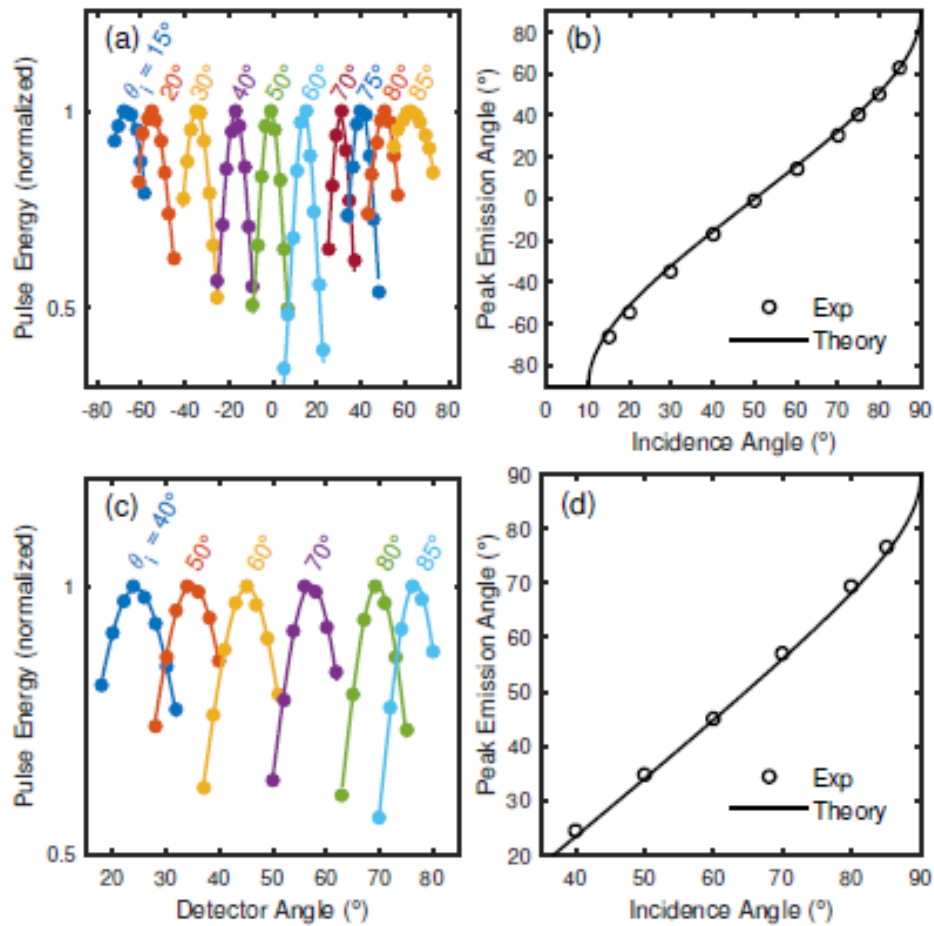


Figure 17. Measured distributions of THz radiation versus angle of emission (a) in the forward direction and (c) in the backward direction, for different optical pulse angles of incidence. The circles are calculated THz energies from measured time-domain waveforms and the lines are Gaussian fits. The peak emission angles are plotted versus angle of incidence in (b) and (d). The solid curves are theoretical fits to Eq. (2.2.13).

An important conclusion of the analysis is that the direction of coherent emission does not depend on the mechanism of THz emission (recognizing that source elements such as dipoles produce a radiation pattern but do not change the direction in which the combined emission of THz radiation from many point sources is temporally coherent). However, the actual amount of energy radiated in the coherent direction will depend on the mechanism of generation as well as losses from interface reflections and THz absorption in each medium. Thus in the case of magneto-electric interactions which generate a longitudinal dipole, no energy will be radiated in the direction of THz propagation if $v_s = v_p$. For equal velocities one can infer that $n_{\text{thz}} = n_{\text{opt}}$, so that the Cerenkov angle in Eq. (2.2.11) is zero. Since no THz energy can radiate from the system under these circumstances, a very important conclusion that emerged from these studies was that for successful observation of THz generation by the M-E mechanism, samples must have very different indices in the optical and THz frequency ranges. For this reason ongoing tests of samples synthesized at UM and Northwestern by the Kim and Marks groups were focused on determinations of their low frequency indices (n_{thz}), seeking samples in which $n_{\text{thz}} \gg n_{\text{opt}}$.

In the lower half of Fig. 18, photoconductive (PC) THz detectors are sketched for two example generation mechanisms – THz arising from optical magneto-electric rectification (Case 1) and from optical-all-electric-field rectification (Case 2) – and for three separate optical-pulse incident angles – normal and left and right oblique. The conventional optical rectification of Case 2 will generate THz pulses of the same polarity for both the normal and oblique optical incident angles. However, for the M-E rectification THz generation, the output pulses will be

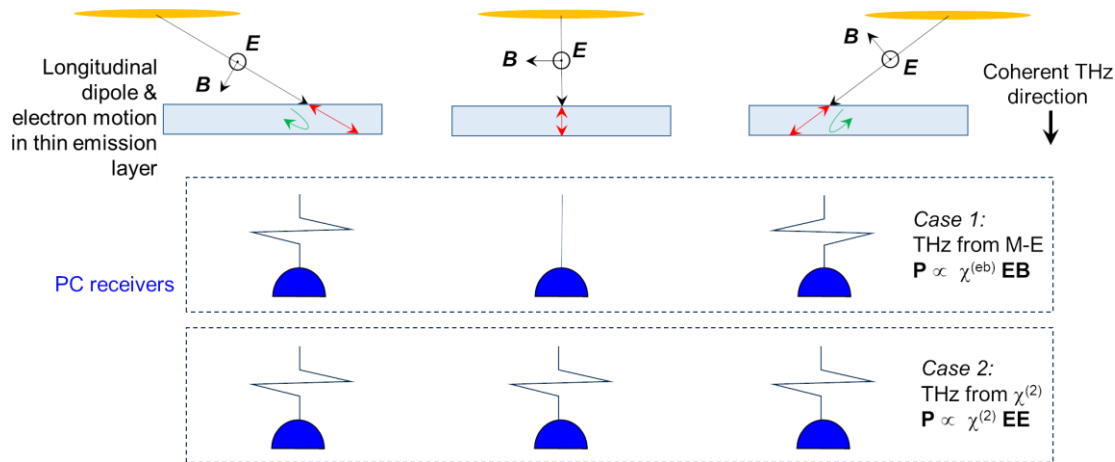


Fig. 18. Optical pulse-front excitation of pulsed-THz radiation for pulse-fronts that are parallel to the surface of a thin-film emitter and incident excitation angles that are both oblique and normal. A photoconductive detector should allow one to distinguish if the THz pulses were generated by M-E or E-E rectification dipoles.

negligible for normal incidence (because there will be no dipole radiation in the direction of the dipole), but they should be of opposite polarity for the left and right oblique incidence angles (because the in-plane components of the longitudinal dipoles are expected to be out of phase with each other). These features actually help distinguish THz generation that arises from M-E charge separation from all-electric sources.

Part of the significance of the tilted pulse-front technique was that it pointed to new methods for steering pulsed-THz beams. It might even lead to raster-scanning of THz probes for imaging applications. In the publication B.C. Smith, J.F. Whitaker and S.C. Rand, "Steerable THz pulses from thin emitters via optical pulse-front tilt", *Optics Express*, 24, Issue 18, pp. 20755-20762 (2016), mechanical steering of a THz beam through adjustment of the pulse front tilt angle was demonstrated. Electronic steering of the beam in materials with voltage controllable group velocity dispersion would greatly speed up the scanning rate and enhance the usefulness of such a THz source for a variety of applications.

Non-mechanical steering over large angles could be achieved by manipulating the tilt angle of the optical pulse-fronts electronically. Then it would be possible to image objects much more quickly and efficiently than with other scanning methods. As illustrated in Fig. 19, to facilitate the rapid steering of THz pulses, one could spatially chirp the pulse-fronts using a grating pair before passing them through a device such as a liquid crystal spatial modulator with a voltage-tunable group-velocity dispersion. Media with this property would allow the imposition of an electrically-controllable tilt on the pulse-fronts due to the different speeds experienced by different wavelengths in the broad spectrum of the optical pulses. Given a

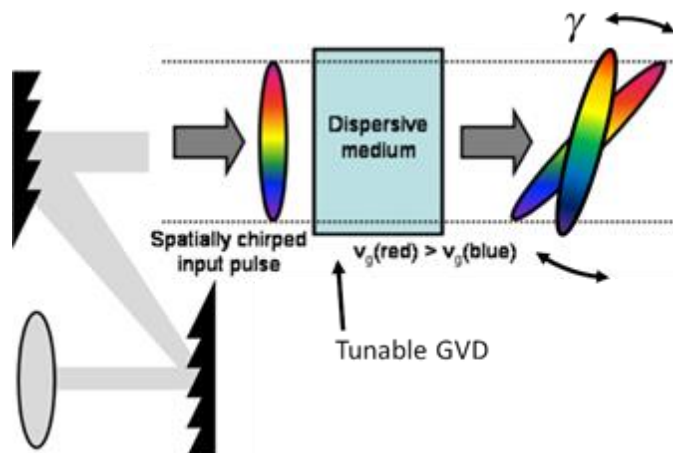


Fig. 19. Illustration of a means to spatially chirp an ultrafast pulse-front before electro-optically controlling its tilt angle (γ) in a medium with a voltage-controlled group-velocity dispersion (GVD).

method for rapid variation of pulse-wavefront tilt in the future, it will be possible with this approach to rapidly vary the output angle of THz beams with no moving parts. In addition to this application, a distinct benefit of the development of tilted pulse-front technology for this research program was that it enabled the first observation of M-E charge separation (Section 2.2.2).

2.3. Optical Magnetization

University of Michigan (S.C. Rand)

2.3.1. Magnetic Light Scattering in Small Molecules

Magnetic light scattering experiments were performed using apparatus depicted in Figure 20. Results from a series of studies in liquid samples of small molecules confirmed the mechanism of optically-induced magnetization previously theorized by UM researchers. Since magnetism is ordinarily a relativistic effect involving spin, it was important to explain in detail how induced

magnetic moments could be enhanced through dynamic exchanges of angular momentum. This work is described in recent publications A.A. Fisher et al., *Opt. Express* 24, 26055(2016) and M.T. Trinh et al., *Opt. Express* 27, 21295(2019) and a forthcoming review by Smail.

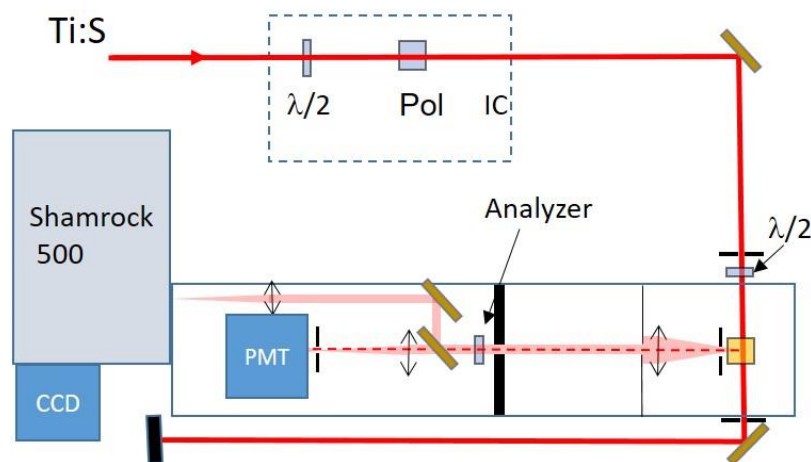


Figure 20. Experimental apparatus to record radiation patterns and spectra of ultrafast nonlinear light scattering. Pulses from a mode-locked Ti:sapphire laser are shown impinging on a liquid sample in a quartz cuvette within a light-tight box. Light scattered at 90° is collected by a collimating lens and apertures positioned along the detection axis determine the detector solid angle. The signal passes through an analyzer and interference filter (or spectrometer) and is detected with a photomultiplier or charge-coupled device (CCD).

The quantum picture of M-E dynamics at the molecular level is shown in Fig. 21. To provide a benchmark test of the theory, scattered light spectra of a series of tetrahedral, nonmagnetic molecules were recorded that included CCl_4 , SiCl_4 , SiBr_4 , $\text{Si}(\text{OCH}_2)_4$, and $\text{Si}(\text{OC}_2\text{H}_5)_4$. Measurements at moderate intensities (10^8 W/cm^2) with femtosecond laser pulses ($<150 \text{ fs}$) revealed the generation of molecular rotations in the cross-polarized scattering process,

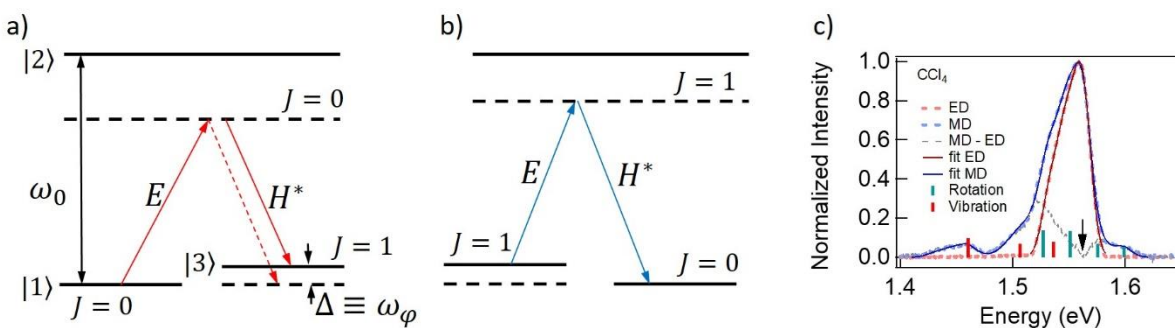


Fig. 21. Two-photon transitions responsible for second-order magneto-electric scattering driven by E and H fields and the scattered light spectrum. (a) In the Stokes process, the H field stimulates two classes of magnetic transition back to the ground state, as indicated by the two downward arrows. (b) In the "reverse" process, an anti-Stokes MD transition. (c) Normalized co- and cross-polarized scattered light spectra in CCl_4 , dashed-red (labelled ED) and -blue (labelled MD), respectively. The black arrow indicates the spectral peak. The solid curve showing a best fit that takes instrumental linewidth into account together with inelastic components due to vibrational and rotational transitions as indicated by vertical red and blue bars. The grey curve is the difference between the red and blue curves, highlighting the inelastic components in the MD spectrum.

providing direct evidence of theorized torque dynamics driven jointly by the electric and magnetic field components of light. The experimental findings were therefore in excellent agreement with the most crucial aspect of quantum theory, which predicted that molecules undergoing magneto-electric transitions terminate in rotationally excited states (as depicted in Figs. 21(a), 21(b)), leading to inelastic (shifted) features in the light scattering spectra.

Figure 21(c) displays the normalized co-polarized and cross-polarized spectra of scattered light in CCl_4 recorded with a 0.5 m grating spectrometer. The co-polarized (Rayleigh scattering) spectrum in red is virtually indistinguishable from the instrumental response over the bandwidth reflecting the pulse duration. The cross-polarized spectrum in blue has large additional features in it. These have been emphasized by subtracting the co-polarized signal to obtain the difference spectrum shown in grey. The extra features appearing in the cross-polarized spectrum are then found to correspond to inelastic scattering from known rotations and vibrations of individual CCl_4 molecules. Below the grey curve are the expected positions and relative heights of rotationally- and vibrationally-shifted satellite lines, indicated by vertical bars displaced from the origin (downward arrow at the peak of the pulse spectrum). Experimental values of the rotation and vibration energies were determined from a best fit convolution of the instrumental response $I(\omega)$ with an assumed spectrum of satellite lines of variable height and position. The widths of these features were assumed to be instrument-limited. The results for fitted vibration and rotation frequencies in Figure 21(c) are in good agreement with literature values (Fig. 22). The comparison of experimental rotation frequencies with results from prior spectroscopy shown in Figure 22(d) provides compelling evidence for our rotational assignments and confirms that rotations (or more correctly librations) are generated during the interaction responsible for cross-polarized scattering.

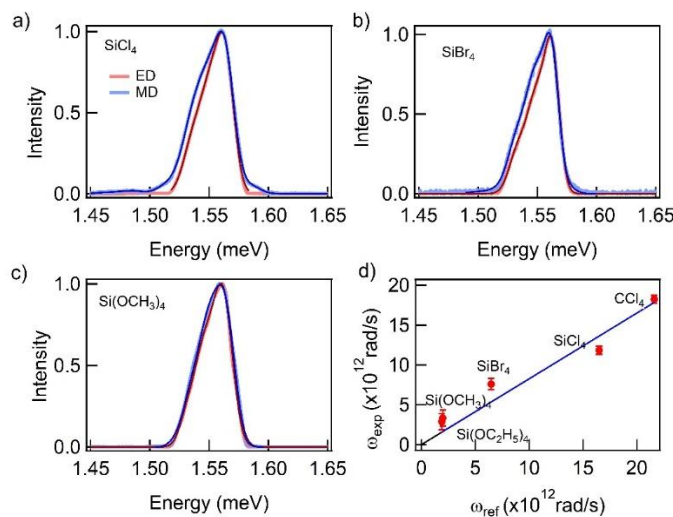


Fig. 22. Normalized co- and cross-polarized scattered light spectra for various compounds. (a) SiCl_4 , (b) SiBr_4 and (c) $\text{Si}(\text{OCH}_3)_4$ with fitted curves. (d) The experimental rotation frequencies (ω_{exp}) plotted versus literature values (ω_{ref}) for all samples. The solid line is a linear fit with a slope of 0.85. A slope slightly less than unity is consistent with heavy rotational damping in these molecular compounds.

Magnetic light scattering in these molecular liquids permitted a direct comparison between experiments and theory of magneto-electric interactions. According to our analysis the intensity of M-E scattering is proportional to the square of the induced magnetic moment, which has been

calculated by density matrix theory (see Publications: Smail and Rand (2020)). The expression for the moment itself is

$$M_y^{(2)}(\omega) = \frac{i}{\sqrt{2}} (\mu_0^{(m)})_{23} \left(\frac{(\Omega_{21}/2)(\Omega_{23}^*/2)}{(\Delta_{12} - i\Gamma_{12})(\Delta_{13} - i\Gamma_{13})} \right) + c.c. \quad (2.3.1)$$

Based on Eq. (2.3.1), a figure of merit (FOM) suitable for predicting M-E scattering intensity with pulsed excitation may be shown to be

$$FOM \equiv \left| \frac{(\mu_0^{(e)})^2 (\omega_0 / \omega_\phi)}{[(\omega_0 - \omega)^2 + (\Gamma^{(e)})^2][\omega_\phi^2 + (\Gamma^{(m)})^2]} \right|^2. \quad (2.3.2)$$

A comparison of FOMs based on Eq. (2.3.2) is presented in Table 2 for the tetrahalide samples described in this section. Comparative strengths of magnetic scattering from these compounds is presented in Figure 23. Note first that the general trend of scattering intensities at a fixed input intensity of $\sim 10^8$ W/cm² is CCl₄<SiCl₄<SnCl₄<GeCl₄. This agrees with the trend of tabulated FOMs for these compounds in the table. Additionally, the relative extremes of scattering intensities in CCl₄ and GeCl₄ are in quite good quantitative agreement with predicted intensity ratios given in the right-most column of the table, referenced to the response measured in CCl₄ which is taken to have a FOM of unity. Even the relative intensities of SiCl₄ and SnCl₄, which are very similar in the experimental data set, are in basic agreement with theory. The

Compound	ω_0 (10 ¹⁵ rad/s)	$\mu_0^{(e)}$ (10 ³⁰ C.m)	$\Gamma^{(e)}$ (10 ¹⁵ rad/s)	ω_ϕ (10 ¹² rad/s)	$\Gamma^{(m)}$ (10 ¹² rad/s)	Relative FOM
CCl ₄	10.7	4.1	0.548	21.6	3.70	1.0
SiCl ₄	13.6	11.3	0.654	16.5	2.86	151
GeCl ₄	10.7	12.1	0.596	15.5	0.898	293
SnCl ₄	9.47	13.2	0.585	12.3	1.26	112

Table 2. Molecular parameters for calculating the induced magnetic moments of liquid tetrahalides. Transient rather than steady-state conditions are assumed and all measurements were made with the same pulse duration and electric field. For each compound the FOM is calculated using Eq. (2.3.1) and normalized to CCl₄ at an optical frequency of $\omega = 2.35 \times 10^{15}$ rad/s.

accord between theory and experiment over more than two orders of magnitude in relative scattering strength provides compelling evidence that the theoretical analyses developed during this program capture the correct dynamics of magneto-electric interactions and the dependence of induced magnetization on the properties of small molecules.

The excellent agreement obtained between the relative scattering intensities plotted in Fig. 23 and quantum theory (that furnished the figures of merit (FOMs) in Table 2) constituted important milestones of this research program. First, it established that seemingly similar compounds could have wide-ranging response. Second it confirmed the basic mechanism of M-E interactions at the molecular level by identifying the key physical properties that cause variations of M-E response among simple liquids at the molecular level. It thereby provided material design guidelines necessary to reach other milestones of the program.

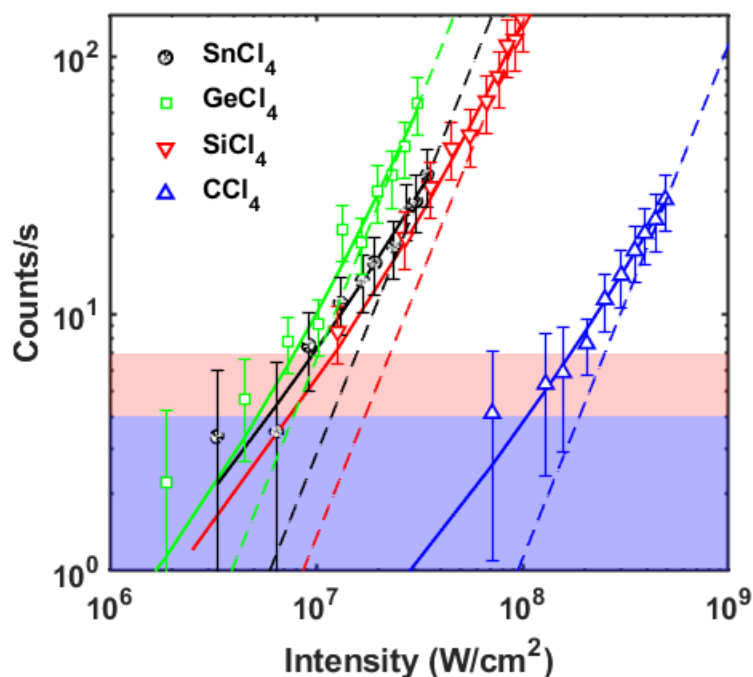


Figure 23. Comparison of total cross-polarized scattering intensities versus input intensity in a series of liquid tetrahalides. The dashed lines are quadratic extrapolations of the magnetic scattering intensities. The ratio of counts at a fixed input intensity for two different compounds, such as CCl_4 and SiCl_4 , is to be compared with the relative scattering strengths listed as figures-of-merit in Table 2.

2.3.2. Magnetic Light Scattering in Macromolecules

Following successful observations and explanations of M-E scattering in small molecules, experiments in compounds composed of large molecules and solids were undertaken. Ultrafast light scattering experiments were performed by Dr. K. Makhmal and Dr. M. Tuan Trinh on a series of novel silsesquioxane compounds (Figure 24) synthesized by Prof. Richard Laine's group at the University of Michigan. In these nonlinear scattering experiments it was shown that subtle differences in the shapes of 3D-conjugated LUMO at the center of silsesquioxane cage structures could be measured in a unique way that exploits their susceptibility to 2-photon, magneto-electric transitions.

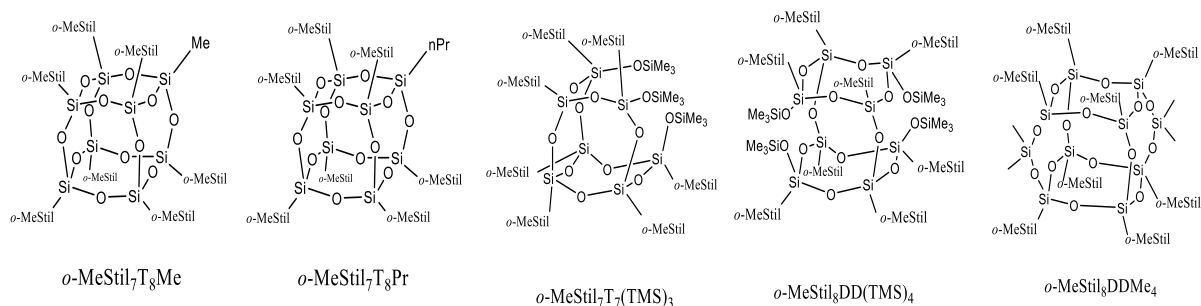


Figure 24. Structure of the silsesquioxane molecular compounds synthesized and studied in this work using ultrafast nonlinear light scattering.

Silsesquioxanes samples were prepared in dichloromethane solvent and were studied in 1 cm x 1 cm quartz cuvettes. Nonlinear scattering experiments offered the potential to characterize 3-D silsesquioxane structures in a novel way that exploited their susceptibility to the joint magneto-electric forces of laser light. The first step in these studies was to record and analyze co- and cross-polarized scattered light intensities to distinguish signals of electric and magnetic origin respectively. Then it was found to be possible to determine the comparative sphericity of the electron orbital from the ratio of unpolarized to polarized magnetic signal intensity. This ratio could be determined by mapping out complete radiation patterns by scanning the input polarization angle for two fixed analyzer orientations (Figure 25). The analyzer in the detection arm either transmits (red) or blocks Rayleigh scattering (blue) in these two orientations while the input polarization is rotated through 360 degrees.

In scattering experiments on Methyl, Propyl & 3TMS versions of the SSQ molecules, two separate components are visible in all scattering data, one with a (polarized) purely dipolar variation and another which contributes a constant background (unpolarized). Both components are of magnetic origin and were extracted by simple fits to the data. The polarized component in magnetic dipole scattering is a little bigger in 3TMS than in the methyl or propyl variants (Figure 25). An increase of this component, measured by the ratio of the angular variation over the constant background in the scattering data, could be interpreted as the result of a deformation in the potential well of the caged electron density. This interpretation follows from the connection

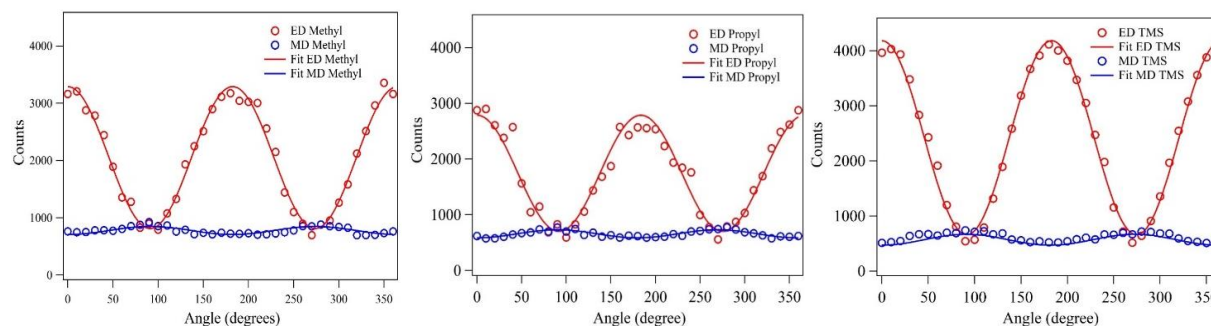


Figure 25. Co-polarized (red) and cross-polarized (blue) scattered light intensity vs. polarization angle of the incident light in three SSQ samples. The cross-polarized (magnetic) scattering shows very weak angle dependence but has a strong, unpolarized component. This may be interpreted as indicating an exceptionally small libration frequency ω_ϕ which promotes the downward magnetic transition depicted by a solid arrow in Fig. 20(a). This transition terminates by exciting librations that depolarize scattered light.

between the restoring force in molecular rotation and the azimuthal slope of the intra-molecular potential. A classical analysis yields

$$\omega_\phi \cong \frac{b}{\sqrt{I}} \left(\frac{dV}{d\phi} \right)_{av}, \quad b = (a)^{-1/2} = \text{constant}. \quad (2.3.3)$$

Thus the molecular rotation frequency is proportional to the average *azimuthal* slope of the intramolecular potential. Small rotation frequencies promote the scattering process that follows the solid downward arrow in Fig. 21(a), by reducing the frequency offset with respect to resonance and thereby resonantly exciting rotational motion. Since the rotational motion

depolarizes light scattering, a larger depolarized scattering component corresponds to a more nearly spherical potential with near-zero slope.

The data of Figure 25 have been re-plotted in Figure 26 in polar form. Note that in both figures the unpolarized component (in blue) is the cross-polarized scattering of magneto-electric origin. The polarized component (in red) is electric dipole scattering (Rayleigh). Note that the (red) electric dipole scattering and the (blue) magnetic dipole scattering share the same unpolarized (circular) component due to magneto-electric scattering.

Some basic observations from these studies are as follows. The MD unpolarized component decreases in the order:

$$\text{Methyl}_{\text{unpol,MD}} > \text{Propyl}_{\text{unpol,MD}} > \text{TMS}_{\text{unpol,MD}}$$

The MD polarized component decreases in the order:

$$\text{TMS}_{\text{pol,MD}} > \text{Propyl}_{\text{pol,MD}} > \text{Methyl}_{\text{pol,MD}}$$

The ED polarized component follows the trend as:

$$\text{TMS}_{\text{pol,ED}} > \text{Methyl}_{\text{pol,ED}} > \text{Propyl}_{\text{pol,ED}}$$

The trends listed above may be interpreted with the help of the quantum theory of magneto-electric interactions on the atomic scale. First, it may be noted that the progression of

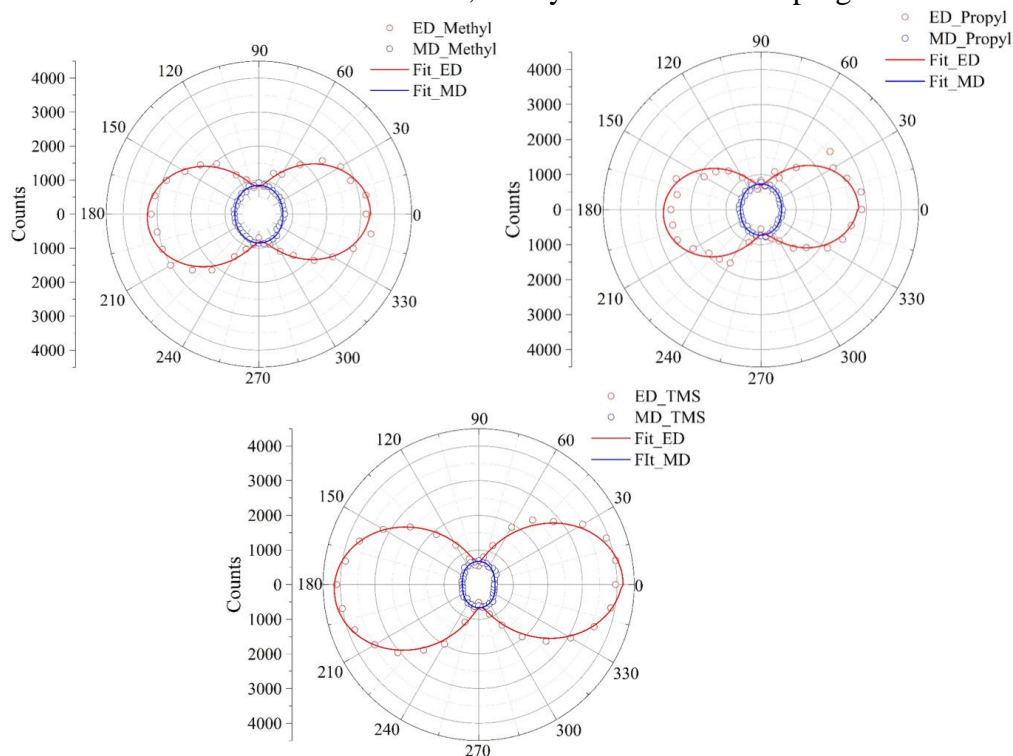


Figure 26. Polar plots of raw light scattering data for all SQs after solvent subtraction. The solid curves are least squares fits to dipole radiation patterns.

unpolarized MD intensity is opposite that of the polarized intensities. The proportion of these two components is determined by the magnitude of the librational resonance frequency ω_ϕ of

electrons responding to incident light. Presuming the active electron density occupies the orbital centered in the cage, the trend is consistent with resonance frequencies in the order

$$\omega_{\phi}(\text{TMS}) > \omega_{\phi}(\text{Propyl}) > \omega_{\phi}(\text{Methyl}).$$

This ordering is justified by the conclusion reached in that the unpolarized scattering channel experiences resonant enhancement as ω_{ϕ} decreases. The intensity of magnetic scattering should also be proportional to the polarized Rayleigh or ED component, provided the character of the orbital does not change appreciably from one compound to another. This trend is upheld in a comparison of the data for Methyl and Propyl which differ only in the substituent outside the cage. However the MD component in the TMS data is reduced in intensity despite a sizeable increase in its Rayleigh component, as compared to the other two compounds. This is most obvious in Figure 26 where TMS clearly exhibits the largest polarized ED and the lowest MD signals.

In the quantum picture of magneto-electric dynamics, it is the slope of the orbital potential function that determines the torsional restoring force and the librational resonance frequency. A spherical or nearly spherical potential has a slope close to zero which promotes unpolarized MD scattering. Hence one interpretation of the scattering data presented in this section is that they are consistent with the idea that removing a corner of the cage in the TMS compound distorts the sphericity of the electron orbital in the cage. It is quite reasonable to expect that the electron potential develops an axis passing through the corner from the center of the cage. The introduction of this axis could be argued to lead to an increase in the ED transition moment accompanied by an anisotropy of the potential which raises the librational frequency and diminishes the magnetic scattering intensity, consistent with the scattering data. Thus the scattering experiments suggest there is a reduction in the sphericity of the LUMO in the cage when a corner is opened, but that the effect is relatively subtle.

2.3.3. Magnetic Light Scattering in Solids

Experiments were also performed in numerous solids. Typical results are shown in Figure 27, which displays the measured radiation patterns for light scattered by a GGG crystal. Fig. 27(a) plots raw data. Fig. 27(b) displays the polarized components of co-polarized and cross-polarized light to emphasize that these components have nearly the same intensity at their respective peaks. Similar results were obtained for scattering in fused quartz, as seen in Figure 28. However the polarized magnetic component in quartz (Fig. 28(b)) is larger than in GGG. Remarkably, the induced, magnetically-scattered light in quartz has an intensity equal to Rayleigh scattering. This is an unprecedented observation which directly affirms that under non-relativistic conditions ($I \ll 10^{18} \text{ W/cm}^2$), magnetic moments induced by light can be as large as electric dipole moments.

The precise location of ligands active in absorbing or emitting light in solids is difficult to determine. Similarly, the natural libration frequency is unknown. Nevertheless, some inferences can be made from radiation patterns like those in Figures 27 and 28 that were common to all the solids studied for this program. The large unpolarized component that is observed in nonlinear light scattering from solids has the same implication as for SSQ macromolecules. It indicates that the libration frequency in hard solids is low so that the two channels indicated by downward arrows in Fig. 21(a) produce comparable scattering intensities. Unlike the situation analyzed in

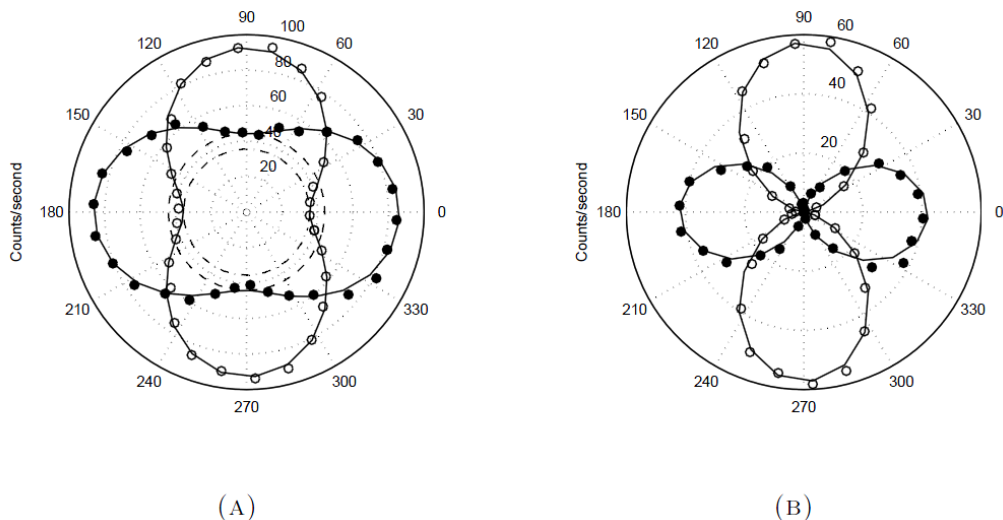


Figure 27. Radiation patterns measured by light scattering in a GGG crystal. Co-polarized data is coded as open circles. Cross-polarized data is shown as filled circles. (a) Raw data. (b) Data after subtraction of the angle-independent background. Incident light was from a mode-locked laser emitting pulses of duration 100 fs and operating at 800 nm at an intensity of $I \sim 5 \times 10^9 \text{ W/cm}^2$.

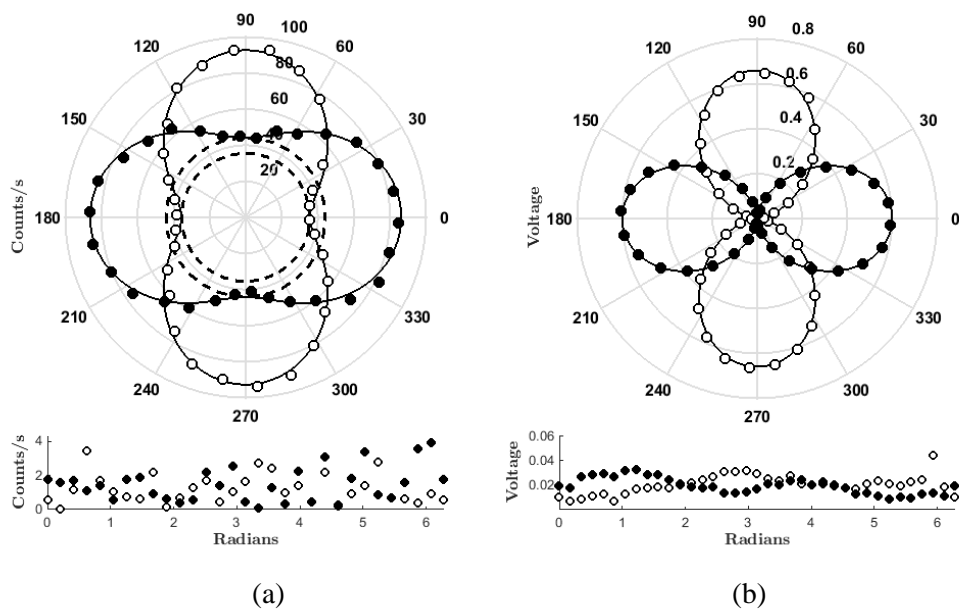


Figure 28. Radiation patterns measured by light scattering in a fused quartz sample. Co-polarized data is coded as open circles. Cross-polarized data is shown as filled circles. (a) Raw data. (b) Data after subtraction of the angle-independent background. Residuals from the fits are shown below the radiation patterns. Incident light was from a mode-locked laser emitting pulses of duration 100 fs and operating at 800 nm at an intensity of $I \sim 5 \times 10^9 \text{ W/cm}^2$.

tetrahalide molecules, the libration frequencies in solids are not determined by the molecular moment of inertia of a small molecular structure. Instead, in view of the intense unpolarized components evident in the data of Figs. 27 and 28, it seems plausible that solid hosts act like super-macromolecules with extremely large *effective* moments of inertia I . Through the usual

expression for libration frequency of a rigid rotor $\omega_\phi = h/I$, a large *effective* value of I consistent with the many atoms surrounding active ligands would imply a very low libration frequency. In turn an exceptionally small value of ω_ϕ promotes intense unpolarized scattering.

2.4. Magneto-electric Second Harmonic Generation

Stanford University (Tony Heinz)

2.4.1. Observation of M-E SHG in Graphene

Second (M-E) harmonic generation is the third nonlinearity in the family of magneto-electric phenomena under investigation in this project. In the first year of research the possible role of magnetic field-induced optical effects in the Dirac Fermion system of graphene was explored (Figure 29). This material is not an insulator and therefore does not localize charges as required for the other nonlinearities of the M-E family. However it does confine Lorentz-force-mediated motion to a plane just like the charge separation and magnetization nonlinearities as a result of its two-dimensional character. Additionally it features a unique linear dispersion relation for charge carriers near the K/K' points of the Brillouin zone and provides a fascinating test case for magnetic effects in a class of electronic materials of great current interest.

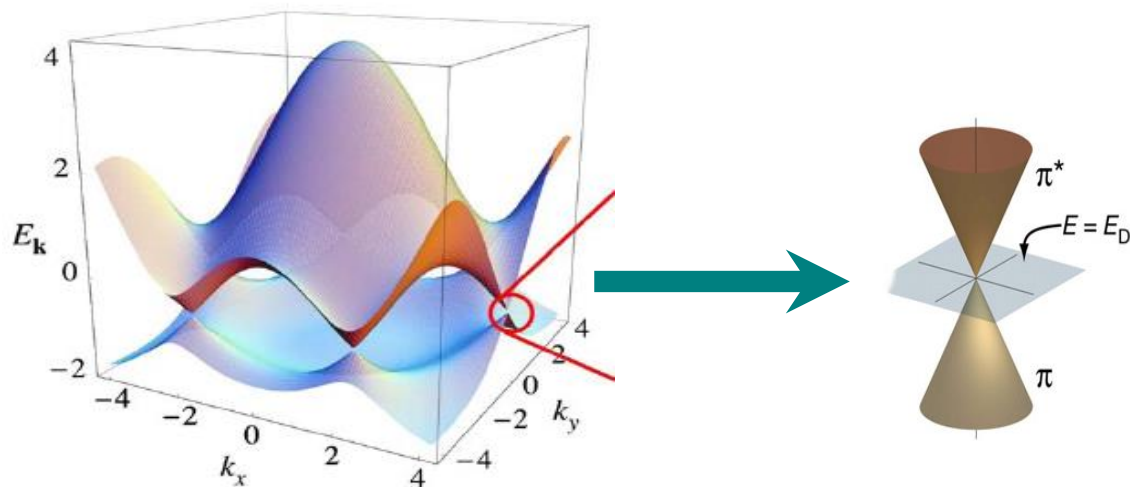


Figure 29. Energy surfaces for graphene, showing an enlargement of the Dirac point where conduction and valence bands touch. This material has no energy gap at this point and exhibits linear dispersion that is usually associated with relativistic dynamics.

The first observation of Lorentz-force-mediated second harmonic generation in graphene was made late in 2014 by the DYNAMO team directed by Prof. Heinz, then at Columbia University. The group subsequently relocated to Stanford but Heinz remained a principal investigator on the MURI team. In the graphene work, monolayer samples were prepared by micromechanical exfoliation onto both transparent substrates and Si wafers covered by a 300-nm thick oxide layer. The former sample provides less background signal for the SHG measurements, while the latter allowed variations of carrier density within the graphene monolayer by electrostatic gating.

SHG response was measured for a graphene monolayer prepared on a bulk fused silica substrate. The graphene monolayer was unintentionally doped at a level of $\sim 10^{11}/\text{cm}^2$ and placed on a substrate with very low second-harmonic response. The experiment revealed a

strong response for the configuration of s polarized pump radiation giving rise to a p -polarized SHG signal ($s \rightarrow p$). The measurements were performed for an angle of incidence of approximately 45° and exhibited negligible SHG signals for other polarization combinations (*i.e.*, $s \rightarrow s$, $p \rightarrow s$, and $p \rightarrow p$). Notably, the signal was negligible for normal incidence, an orientation which prohibits Lorentz-force-mediated motion within the graphene layer.

The SH signal intensity was therefore maximized by the orientation displayed in Fig. 30. This result shows that the output is p -polarized in character. The observed polarization dependence is completely compatible with a model of the SHG process that relies on the effect of magnetic forces through the action of the Lorentz term. In this picture, the electrons are driven at the fundamental frequency through their interaction with the electric field. The observed SH response then arises from the $\bar{v} \times \bar{B}$ term in the expression for the Lorentz force. Since \bar{v} for a two-dimensional material must necessarily lie in the plane of the material, this term can drive a response current in the plane of the material only if the optical magnetic field \bar{B} has a component perpendicular to the plane of the graphene. This is achieved for p -polarized optical excitation, with the $\bar{v} \times \bar{B}$ term, which is parallel to $\bar{E} \times \bar{B}$ giving rise to p -polarized emission.

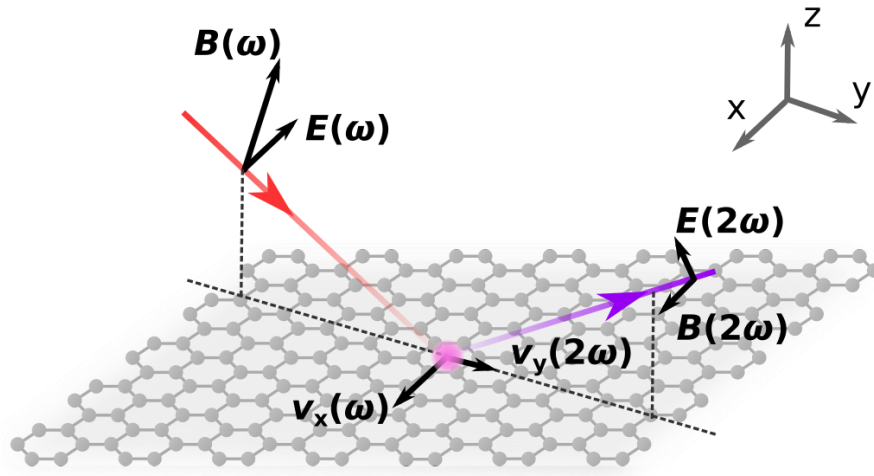


Figure 30. Input polarization that results in the maximum SHG signal from graphene. Note that the electric field vector lies in the plane whereas B has a perpendicular component. Thus E can initiate charge motion within the graphene plane and B can deflect it as required to enable magneto-electric second harmonic generation.

2.4.2. Experiments on Magnetic Effects in 2-D Materials

Following this successful, experiment on ME-SHG in graphene, an investigation was undertaken of optical magnetic field effects in second and higher-order nonlinear response of electrons in a broad class of 2-D materials. Biexcitons in monolayer WSe_2 were targeted as important to this project for a number of reasons. In addition to forming a stable four-body correlated state, biexcitons exhibit strong nonlinearity at low power and, under radiative decay, can also be a source of the emission of entangled photons.

In our investigations we have examined monolayer samples of WSe_2 , a well-known representative of the new class of two-dimensional semiconductors in the TMDC family. In these systems, the three-dimensional bulk crystal is known to be an indirect-gap material, while the monolayer exhibits direct-gap character with optical transitions at the K and K' points in the Brillouin zone. Because of weak dielectric screening in these monolayer materials, the optical

properties at the band-edge are dominated by excitonic transitions, leading to sharp emission features in the photoluminescence spectrum. In addition to the presence of the neutral exciton (X_0), in samples with free charges, the spectra exhibit emission from charged excitonic species or trions. In our case, we have unintentional doping leading to the presence of free electrons and the formation of the negative trion state (X_T). These additional species contribute spectral features that are shown in Fig. 31 for the emission from monolayers of WSe₂. Additional low-energy emission features associated with localized excitons are also present (but are not shown in Fig. 31).

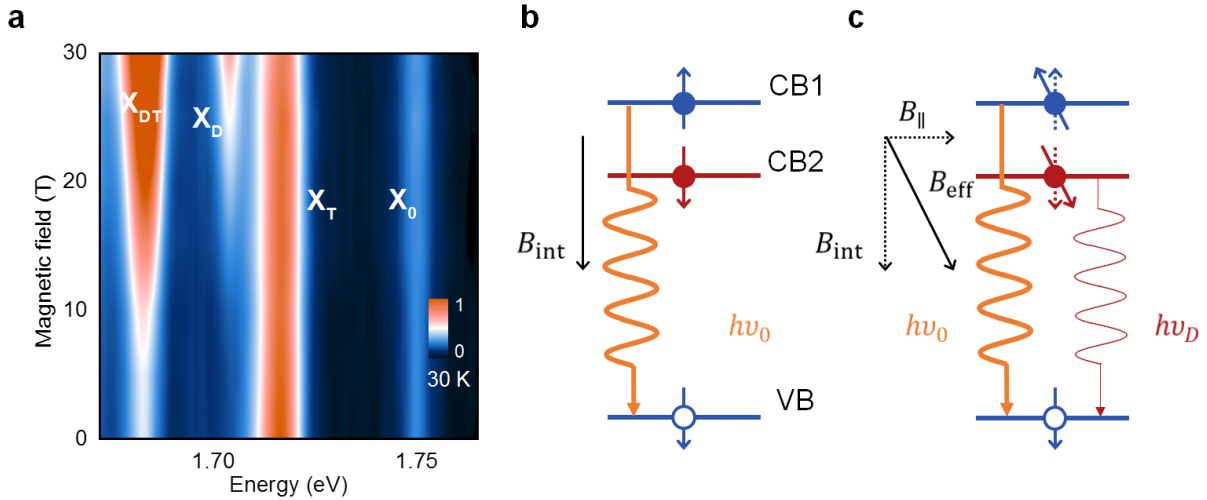


Fig. 31: Magnetic brightening of dark excitons in monolayer WSe₂. a) False color plot of the emission spectrum as a function of the strength of an in-plane magnetic field $B_{||}$. In the absence of the magnetic field, we observed emission from the neutral exciton (X_0) and the charged exciton or trion state (X_T). With increased magnetic field, two strong new features emerge associated with the magnetically brightened dark neutral exciton (X_D) and the brightened trion state (X_{DT}). b and c) Schematic representation of the band structure of WSe₂ at the band structure extrema at the K and K' valleys. The conduction band is split into to spin-polarized components. The lower band has the opposite spin compared to the (upper) valence band, thus rendering the lowest lying optical transition spin forbidden. c) In the presence of an in-plane magnetic field, the conduction band spin states become slightly tilted by the mixing between the two bands. Optical transitions from the lower conduction band, the previously dark excitonic states, become weakly allowed.

Under the application of an in-plane magnetic field $B_{||}$, we observed the emergence of two distinct new features in the emission spectrum, as shown in Fig. 31. The two new emission features are magnetically brightened dark excitons (X_D and X_{DT}) associated with exciton and trion emission, respectively. The origin of the initially dark excitonic states lies in the spin configuration of the valence and conduction bands. Because of spin-orbit interactions both the valence and conduction bands are split into spin-polarized bands. While the spin splitting of the valence band is large (several hundred meV) due to the angular momentum of the relevant orbitals, the spin splitting in the conduction band is relatively small, on the order of a few tens of meV. The relative spin configuration of the upper valence band and of the lower conduction band is of critical importance in defining the optical characteristics of the material. If the initial and final spin states are the same, then we have an optically allowed direct transition with efficient light emission. However, if the two spin states are opposite, then the transition is spin-

forbidden. In this case, emission from the lowest-lying optical transition is forbidden. Provided the energy separation to the higher-lying optically-allowed transition is large compared to the thermal energy in the system, then the overall emission rate of the system will be dramatically reduced. It has been predicted theoretically that for the tungsten-based dichalcogenide crystals, like WSe_2 , the upper valence band and lower conduction band have opposite spin, corresponding to the case of a band-edge dark exciton (Fig. 11b). This situation has significant implications for the possibility of efficient light emission from this system.

In our measurements, use was made of magnetic fields to brighten the otherwise dark band-edge exciton states by changing the spin configuration of the conduction band. Under the presence of an in-plane magnetic field B_{\parallel} , the weakly split conduction bands mix with one another. This situation can be understood within a picture where the spin splitting of the bands is attributed to the Zeeman effect induced by an effective out-of-plane magnetic field. In the presence of an applied in-plane magnetic field, the total effective magnetic field now lies at an oblique angle, giving rise to new mixed spin states (Fig. 31(c)). The consequence of this reorientation of the spins in the conduction band is that there is now a finite projection of the spin of the lower conduction band on the spin state of the upper valence band, rendering the corresponding optical transition (weakly) spin-allowed. This mechanism explains the emergence of new emission peaks associated with the dark exciton and trion states under the application of the in-plane magnetic field.

Further results supporting the picture of magnetic brightening of dark states are presented in Fig. 32. Figs. 32(a) and (b) exhibit the emergence of field-induced emission features at low and higher temperatures, respectively. Fig. 32(c) shows the expected quadratic variation of the intensity of the brightened dark exciton and trion with increasing applied magnetic field, as predicted theoretically from a picture of weak spin mixing in the split conduction band. Fig. 32(d) shows the emission dynamics from the bright and dark exciton states using time-resolved photoluminescence. As expected, based on the relatively weak induced mixing of the conduction bands, the magnetically-brightened dark state exhibits much longer emission lifetime than the bright exciton state.

Key features of the emission spectrum include the bright exciton peak (X^0), the spin-forbidden dark exciton (X^D), and a newly identified feature labeled as XX in Figure 33. While the bright and dark exciton peaks exhibit essentially linear power dependence, the XX feature varies quadratically with power. Through this and other experimental observation, we have identified feature XX as originating from neutral biexciton emission. A feature previously identified as a biexciton, appearing at lower emission energy, has now been recognized as a charged biexciton species.

The present investigation illustrated how the basic optical properties of the states in semiconductors can be tuned by magnetic interactions. Our experiments directly demonstrated the possibility of continuous tuning of radiative lifetimes, as well as the increase in valley lifetime. The long-lived, but radiatively-coupled brightened dark states are candidates for “valleytronic” applications and the creation of new many-body correlated states, such as exciton or polariton condensates. In addition, the spectral shifts between the dark and bright exciton and trion states provided quantitative information about the conduction band splitting and the many-body excitonic interactions, such as the strength of exchange interactions. The theoretical aspects of this work were pursued through a collaboration with the group of Prof. Steven Louie at UC

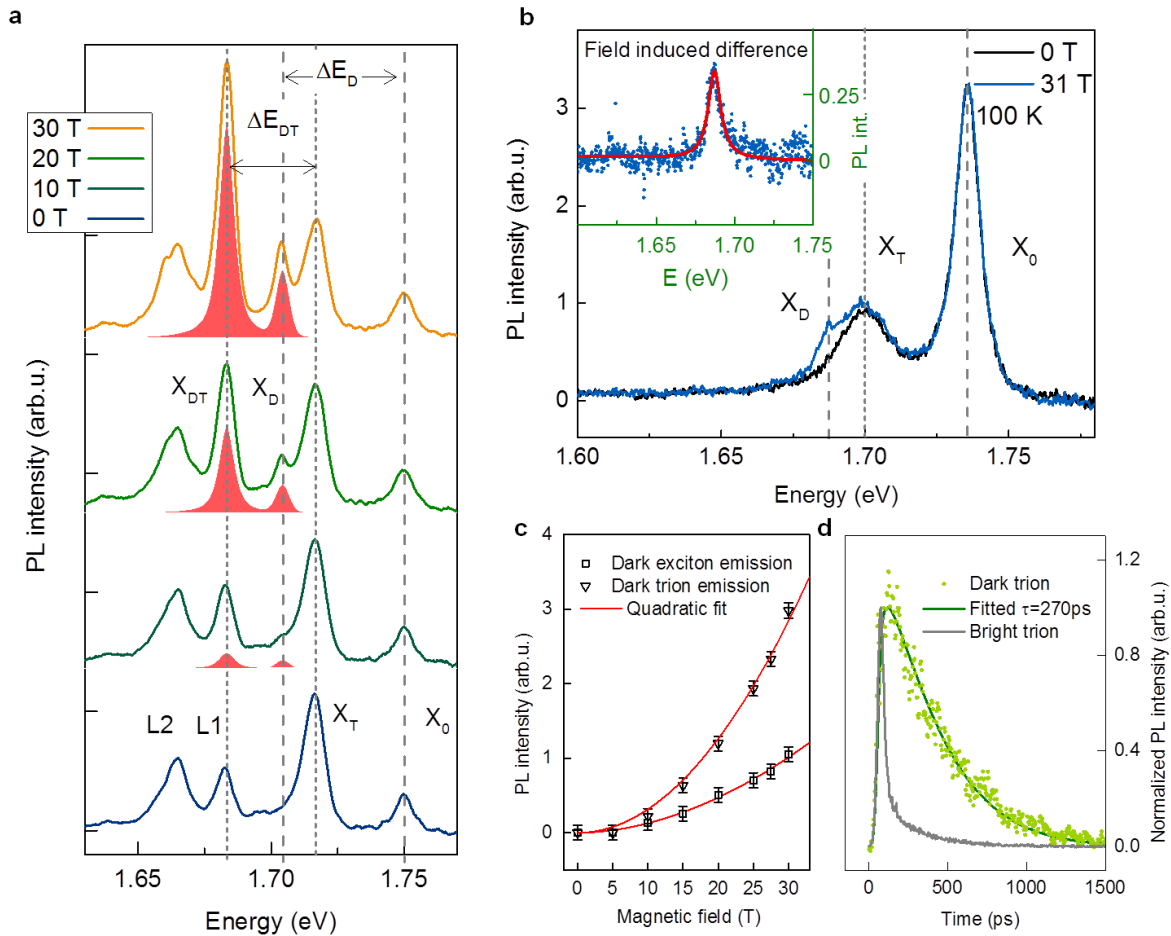


Fig. 32: Spectroscopic investigations of magnetically brightened dark exciton states in monolayer WSe_2 . a) Emission spectra at 30 K as a function of magnetic field, showing the growth of the magnetically brightened dark exciton states. The lower energy emission features arise from localized excitons at defect sites. b) The emission spectrum at 100 K, showing the emergence of the brightened dark exciton in a regime where the localized states are absent. c) The quadratic variation of the magnetically brightened exciton and trion states with magnetic field for the spectra in a). d) Time-resolved emission spectrum from the bright and dark trion states, showing the long lifetime of the magnetically brightened dark states compared to that of the corresponding bright state.

Berkeley. On the experimental side, the Heinz group collaborated with Drs. Dmitri Smirnov and Zhiqiang Li at the National High Magnetic Field Laboratory in Tallahassee for the magnetic field measurements, with support on sample preparation from Jim Hone's group at Columbia University and Joshua Robinson's group at Pennsylvania State University. (For published work see Publication List).

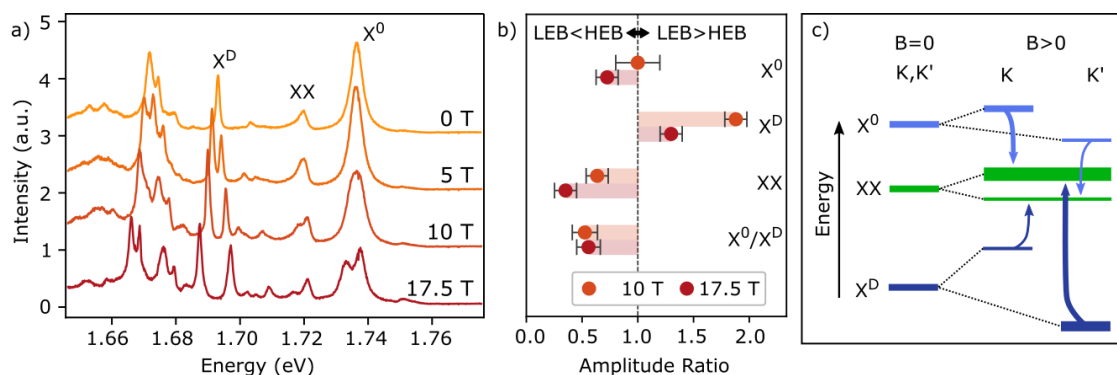


Fig. 33. Magneto-optical measurements on monolayer WSe_2 . The left panel shows the evolution of the emission spectra for the different excitonic features as a function of the strength of the perpendicular magnetic field. The neutral bright (X^0) and dark (X^D) excitons, as well as the biexciton (XX), are split into two features, corresponding to excitons in the two available (K/K') valleys. The rate of splitting reflects the magnetic moments of the species. From an analysis of the heights of the two features we can infer that the biexciton is preferentially formed as a combination of excitons in opposite valleys.

2.5. Rational Design & Characterization of M-E Materials Northwestern University (Tobin Marks)

In order to elucidate the governing rules of magneto-electric (M-E) susceptibility in molecular/macromolecular materials, experimental and computational evidence was sought for structure-property relationships and concepts from conventional nonlinear optics (NLO) that might assist this endeavor. Our goals included: (1) establishment of design criteria for enhanced M-E susceptibility in molecules based on experimental and theoretical evidence, and (2) synthesis and characterization of high-performance materials with enhanced third-order susceptibilities $\chi^{(3)}_{xxxx}$ and $\chi^{(3)}_{zxzx}$. The main goal is to develop design guidelines and materials with significantly enhanced M-E susceptibility that are suitable for charge separation and magnetization technologies.

2.5.1. A Link between Conventional and M-E NLO Materials

A formal connection was discovered in 2018 between M-E and conventional nonlinear optical (NLO) response (see A. Lou et al. in Publications List). This previously unknown connection was derived by recognizing that M-E interactions are not governed by the symmetry rules of conventional NLO processes, which are based on symmetry elements of the unperturbed medium or crystal. M-E interactions are governed by combined parity-time (P-T) symmetry which breaks inversion symmetry of centrosymmetric media, rendering second-order M-E nonlinearities universal. This advance enabled the Northwestern and UCF teams to leverage their considerable expertise in NLO to synthesize and investigate promising classes of molecules for M-E magnetization and rectification. These two phenomena are governed by conventional (all-electric) susceptibility elements $\chi^{(3)}_{xxxx}$ and $\chi^{(3)}_{zxzx}$ respectively. Hence it became possible to design high-performance chromophores specifically for M-E rectification and M-E magnetization applications based on long-established optimization techniques from conventional nonlinear optics.

2.5.2. Design Guidelines for M-E Magnetization Materials

The first series of molecules targeted for synthesis at NW were tri-substituted benzene derivatives (Figure 34). These compounds were chosen on the basis that benzene itself showed heightened cross-polarized scattering in preliminary experiments and because they vary in electron density within their conjugated ring structure. They have the potential merit of possessing centrosymmetry, which prohibits all-electric second-order nonlinearities that could confuse the interpretation of nonlinear scattering experiments. They also provide a range of refractive index (n), moments of inertia, and are transparent.

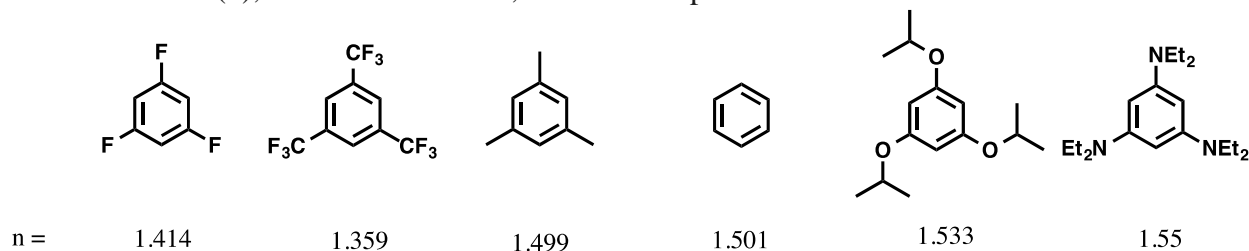


Figure 34. Tri-substituted benzene survey materials in order of increasing refractive index (n)

An early finding with these benzene derivatives however was that the high cross-polarized scattering intensity observed in preliminary experiments was not an indication of magneto-electric behavior at all. In planar, anisotropic molecules like benzene an all-electric third-order effect competes very effectively with M-E interactions, creating an anisotropic electric polarization on which optical fields can exert electric torque to rotate the molecules. Thus, in such systems, all-electric interactions can give rise to nonlinear crossed-polarized light scattering.

To eliminate this source of confusion in scattering experiments, it became necessary to synthesize isotropic, centrosymmetric media for the project. Consequently the second phase of synthetic efforts at NW focused on materials with exceptional values of hyperpolarizability. It had been shown previously at NW that the inclusion of a twisted biaryl in push-pull chromophores led to high values of second hyperpolarizability. However, the difficulty of synthesizing twisted chromophores had impeded research on them. Thus the primary goal of this effort turned to development of an efficient route for synthesis of a variety of twisted chromophores. Several of these compounds were successfully synthesized on a five-gram scale and purified by column chromatography. However, it was discovered that even triethylene glycol side chains were insufficient to render all target compounds liquid at room temperature. Hence it was not always possible to deliver samples suitable for light scattering investigations in standard quartz cuvettes.

One sample, which proved to be a transparent liquid when glycol side chains were added, and which was expected to have exceptionally high hyperpolarizability, was the twisted chromophore TMC-3. Because this molecule seemed to be very promising, a scheme was developed that maximized the use of versatile and robust reactions as illustrated in Figure 35. A reliable *E*-selective Horner-Wadsworth-Emmons reaction was employed and strategic alkylation significantly improved on previous synthetic routes by reducing the number of steps from ten to four. Considerable effort was also made to optimize reaction conditions for the key Kumada or Suzuki cross-coupling (step *i*).

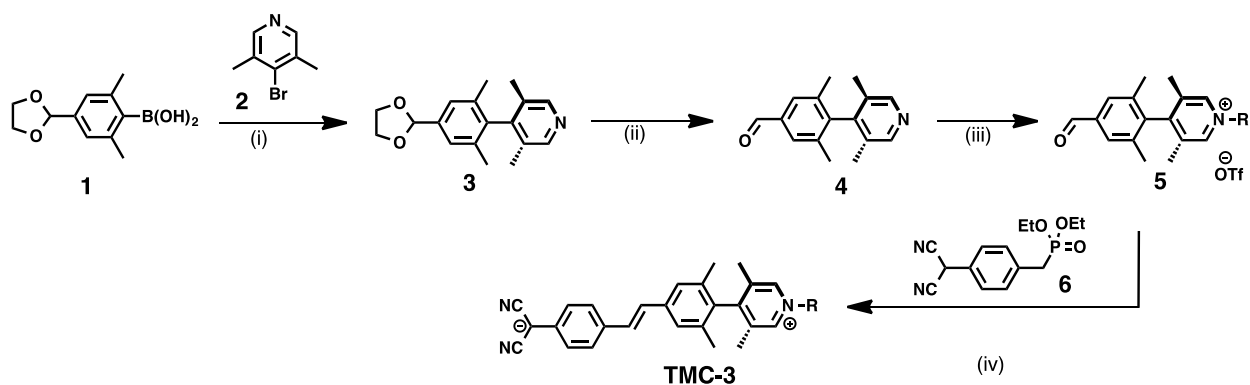


Figure 35. Improved synthesis of the twisted *p*-system chromophore TMC-3.

The focus on hyperpolarizability was justified in 2018 by the discovery of a link between the third order M-E susceptibility for magnetization and the diagonal element for a third-order, all-electric nonlinearity. The specific relationship deduced was

$$\chi_{yyx}^{(meme)} = \chi_{xxx}^{(3)} \quad (2.5.1)$$

Because preliminary measurements had indicated large hyperpolarizability in TMC-3, a thorough characterization of this chromophore was undertaken at the University of Central Florida. When characterization by Z-scan measurements at CREOL were completed, they revealed that extension of the dipole moment on the molecule led to improved γ_{xxx} (to which χ_{xxx} is proportional) on the order of $\sim 10^{-33}$ esu, causing a large nonlinear refraction (NLR) response. An unexpected excited state-derived nonlinearity was found to derive from the type of conjugation created in the molecular structure. The effort made to improve beam-deflection experiments for the measurement of M-E nonlinearity are described in Sec. 2.5.4.

2.5.3. Design Guidelines for M-E Rectification Materials

Establishment of the theoretical link between all-electric and M-E nonlinearities specifically predicted that rectification was optimized by the susceptibility element $\chi_{zxx}^{(3)}$ according to the relation:

$$\chi_{zyx}^{(eme)} = -\eta_0 \chi_{zxx}^{(3)} \quad (2.5.2)$$

Multi-directional charge transfer was previously shown to be a key factor in enhancing $\chi_{zxx}^{(3)}$. Hence this factor infused the strategy to optimize materials for M-E rectification. A consequence of this was that it led to the selection of Λ -shaped, X-shaped, octupolar molecules, and 2-D planar systems such as porphyrins and phthalocyanines for the rectification task. Thus numerous conjugated polymers, phthalocyanines, and porphyrin films, as well as solutions of these compounds were provided for the pump-probe and THz generation experiments performed at University of Michigan. Computations were also performed on X-shaped, Λ -shaped, and octupolar (OB2) twisted chromophores (Figure 36). In these structures, enhancements in hyperpolarizability elements γ_{xxx} and γ_{zzz} were predicted with increasing dihedral angle. Systematic studies were therefore undertaken of the spectroscopic properties, geometric conformations, and lower-order nonlinear responses of the 1-D derivative compound B2TMC-2. These studies confirmed that the benzimidazolium acceptor group in the B2TMC-2 series

maintained both large torsional angles and very large nonlinear response. They also revealed that the impact of chromophore environment on NLO response was highly dependent on the acceptor group.

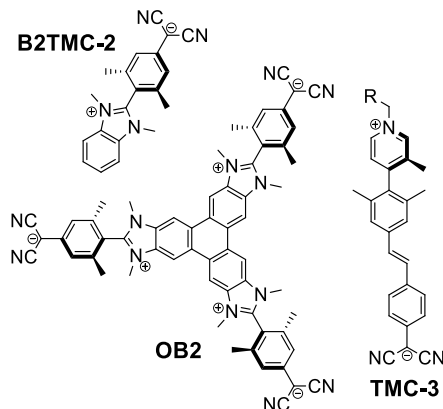


Figure 36. Depiction of the 1-D derivative B2TMC-2 in which the benzimidazolium acceptor group maintains both large torsional angles and very large nonlinear response.

2.5.4. Measurements of M-E Susceptibilities University of Central Florida (David Hagan)

Many experimental techniques exist for measuring the nonlinear optical (NLO) response of materials. However, the polarization combinations that can be applied to determine specific elements of the susceptibility tensor are often limited because the interaction geometry is limited. Full characterization of the M-E susceptibility tensor is difficult unless beams can cross at 90° . Unfortunately, a right-angle geometry typically reduces the attainable temporal resolution, creating a challenge that must be overcome either with a beam-focusing technique or by introducing tilted pulse fronts, as described in the earlier Section 2.1.2.

A beam deflection technique typically employed at CREOL was therefore modified to study the elements of the third-order susceptibility tensor with field components along the propagation direction. This technique can be of use in detecting magneto-electric (ME) contributions to the nonlinear susceptibility. To maintain good temporal resolution, focused beams were used at first to limit the spatial extent of the interaction region. Later tilted wavefronts of the pump and probe beams were employed in a cross-beam geometry. The tilted wave approach was conceived by Dr. Trinh at Michigan and introduced into experiments at CREOL by him during a collaborative exchange. The UCF group was then able to make progress in the characterization of twisted chromophores provided by Tobin Marks' group at various wavelengths in the search for candidate magneto-electric materials.

Nondegenerate excitation and probe beam wavelengths were employed to characterize the time-resolved ultrafast nonlinear refraction and absorption. This avoided complications that occur in experiments with degenerate wavelengths. For tilted wave experiments, independent control of the tilt angle of the excitation and probe beams was necessitated. Consequently two independent adjustments of tilt angle had to be introduced into the crossed beam experiment, as shown in Fig 37. The spatio-temporal interaction of two beams crossing each other depends

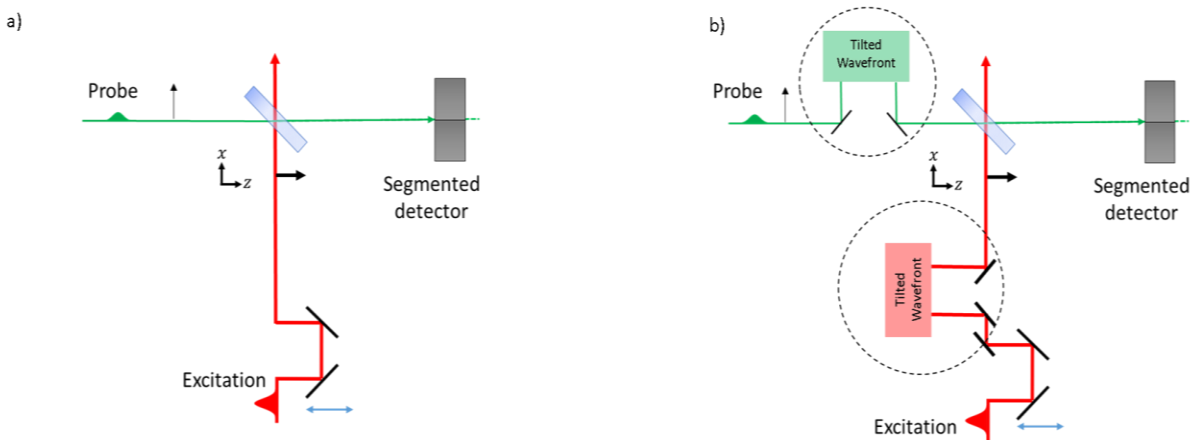


Figure 37. (a) Conventional cross-propagating beam geometry and (b) tilted pulse front setup allowing independent adjustment of tilt angle for excitation and probe beams.

upon the wavefront tilt of each individual beam. For a nondegenerate experiment, the tilt is produced independently in each beam as shown in Figure 37(b). In a degenerate pump-probe geometry, the tilt can be suitably adjusted before splitting the laser into pump and probe, but in the case of nondegenerate wavelengths the dispersion is different for each beam, requiring independent adjustments.

In the tilted pulse approach to characterization depicted in Fig. 38, wavefronts that are

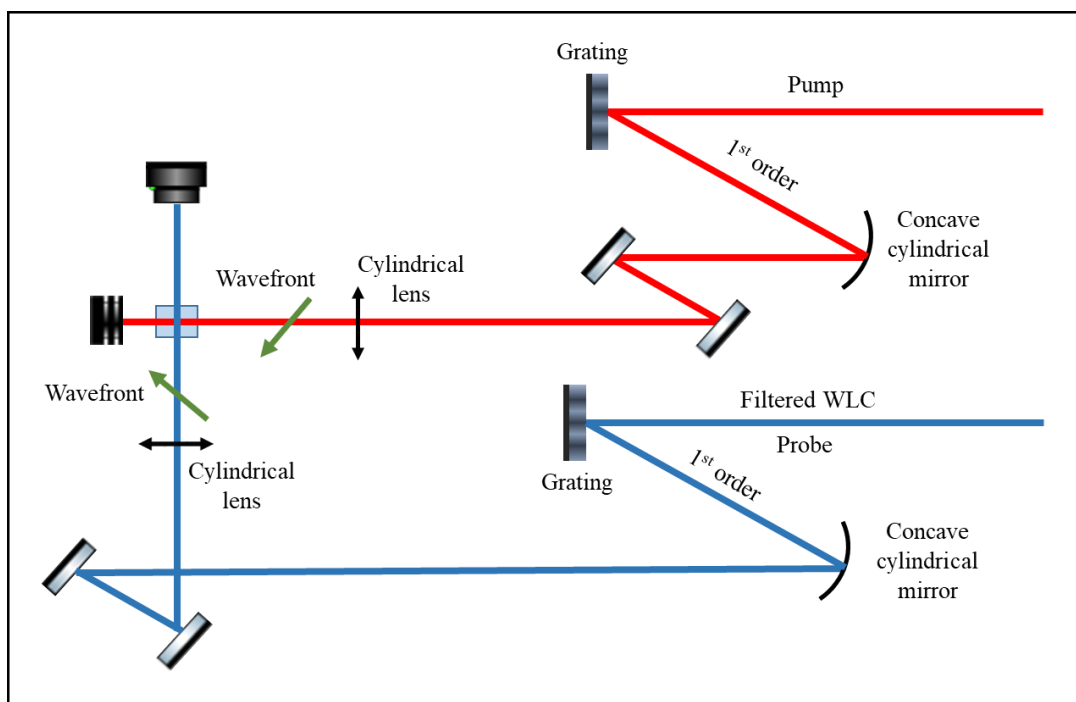


Figure 38. Method for producing tilt in nondegenerate pump-probe setup. Note that the number of mirrors in each beamline is the same.

perpendicular to the direction of propagation intersect in the interaction region along a line. This restricts the interaction to a small volume and is accompanied by significant transit time broadening. However, when the wavefronts were tilted away from perpendicular, it was possible to optimize the interaction as illustrated in Fig 39(a). For example, when the pump and probe wavefronts were tilted by 20° in the correct mutual orientation, the cross correlation width was greatly reduced compared to the case with no tilt in the wavefront, as shown in Fig 39(b) for normalized signals.

In view of the need to make the difficult adjustment of tilt angles in the setup of Fig. 38, full characterization of the M-E tensor was not completed during this project. Instead, elements of $\chi^{(3)}$ for a class of TICT chromophores (TMC-3') was ultimately performed using a dual-arm (DA) Z-scan technique to measure diagonal components of the all-electric susceptibility. The impact of structural modifications of TICT chromophores on the nonlinear response was then successfully determined in hybrid TICT chromophores using the link between M-E and all-electric tensor elements. It was found that this particular class of TICT chromophores exhibited nonlinear refraction that was predominantly excited by two-photon-excited-state processes with comparatively small contributions from second-order hyperpolarizability. This behavior was attributed to orbitals of the stilbene fragment which led to significant 2-photon absorption (2PA).

DA Z-scans were performed at 800, 1100, and 1300 nm to characterize the spectral response of the third- and fifth-order nonlinear response of the TICT chromophores provided by Northwestern University. Figure 40 shows signals from open aperture (OA) and closed aperture (CA) Z-scans after removing the effect of the OA (CA/OA) at 1100 nm. Figure 40(c) also reveals a dependence of the peak-valley normalized nonlinear refraction signal on fluence. This dependence verified that fifth-order nonlinearities contributed significantly to this response, confirming that the nonlinear properties of TICT chromophores were dominated by excited state nonlinear refraction following 2-photon absorption.

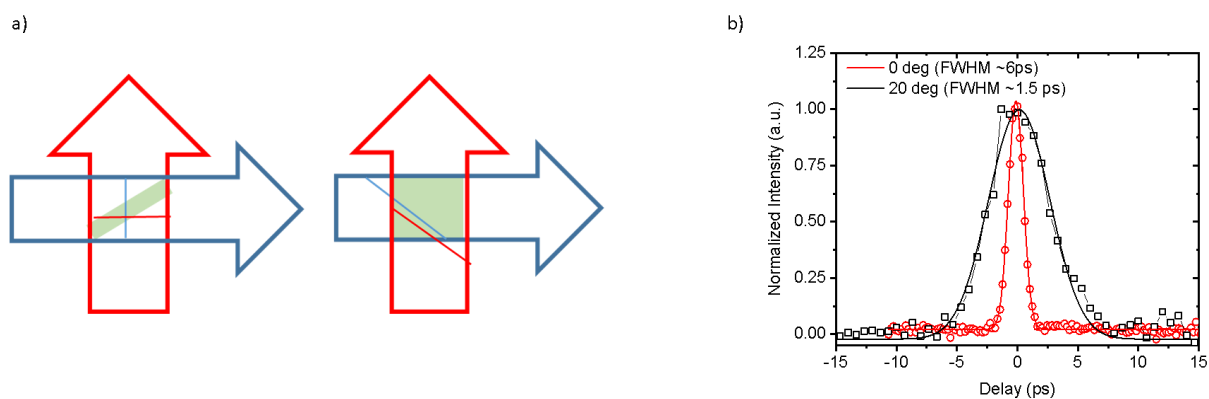


Figure 39. (a) The interaction geometry and effect of wavefront tilt in spatio-temporal interaction, (b) experimental observation of the optimization of the cross-correlation width.

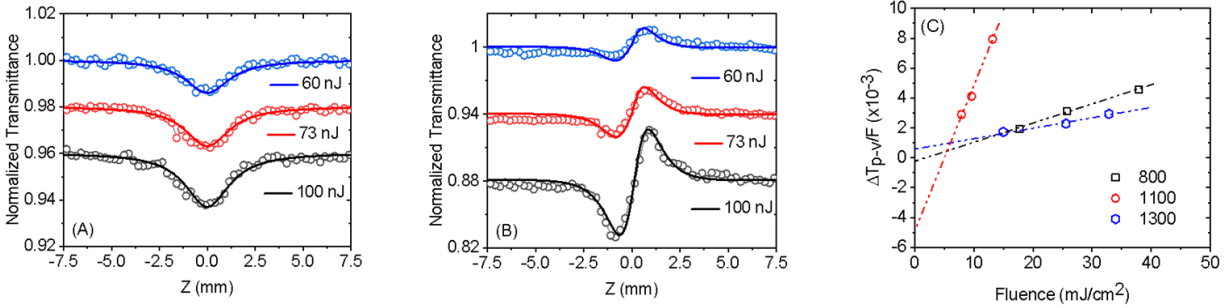


Figure 40. (a) OA, (b) CA/OA at 1100 nm measured via dual arm Z-scan. (c) The fluence dependence of the peak-valley normalized signal for different wavelengths.

2.6. Angular Momentum Theory and Dual Field Interactions

RIKEN, Saitama, Japan (Franco Nori)

Theoretical research at RIKEN focused on the analysis of dual field interactions and parity-time (P-T) symmetry in optical systems. P-T symmetric systems are ones in which parity and time symmetries are individually broken but leave a system invariant when considered together. In such systems, novel optical functionality can be encountered as the result of this unusual symmetry itself or through the coupling of various forms of angular momentum. The main advances contributed by this task consisted of linking angular momentum properties of light to magneto-electric effects. It went on to investigate angular momentum at surfaces, discovering new Hall effects and finding analogies to the properties of topologically-protected optical systems. These efforts drew the topic of magneto-electric interactions much closer to two fields of great current interest, namely generalized Hall effect theory and topological insulators.

In several highly cited publications of 2014, Franco Nori and his collaborators reported results on P-T symmetry in optics with strong relevance to non-reciprocal (magneto-electric) optical devices. One advance was analysis of the relativistic optical Hall effect. This work explained how at relativistic intensities a transverse Hall field arises through symmetry-breaking by the Lorentz force. This was closely related to the report of dynamic symmetry-breaking in the theories of magneto-electric interactions from Rand's group at UM. Magneto-electric processes were shown to be P-T symmetric. Nori's team also investigated novel examples of symmetry-breaking at interfaces where it was predicted that evanescent waves can carry spin that is transverse rather than longitudinal. This finding, referred to as the quantum spin Hall effect of light, uncovered previously unknown angular momentum properties of light at interfaces. RIKEN research noted that in evanescent fields light acquires transverse spin, altering the usual longitudinal spin associated with photon propagation in free space. This fundamental advance contributed importantly to unifying the new phenomena of interest in our MURI research with more established topics in conventional nonlinear optics.

Propagating optical waves (photons) ordinarily carry momentum and longitudinal spin determined by the wave vector and circular polarization, respectively. Nori and colleagues showed that exactly the opposite was the case for evanescent optical waves at interfaces (Figure 41). A single evanescent wave possesses a spin component, which is independent of the polarization and is orthogonal to the wave vector. Furthermore, such a wave carries a momentum component, which is determined by the circular polarization and is also orthogonal to the wave vector. These extraordinary properties reveal a fundamental Belinfante's spin momentum, previously known in field theory but absent in propagating fields. The effort at RIKEN

demonstrated that the spin momentum transverse to the boundary can theoretically push and twist probe particles in non-propagating, evanescent fields.

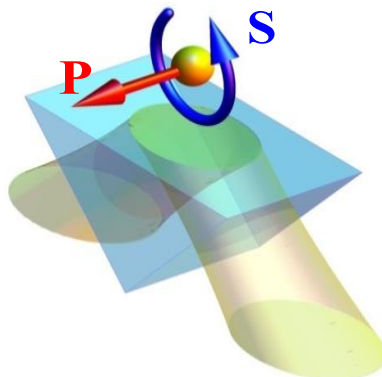


Figure 41. Extraordinary momentum and spin in evanescent waves. In sharp contrast to the usual electromagnetic waves (photons), evanescent waves possess transverse helicity-dependent momentum P and transverse helicity-independent spin S .

Wide-ranging investigations by RIKEN researchers on the coupling between electric and magnetic properties of both light and matter led to other important developments and device technology as part of this program. In particular, non-reciprocal transmission was demonstrated in coupled micro-cavities that were adjusted to balance optical gain and loss. By operating at exceptional points in P-T symmetric arrays of paired micro-cavities (Figure 42), Nori and collaborators demonstrated non-reciprocal transmission by balancing gain and loss to obtain P-T symmetry in their micro-cavities. The addition of loss to the system permitted tuning the coupled cavities to so-called exceptional points where broken symmetry could be realized. This gave rise to non-reciprocal behavior (uni-directional transmission) in a non-magnetic system. They also reported the paradoxical reduction of absorptive loss by increasing optical coupling losses in arrays of coupled whispering gallery micro-cavities. (See Publications)

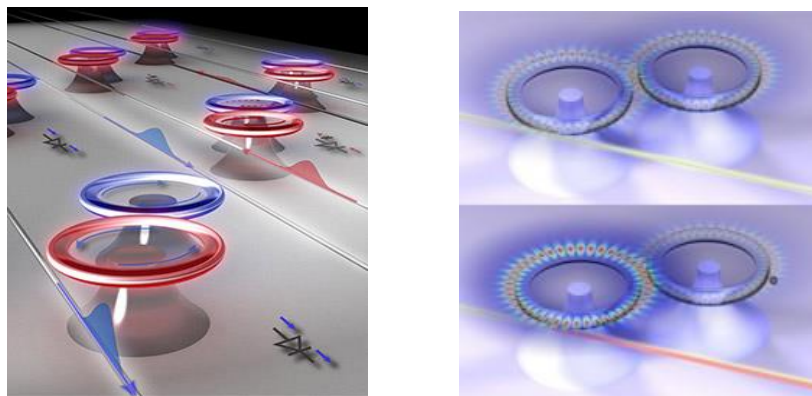


Figure 42. Parity-Time (PT) Symmetric Photonics. (Left) Optical diode produces nonreciprocal light transmission as the result of PT-symmetric coupled cavities. (Nori et al., Nature Physics 10, 394(2014)) (Right) Winning by losing: PT-symmetric waveguide structures can paradoxically reverse the effect of absorptive loss by introducing more loss. (Nori et al., Science 346, 328(2014)).

2.7. Summary

This MURI research project was established to investigate magneto-electric phenomena at the molecular level and to evaluate their possible utility for energy conversion. While M-E processes are well-known in bulk magnetic material, and have been studied for energy conversion and sensor technology, magneto-electric rectification, magnetization and harmonic generation at the molecular level can arise in non-magnetic materials and have not previously been investigated in any detail. The three nonlinear optical phenomena at the core of this program are unique in their dependence on the magnetic (Lorentz) force of light under non-relativistic conditions (i.e. at intensities $< 10^{18}$ W/cm²). While magneto-optic effects are generally expected to be extremely weak at low intensities, this project found that parametric resonance and the dynamic exchange of orbital and rotational angular momenta could intensify nonlinearities mediated by the optical Lorentz force. This picture was confirmed experimentally and the project was successful in elucidating the mechanism of nonlinear enhancement. More specifically, spectra of magneto-electrically scattered light revealed rotational features that confirmed the importance of librational motion and low libration frequencies in magneto-electric transitions at the molecular level. The program also developed three different analytic approaches to understand charge separation, magnetization, and harmonic generation and provided a reliable platform for predicting their applications. Predictive tools comprised a classical torque model, an exact dressed state analysis, and a density matrix treatment which displayed the dependences of M-E processes on transition moments, detuning, relaxation rates, intensity, and polarization.

Through efforts at the collaborating institutions - the University of Michigan, Northwestern University, Stanford University, RIKEN in Japan, and the University of Central Florida - magneto-electric interactions were investigated in simple molecules, oriented polymers, macromolecules, and solids. Material synthesis played a key role in providing not only several series of compounds that systematically varied the librational frequencies of M-E samples to confirm key theoretical expectations but also optimized charge separation and magnetization response. An important milestone of the program was the demonstration of quantitative agreement between experiment and theory regarding the magnitude of magneto-electric magnetization in a series of tetrahalide liquids. Subsequently it was found that solids with optical transitions near the wavelength of incident light gave the highest response at the lowest intensities. In undoped fused quartz, at visible wavelengths far from any electronic resonances and at an intensity of only 5×10^9 W/cm², the magnetic moments induced by light were shown to equal the electric dipole moments responsible for Rayleigh scattering. This observation reflected an unprecedented strength of magneto-electric processes compared to all-electric processes driven by light under non-relativistic conditions. Another milestone was the successful linkage of even-order, magneto-electric susceptibilities to odd-order, all-electric susceptibilities of conventional nonlinear optics. This relationship between nonlinear processes relying on an axial field (the H field) versus those that do not was hitherto unknown in nonlinear optics. One of the unique outcomes of it is that light-by-light switching becomes possible in a new geometry involving light beams propagating at right angles to one another. Thus, it seems likely that this research will spawn new device technology inspired by magneto-electric photonics. Finally the research reported here has confirmed that M-E charge separation at intensities of $\sim 10^8$ - 10^9 W/cm² in many materials could support fast, efficient energy conversion without substantial heat generation to support future mission capabilities.

3. Cumulative List of MURI Awards & Honors

November 2019: Franco Nori was selected for the 2018 Clarivate Analytics Highly Cited Researcher list. This list identifies the top 1% of researchers based on citations in their field. The Web of Science sponsors this evaluation.

November 2018: Franco Nori was selected for the 2017 Clarivate Analytics Highly Cited Researcher list.

November 2017: Franco Nori was selected for the 2016 Clarivate Analytics Highly Cited Researcher list.

September 2018: Stephen Rand elected Fellow of the American Physical Society

May 2018: Stephen Rand elected Fellow of the Institute of Physics (United Kingdom)

November 2017: Franco Nori was selected for the 2017 Clarivate Analytics Highly Cited Researcher list. This list identifies the top 1% of researchers based on citations in their field. The Web of Science sponsors this evaluation.

2016: Franco Nori elected as Foreign Member of the Swedish Royal Society of Arts and Sciences, in Gothenburg, Sweden

July 2015: Tobin Marks awarded the 2014 Sir Geoffrey Wilkinson Award for pioneering organometallic chemistry, particularly with regard to catalysis, and is awarded by the Royal Society of Chemistry.

May 2015: Tobin Marks awarded the 2015 Luigi Sacconi Medal of the Italian Chemical Society. The award recognizes outstanding research in the field of inorganic chemistry and was awarded at the annual meeting of the Italian Chemical Society in Camerino Italy in September.

May 2015: Tony F. Heinz was a Plenary Speaker discussing “Electrons in Atomically Thin Two-Dimensional Crystals” at CLEO/QELS in San Jose, CA.

April 2015: DYNAMO Graduate Student Brad Smith awarded two prestigious fellowships; [1] University of Michigan Dow Sustainability Fellowship and [2] a National Science Foundation Graduate Research Fellowship!

February 2015: Stephen Rand received the Outstanding Achievement Award from the EECS Department at the University of Michigan.

October 2014: Franco Nori elected Fellow of the Optical Society of America for “fundamental contributions to quantum information science and optics, including circuit quantum electrodynamics, and the interface between quantum optics and quantum circuits”

May 2014: Fred Adams awarded a Collegiate Professorship by the College of Literature, Science & the Arts at the University of Michigan

April 2014: Stephen Rand awarded Distinguished Honorary Professorship in Applied Science at Amity University Gurgaon, India

March 2014: T.F. Heinz awarded APS Frank Isakson Prize for Optical Effects in Solids

February 2014: S.C. Rand awarded J. Erskine Professorship at the University of Canterbury, Christchurch, NZ

February 2014: S.C. Rand awarded APS-IUSSTF Fellowship by the American Physical Society

January 2014: S.C. Rand invited as Distinguished Lecturer at Institute of IIT-Kharagpur, India

January 2014: S.C. Rand awarded OSA Travelling Fellowship to visit IIT-Kharagpur, IIT-Delhi, IIT-Bhubaneswar, IITK, & Amity universities in India

4. Cumulative List of MURI Publications

4.1. Journal Articles

2020:

G. Smail and S.C. Rand, Magneto-electric Phenomena in Atoms and Molecules, Reviews of Modern Physics (to be published).

A. J.-T. Lou, S. Benis, M. Gao, A. Baev, D. Kim, E. W. Van Stryland, D. J. Hagan, T. J. Marks. Third and Fifth Order Nonlinear Optical Response of a TICT/Stilbene Hybrid Chromophore, J. Phys. Chem. C, 2020. <https://pubs.acs.org/doi/10.1021/acs.jpcc.9b11735>

M. Tuan Trinh, Gregory Smail, Krishnandu Makhal, Da S. Yang, Jinsang Kim, and Stephen C. Rand, Observation of Magneto-Electric Rectification at Non-relativistic Intensities, Nature Communications (submitted).

Da Seul Yang, Kyeongwoon Chung, Jinsang Kim “Controlled Alignment of Polymer Chain Near the Semiconductor-Dielectric Interface” Organic Electronics 76, 105484(2020).

2019:

Kyeongwoon Chung, Da Seul Yang, Woo-Hwan Sul, Bong-Gi Kim, Jongho Kim, Geunseok Jang, Min Sang Kwon, Maciej Barlog, Taek Seung Lee, Soo-Young Park, Mohammed Al-Hashimi, Jinsang Kim “Molecular Design Approach for Directed Alignment of Conjugated Polymers” Macromolecules 52, 6485(2019).

M.T. Trinh, K. Makhal, E. Dreyer, A. Shanker, S. Yoon, J. Kim, S. Rand, “Optical torque induces magnetism at the molecular level”, Opt. Express 27, 21295 (2019)

J. Guan, K. Tomobe, I. Madu, T. Goodson III, K. Makhal, M.T. Trinh, S.C. Rand, N. Yodsudin, S. Jungstittiwong, R.L. Laine, “Photophysical properties of partially functionalized phenylsilsesquioxanes: [RSiO_{1.5}]₇[Me/nPrSiO_{1.5}] and [RSiO_{1.5}]₇[O_{0.5}SiMe₃]₃ (R = 4-Me/4-CN-stilbene)”, Macromolecules 52, 4008(2019).

Lou, A.; Marks, T.J. Nonlinear Optical Response of π -Twisted Chromophores (Submitted for publication)

K.Y. Bliokh, F. Nori, “Transverse spin and surface waves in acoustic metamaterials” Phys. Rev. B 99, 020301(R) (2019).

T. Liu, Y.R. Zhang, Q. Ai, Z. Gong, K. Kawabata, M. Ueda, F. Nori, “Second-Order Topological Phases in Non-Hermitian Systems”, Phys. Rev. Lett. (2019).

K.Y. Bliokh, D. Leykam, M. Lein, F. Nori, “Topological non-Hermitian origin of surface Maxwell waves”, Nature Communications (2019).

S.K. Ozdemir, S. Rotter, F. Nori, L. Yang, “Parity-time Symmetry and Exceptional Points in Photonics”, *Nature Materials* (2019).

Lou, A.; Marks, T.J. Nonlinear Optical Response of π -Twisted Chromophores (submitted for publication).

Lou, A.; Benis, S.; Guo, M.; Baev, A.; Prasad, P.N.; Van Stryland. E.W.; Hagan, D.J.; Marks, T.J. Enhancing the Dipolar Contribution of Extended Twisted Chromophores for Increasing Third-order Optical Nonlinearity (Manuscript in preparation).

Pati, S.; Marks, T.J.; Calculation of Magneto-Electric Coefficients from the Many Body Electronic Hamiltonians (Manuscript in preparation).

Lou, A.; Benis, S.; Guo, M.; Baev, A.; Prasad, P.N.; Van Stryland. E.W.; Hagan, D.J.; Marks, T.J. Enhancing the Dipolar Contribution of Extended Twisted Chromophores for Increasing Third-order Optical Nonlinearity (Manuscript in preparation).

E. Barre, J. A. Incorvia, S. H. Kim, C. J. McClellan, E. Pop, H. P. Wong, and T. F. Heinz, “Spatial Separation of Carrier Spin by the Valley Hall Effect in Monolayer WSe₂ Transistors,” *Nano Lett.* 19, 770–774 (2019).

2018:

Da S. Yang, M. Barlog, J. Park, K. Chung, A. Shanker, J. Sun, J. Kang, K. Lee, M. Al-Hashimi, J. Kim “Alignment of Lyotropic Liquid Crystalline Conjugated Polymer in Floating Film” *ACS Omega* 3, 14807(2018).

Lou, A.; Cariati, E.; Barger, C.; Zuccaccia, C.; Macchioni, A.; Marks, T.J. Unprecedented Large Hyperpolarizability of Twisted Chromophores in Polar Media. *J. Am. Chem. Soc.* 2018, 140, 8746-8755. DOI: 10.1021/jacs.8b04320

Lou, A.; Cariati, E.; Zuccaccia, C.; Macchioni, A.; Marks, T.J. “Organic Salts Suppress Aggregation and Enhance the Hyperpolarizability of a π - Twisted Chromophore”, *Chem. Eur. J.* 2018, 24, 15801-15805. DOI:10.1002/chem.201804365

K.Y. Bliokh, F.J. Rodríguez-Fortuño, A.Y. Bekshaev, Y.S. Kivshar, F. Nori, “Electric-current-induced unidirectional propagation of surface plasmon-polaritons”, *Optics Letters* 43, pp. 963-966 (2018).

D.A. Smirnova, V.M. Travin, K.Y. Bliokh, F. Nori, “Relativistic spin-orbit interactions of photons and electrons”, *Phys. Rev. A* 97, 043840 (2018).

F. Quijandría, U. Naether, S.K. Ozdemir, F. Nori, D. Zueco, “PT-symmetric circuit QED”, *Phys. Rev. A* 97, 053846 (2018).

- F. Alpeggiani, K.Y. Bliokh, F. Nori, L. Kuipers, “Electromagnetic Helicity in Complex Media”, *Phys. Rev. Lett.* 120, 243605 (2018).
- Y.R. Zhang, Y. Zeng, H. Fan, J.Q. You, F. Nori, “Characterization of Topological States via Dual Multipartite Entanglement”, *Phys. Rev. Lett.* 120, 250501 (2018).
- S. Maayani, R. Dahan, Y. Kligerman, E. Moses, A.U. Hassan, H. Jing, F. Nori, D.N. Christodoulides, T. Carmon, “Flying couplers above spinning resonators generate irreversible refraction”, *Nature* 558, pp. 569–572 (2018).
- J. Zhang, B. Peng, S.K. Ozdemir, K. Pichler, D.O. Krimer, G. Zhao, F. Nori, Y.X. Liu, S. Rotter, L. Yang, “A phonon laser operating at an exceptional point”, *Nature Photonics* 12, pp. 479–484 (2018).
- M.F. Picardi, K.Y. Bliokh, F.J. Rodríguez-Fortuño, F. Alpeggiani, F. Nori, “Angular momenta, helicity, and other properties of dielectric-fiber and metallic-wire modes”, *Optica* 5, pp. 1016–1026 (2018).
- R. Huang, A. Miranowicz, J.Q. Liao, F. Nori, H. Jing, “Nonreciprocal Photon Blockade”, *Phys. Rev. Lett.* 121, 153601 (2018).
- H. Jing, H. Lu, S.K. Ozdemir, T. Carmon, F. Nori, “Nanoparticle sensing with a spinning resonator”, *Optica* 5, pp. 1424–1430 (2018).
- K. Xia, F. Nori, M. Xiao, “Cavity-Free Optical Isolators and Circulators Using a Chiral Cross-Kerr Nonlinearity”, *Phys. Rev. Lett.* 121, 203602 (2018).
- Y. Jiang, S. Maayani, T. Carmon, F. Nori, H. Jing, “Nonreciprocal Phonon Laser”, *Phys. Rev. Applied* 10, 064037 (2018).
- J. K. Kim, X. Shi, M. J. Jeong, J. Park, H. S. Han, S. H. Kim, Y. Guo, T. F. Heinz, S. Fan, C.-L. Lee, J. H. Park, and X. Zheng, “Enhancing Mo:BiVO₄ Solar Water Splitting with Patterned Au Nanospheres by Plasmon-Induced Energy Transfer,” *Adv. Energy Mater.* 8, 1701765 (2018).
- Y. D. Kim, Y. Gao, R.-J. Shiue, L. Wang, O. B. Aslan, M.-H. Bae, H. Kim, D. Seo, H.-J. Choi, S. H. Kim, A. Nemilentsau, T. Low, C. Tan, D. K. Efetov, T. Taniguchi, K. Watanabe, K. L. Shepard, T. F. Heinz, D. Englund, and J. Hone, “Ultrafast graphene light emitters,” *Nano. Lett.* 18, 934–940 (2018).
- P. Gallagher, Y. Li, K. Watanabe, T. Taniguchi, T. F. Heinz, and D. Goldhaber-Gordon, “Optical Imaging and Spectroscopic Characterization of Self-Assembled Environmental Adsorbates on Graphene,” *Nano. Lett.* 18, 2603–2608 (2018).
- O. B. Aslan, I. M. Datye, M. J. Mleczko, K. S. Cheung, S. Krylyuk, A. Bruma, I. Kalish, A. V. Davydov, E. Pop, and T. F. Heinz, “Probing the Optical Properties and Strain-Tuning of Ultrathin Mo_{1-x}W_xTe₂,” *Nano Lett.* 18, 2485 (2018).

K. K. H. Smithe, A. V. Krayev, C. S. Bailey, H. R. Lee, E. Yalon O. B. Alsan, M. Muñoz Rojo, S. Krylyuk, P. Taheri, A. V. Davydov, T. F. Heinz, and E. Pop, "Nanoscale Heterogeneities in Monolayer MoSe₂ Revealed by Correlated Scanning Probe Microscopy and Tip-Enhanced Raman Spectroscopy," *ACS Appl. Nano Mater.* **1**, 572-579 (2018).

Y. Li and T. F. Heinz, "Two-dimensional models for the optical response of thin films," *2D Mater.* **5**, 025021 (2018).

2017:

Kyeongwoon Chung, Da Seul Yang, Geunseok Jang, Bong-Gi Kim, Min Sang Kwon, Taek Seung Lee, Jinsang Kim "Molecular Design Principle for Directed Alignment of Conjugated Polymers" (in preparation).

X.-X. Zhang, T. Cao, Z. Lu, Y.-C. Lin, F. Zhang, Y. Wang, Z. Li, J. Hone, J. A. Robinson, D. Smirnov, S. G. Louie, T. F. Heinz, "Magnetic brightening and control of dark excitons in monolayer WSe₂," *Nature Nanotech.* **12**, 883–888 (2017).

Y. Li and T. F. Heinz, "Two-dimensional models for the optical response of thin films," *2D Materials* (in press).

P. Gallagher, Y. Li, K. Watanabe, T. Taniguchi, T. F. Heinz, and D. Goldhaber-Gordon, "Optical imaging and spectroscopic characterization of self-assembled environmental adsorbates on graphene," *Nano Letters* (in review).

Z. Ye, L. Waldecker, E. Y. Ma, D. Rhodes, A. Antony, B. Kim, J. Ardelean, X.X. Zhang, M. Deng, Y. Jiang, Z. Lu, D. Smirnov, K. Watanabe, T. Taniguchi, J. Hone, and T. F. Heinz, "Spin-valley configuration of the natural biexciton in WSe₂ monolayers" (in preparation).

A. Lou, S. Benis, M. Gao, A. Baev, P.N. Prasad, E.W. Van Stryland, D.J. Hagan, T.J. Marks, "Enhancing the Dipolar Contribution of Extended Twisted Chromophores for Increasing Third-order Optical Nonlinearity" (in preparation).

M.Cirio, K. Debnath, N. Labert, F. Nori, "Amplified Optomechanical Transduction of Virtual Radiation Pressure", *Phys. Rev. Lett.* **119**, 053601 (2017).

K.Y. Bliokh, A.Y. Bekshaev, F. Nori, "Optical Momentum, Spin, and Angular Momentum in Dispersive Media", *Phys. Rev. Lett.* **119**, 073901 (2017).

K.Y. Bliokh, M.R. Dennis, F. Nori, "Position, spin, and orbital angular momentum of a relativistic electron", *Phys Rev. A* **96**, 023622 (2017).

H. Lu, S.K. Ozdemir, L.M. Kuang, F. Nori, H. Jing, "Exceptional Points in Random-Defect Phonon Lasers", *Phys. Rev. Applied* **8**, 044020 (2017).

K.Y. Bliokh, A.Y. Bekshaev, F. Nori, "Optical momentum , Spin, and Angular Momentum in Dispersive Media", *Phys. Rev. Lett.* 119, 073901 (2017).

K.Y. Bliokh, A.Y. Bekshaev, F. Nori, "Optical momentum and angular momentum in complex media: from the Abraham-Minkowski debate to unusual properties of surface plasmon-polaritons", *New Journal of Physics* 19, 123014 (2017).

H. Jing, S.K. Ozdemir, H. Lu, F. Nori, "High-order exceptional points in optomechanics", *Scientific Reports* 7, 3386 (2017).

Y.L. Liu, R. Wu, J. Zhang, S.K. Ozdemir, L. Yang, F. Nori, Y.X. Liu, "Controllable optical response by modifying the gain and loss of a mechanical resonator and cavity mode in an optomechanical system", *Phys. Rev. A* 95, 013843 (2017).

H. Chandralalim, S.C. Rand, and X. Fan, "Evanescent coupling between refillable ring resonators and laser-inscribed optical waveguides", *Advanced Optical Materials*, 56, 16, 4750-4756 (2017).

Alexander J.-T. Lou, Elizabeth F.C. Dreyer, Stephen C. Rand, Tobin J. Marks, "Molecular Design Principles for Magneto-Electric Materials: All-Electric Susceptibilities relevant to Optimal Molecular Chromophores", *J. Phys. Chem*, 121, 16491-16500. (2017).

E.F.C. Dreyer, A.A. Fisher, P. Anisimov and S.C. Rand, "Optical Magnetization Part III: Theory of Molecular Magneto-electric Rectification", *Opt Express* (in preparation).

S. Benis, D.J. Hagan, E.W. Van Stryland, "Cross-propagating Beam-Deflection measurements of third-order nonlinear optical susceptibility", *SPIE proceedings*, Volume 10088, 2017.

D. Leykam, K.Y. Bliokh, C. Huang, Y.D. Chong, F. Nori, "Edge Modes, Degeneracies, and Topological Numbers in Non-Hermitian Systems", *Phys. Rev. Lett.* 118, 040401 (2017).

A.V. Rozhkov, A.O. Sboychakov, A.L. Rakhmanov, F. Nori, "Single-electron gap in the spectrum of twisted bilayer graphene", *Phys. Rev. B* 95, 045119 (2017).

A.O. Sboychakov, A.L. Rakhmanov, K.I. Kugel, A.V. Rozhkov, F. Nori, "Magnetic field effects in electron systems with imperfect nesting", *Phys. Rev. B* 95, 014203 (2017).

Wang, Xin., Miranowicz, Adam., Li, Hong-Rong., Nori, Franco, "Hybrid quantum device with a carbon nanotube and flux qubit for dissipative quantum engineering", *Phys. Rev. B* 95, 205415 (2017).

DiStefano, Omar., Stassi, Roberto., Garziano, Luigi., Kockum, Anton Frisk., Savasta, Salvatore., Nori, Franco., "Feynman-diagrams approach to the quantum Rabi model for ultrastrong cavity QED: stimulated emission and reabsorption of virtual particles dressing a physical excitation", *New J. Phys.* 19, 053010, (2017).

Yang, Chui-Ping., Su, Qi-Ping., Zheng, Shi-Biao., Nori, Franco., Han, Siyuan, "Entangling two oscillators with arbitrary asymmetric initial states" *Phys. Rev. A* 95, 052341 (2017).

Bliokh, K. Y., Ivanov, I.P., Guzzinati, G, Clark, L., Van Boxem, R., Beche, A., Juctmans, R., Alonso, M.A., Schattschneider, P., Nori, F., Verbeeck, J., "Theory and applications of free-electron vortex states", *Physics Report* 690, 1-70 (2017).

Chen, S.L., Lambert, N., Li, C.M., Chen, G.Y., Chen, Y.N., Miranowicz, A., Nori, F., "Spatio-Temporal Steering for Testing Nonclassical Correlations in Quantum Networks", *Scientific Reports* 7, 3728 (2017).

Kockum, A.F., Miranowicz, A., Macri, V., Savasta, S., Nori, F., "Deterministic quantum nonlinear optics with single atoms and virtual photons", *Phys. Rev. A* 95, 063849 (2017).

Qin, W., Wang, X., Miranowicz, A., Zhong, Z., Nori, F., "Heralded quantum controlled -PHASE gates with dissipative dynamics in macroscopically distant resonators", *Phys. Rev. A* 96, 012315 (2017).

Chen, Z., Wang, Y., Li, T., Tian, L., Qiu, Y., Inomata, K., Yoshihara, F., Han, S., Nori, F., Tsai, J.S., You, J.Q., "Single-photon-driven high-order sideband transitions in an ultrastrongly coupled circuit-quantum-electrodynamics system", *Phys. Rev. A* 96, 0123325 (2017).

Cirio, M., Debnath, K., Lambert, N., Nori, F., "Amplified Optomechanical Transduction of Virtual Radiation Pressure", *Phys. Rev. Lett.* 119, 053601 (2017).

Stassi, R., Macri, V., Kockum, A.F., DiStefano, O., Miranowicz, A., Savasta, S., Nori, F., "Quantum nonlinear optics without photons", *Phys. Rev. A* 96, 023818 (2017).

2016:

Chandralalim H., Rand S., Fan X., "Fusion of Renewable Ring Resonator Lasers and Ultrafast Laser Inscribed Photonic Waveguides", *Scientific Reports*, 6, 32668 (2016).

Teran, N.B., He, G.S., Baev, A., Shi, Y., Swihart, M.T., Prasad, P.N., Marks, T.J. Reynolds, J.R., "Balancing Structural Extremes: Enhancing Intramolecular Charge Transfer in Twisted Thiophene-Based Aromatic/Quinoid Chromophores", *J. Am. Chem. Soc.* 2016, 138, 6975-6984. DOI: 10.1021/jacs.5b12457. (2016).

S.C. Rand, "Lectures on Light: The Density Matrix in Nonlinear and Quantum Optics", Second Edition, Oxford University Press, Oxford, 2016.

A.A. Fisher, E.F.C. Dreyer A. Chakrabarty and S.C. Rand, "Optical magnetization, Part I: Experiments on radiant optical magnetization in solids", *Optics Express*, 24, Issues 23, pp. 26055-26063 DOI: 10.1364/OE.24.026064. (2016).

A.A. Fisher, E.F.C. Dreyer A. Chakrabarty and S.C. Rand, "Optical magnetization, Part II: Theory of induced optical magnetism", *Optics Express*, 24, Issues 23, pp. 26064-26079 DOI: 10.1364/OE.24.026055. (2016).

B.C. Smith, J.F. Whitaker and S.C. Rand, "Steerable THz pulses from thin emitters via optical pulse-front tilt", *Optics Express*, 24, Issue 18, pp. 20755-20762 DOI: 10.1364/OE.24.020755. (2016).

Teran, N.B., He, G. S., Baev, A., Shi, Y., Swihart, M.T., Prasad, P.N., Marks, T.J., Reynolds, J.R., "Balancing Structural Extremes: Enhancing Intramolecular Charge Transfer in Twisted Thiophene-Based Aromatic/Quinoid Chromophores ", *J. Am. Chem. Soc.* 138, 6975-6984. DOI: 10.1021/jacs.5b12457 (2016).

Bloch, A.M., Adams, F.C., Gupta, R. and Razavi, H. "Coupled Hill's equations and the Lorentz Oscillator Model", *Oberwolfach Reports* (2016).

Razavi, H., Adams, F.C., Bloch, A.M., Gupta, R. and Razavi, H. "Stability of Coupled Hill's Equations and the Lorentz Oscillator Model," *SIAM J Dyn Syst*, 15, 2, 1104-1123. <https://doi.org/10.1137/15M1033228> (2016).

J. Fan, Y. Chen, G. Chen, L. Xiao, S. Jia, F. Nori, "Electric-field-induced interferometric resonance of a one-dimensional spin-orbit-coupled electron", *Scientific Reports* 6, 38851 (2016).

K. Bartkiewicz, A. Cernoch, K. Lemr, A. Miranowicz, F. Nori, "Experimental temporal quantum steering", *Scientific Reports* 6, 38076 (2016).

M. Asano, K.Y. Bliokh, Y.P. Bliokh, A.G. Kofman, R. Ikuta, T. Yamamoto, Y.S. Kivshar, L. Yang, N. Imoto, S.K. Ozdemir, F. Nori, "Anomalous time delays and quantum weak measurements in optical micro-resonators", *Nature Communications* 7, 13488 (2016).

Z.P. Liu, J. Zhang, S.K. Ozdemir, B. Peng, H. Jing, X.Y. Lu, C.W. Li, L. Yang, F. Nori, Y.X. Liu, "Metrology with PT-Symmetric Cavities: Enhanced Sensitivity near the PT-Phase Transition", *Phys. Rev. Lett.* 117, 110802 (2016).

R.S. Akzyanov, A.L. Rakhmanov, A.V. Razhkov, F. Nori, "Tunable Majorana fermion from Landau quantization in 2D topological superconductors", *Phys. Rev. B* 94, 125428 (2016).

K.Y. Bliokh, C.T. Samlan, C. Prajapati, G. Puentes, N.K. Viswanathan, F. Nori, "Spin-Hall effect and circular birefringence of a uniaxial crystal plate", *Optica* 3, 10 pp. 1039-1047 (2016).

C.P. Yang, Q.P. Su, S.B. Zheng, F. Nori, "Crosstalk-insensitive method for simultaneously coupling multiple pairs of resonators", *Phys. Rev A.*, 93, 042307 (2016).

F. Monifi, J. Zhang, S.K. Ozdemir, B. Peng, Y.X. Liu, F. Bo, F. Nori, L. Yang, "Optomechanically induced stochastic resonance and chaos transfer between optical fields", *Nature Photonics* 10, 399-405 (2016).

M. Antognozzi, C.R. Bermingham, R.L. Harnman, S. Simpson, J. Senior, R. Hayward, H. Hoerber, M.R. Dennis, A.Y. Bekshaev, K.Y. Bliokh, F. Nori, "Direct measurements of the extraordinary optical momentum and transverse spin-dependent force using a nano-cantilever", *Nature Physics* 12, 731-735 (2016).

2015:

H. Jing, S.K. Ozdemir, Z. Geng, J. Zhang, X.Y. Lu, B. Peng, L. Yang, F. Nori, "Optomechanically-Induced Transparency in parity-time-symmetric microresonators", *Scientific Reports* 5, 9663 (2015).

J. Dressel, K.Y. Bliokh, F. Nori, "Spacetime algebra as a powerful tool for electromagnetism", *Physics Reports* 589, 1-71 (2015).

J. Zhang, B. Peng, S.K. Ozdemir, Y.X. Liu, H. Jing, X.Y. Lu, Y.L. Liu, L. Yang, F. Nori, "Giant nonlinearity via breaking parity-time symmetry: A route to low-threshold phonon diodes", *Phys Rev B* 92, 115407 (2015).

K.Y. Bliokh, F. J. Rodriguez-Fortuno, F. Nori, A.V. Zayats, "Spin-orbit interactions of light", *Nature Photonics* 9, 796-808 (2015).

X.Y. Lu, Y. Wu, J.R. Johansson, H. Jing, J. Zhang, F. Nori, "Squeezed Optomechanics with Phase-matched Amplification and Dissipation", *Phys. Rev. Lett.* 114, 093602 (2015).

(Invited) M. Bass and S.C. Rand, "Linear and Nonlinear Laser Spectroscopy", in *OSA Century of Optics*, Optical Society of America, 2015, pp. 218-222. (2015).

(Invited) S.C. Rand, "One Hundred Years of Laser Spectroscopy at the Optical Society of America", online in *Centennial History of OSA*, 2015.

Shi, Y.; He, G.S.; Lou, A.; Baev, A.; Swihart, M.T.; Prasad, P.N; Marks, T.J., "Cooperative Coupling of Cyanine and Tictoid Twisted- π -Systems to Amplify Organic Chromophore Cubic Nonlinearities", *J. Am. Chem. Soc.* 2015, 137, 4622-4625. DOI: 10.1021/jacs.5b01042. (2015).

Shi, Y.; Frattarelli, D.; Watanabe, N.; Facchetti, A.; Cariati, E.; Righetto, S.; Tordin, E.; Zuccaccia, C.; Macchioni, A.; Wegener, S.L.; Stern, C.L.; Ratner, M.A.; Marks, T.J., "Ultra-High Response Multi- Twisted Electro-Optic Chromophores: Influence of π -System Elongation and Interplanar Torsion on Hyperpolarizability", *J. Am. Chem. Soc.* 2015, 137, 12521-12538. DOI: 10.1021/jacs.5b04636.

A.Y. Bekshaev, K.Y. Bliokh, F. Nori, "Transverse Spin and Momentum in Two-Wave Interference", *Phys. Rev. X* 5, 011039 (2015).

X.Y. Lü, J.Q. Liao, L. Tian, F. Nori, "Steady-state mechanical squeezing in an optomechanical system via Duffing nonlinearity", *Phys. Rev. A* 91, 013834 (2015).

K.Y. Bliokh, F. Nori, "Transverse and longitudinal angular momenta of light", *Phys. Rep.* 592, 1-38 (2015).

K.Y. Bliokh, D. Smirnova, F. Nori, "Quantum spin Hall effect of light *Science*", 348, 1448-1451 (2015).

J.Q. Liao, C.K. Law, L.M. Kuang, F. Nori, "Enhancement of mechanical effects of single photons in modulated two-mode optomechanics", *Phys. Rev. A* 92, 013822 (2015).

X.Y. Lü, Y. Wu, J.R. Johansson, H. Jing, J. Zhang, F. Nori, "Squeezed Optomechanics with Phase-matched Amplification and Dissipation", *Phys. Rev. Lett.* 114, 093602 (2015).

Y.P. Bliokh, V. Freilikher, Z. Shi, A.Z. Genack, F. Nori, "Hidden modes in open disordered media: analytical, numerical, and experimental results", *New J. Phys.* 17, 113009 (2015).

L.G. Mouroukh, F. Nori, "Energy transfer efficiency in the chromophore network strongly coupled to a vibrational mode", *Phys. Rev. E* 92, 052720 (2015).

J. Zhang, B. Peng, S.K. Ozdemir, Y.X. Liu, H. Jing, X.Y. Lu, Y.L. Liu, L. Yang, F. Nori "Giant nonlinearity via breaking parity-time symmetry: A route to low-threshold phonon diodes" *Phys. Rev. B* 92, 115407 (2015).

T. Gao, E. Estrecho, K.Y. Bliokh, T.C.H. Liew, M.D. Fraser, S. Brodbeck, M. Kamp, C. Schneider, S. Höfling, Y. Yamamoto, F. Nori, Y.S. Kivshar, A. Truscott, R. Dall, E.A. Ostrovskaya, "Observation of non-Hermitian degeneracies in a chaotic exciton-polariton billiard", *Nature* 526, 15522 (2015).

2014:

B. Peng, S.K. Ozdemir, W. Chen, F. Nori, L. Yang, "What is and what is not electromagnetically induced transparency in whispering-gallery microcavities", *Nature Communications* 5, 5082 (2014).

B. Peng, S. K. Ozdemir, S. Rotter, H. Yilmaz, M. Liertzer, F. Monifi, C. M. Bender, F. Nori, L. Yang, "Loss-induced suppression and revival of lasing", *Science* 346, 328-332 (2014).

K.Y. Bliokh, A.Y. Bekshaev, and F. Nori, "Extraordinary momentum and spin in evanescent waves", *Nature Communications* 5, 3300 (2014).

A.A. Fisher, E.F. Cloos, W.M. Fisher, and S.C. Rand, "Dynamic Symmetry-breaking in a Simple Quantum Model of Magneto-Electric Rectification, Optical Magnetization, and Harmonic Generation", *Optics Express* Vol. 22, No. 3, 2910 (2014).

J.R. Johansson, N. Lambert, I. Mahboob, H. Yamaguchi, F. Nori, "Entangled-state generation and Bell inequality violations in nanomechanical resonators", *Phys. Rev. B* 90, 174307 (2014).

- J.R. Johansson, G. Johansson, Franco Nori, “Optomechanical-like coupling between superconducting resonators”, *Phys. Rev. A* 90, 053833 (2014).
- T.N. Rokhmanova, S.S. Apostolov, Z.A. Maizelis, V.A. Yampol'skii, F. Nori, “Superposition principle for nonlinear Josephson plasma waves in layered superconductors”, *Phys. Rev. B* 90, 184503 (2014).
- A.M. Satanin, M.V. Denisenko, A.I. Gelman, F. Nori, “Amplitude and phase effects in Josephson qubits driven by a biharmonic electromagnetic field”, *Phys. Rev. B* 90, 104516 (2014).
- A. Miranowicz, J. Bajer, M. Paprzycka, Y.X. Liu, A.M. Zagorskin, F. Nori, “State-dependent photon blockade via quantum-reservoir engineering”, *Phys. Rev. A* 90, 033831 (2014).
- J.Q. Liao, F. Nori, “Single-photon quadratic optomechanics”, *Scientific Reports* 4, 6302 (2014).
- J.Q. Liao, F. Nori, “Spectrometric Reconstruction of Mechanical-motional States in Optomechanics”, *Phys. Rev. A* 90, 023851 (2014).
- H. Wang, X. Gu, Y.X. Liu, A. Miranowicz, F. Nori, “Optomechanical analog of two-color electromagnetically-induced transparency: Photon transmission through an optomechanical device with a two-level system”, *Phys. Rev. A* 90, 023817 (2014).
- P. Schattschneider, Th. Schachinger, M. Stoger-Pollach, S. Löffler, A. Steiger-Thirsfeld, K. Y. Bliokh, F. Nori, “Imaging the dynamics of free-electron Landau states”, *Nature Communications* 5, 4586 (2014).
- H. Jing, S.K. Ozdemir, X.Y. Lu, J. Zhang, L. Yang, F. Nori, “PT-Symmetric Phonon Laser”, *Phys. Rev. Lett.* 113, 053604 (2014).
- K.Y. Bliokh, Y. S. Kivshar, F. Nori, “Magnetoelectric Effects in Local Light-Matter Interactions”, *Phys. Rev. Lett.* 113, 033601 (2014).
- J.Q. You, Z.D. Wang, W. Zhang, F. Nori, “Encoding a qubit with Majorana modes in superconducting circuits”, *Scientific Reports* 4, 5535 (2014).
- L. Wang, L. N. Wu, W. Yang, G. R. Jin, N. Lambert, F. Nori, “Quantum Fisher information as a signature of the superradiant quantum phase transition”, *New J. Phys.* 16, 063039 (2014).
- H. Asai, Y. Ota, S. Kawabata, M. Machida, F. Nori, “Theory of macroscopic quantum tunneling with Josephson-Leggett collective excitations in multiband superconducting Josephson junctions”, *Phys. Rev. B* 89, 224507 (2014).
- P.K. Ghosh, P. Hanggi, F. Marchesoni, F. Nori, “Giant negative mobility of Janus particles in a corrugated channel”, *Phys. Rev. E* 89, 062115 (2014).

S. Okaba, T. Takano, F. Benabid, T. Bradley, L. Vincetti, Z. Maizelis, V. Yampol'skii, F. Nori, H. Katori, "Lamb-Dicke spectroscopy of atoms in a hollow-core photonic crystal fibre", *Nature Communications* 5, 4096 (2014).

Q.S. Tan, J.Q. Liao, X. Wang, F. Nori, "Enhanced interferometry using squeezed thermal states and even or odd states", *Phys. Rev. A* 89, 053822 (2014).

B. Peng, S. K. Ozdemir, F. Lei, F. Monifi, M. Gianfreda, G. L. Long, S. Fan, F. Nori, C. M. Bender, L. Yang, "Parity-time-symmetric whispering-gallery microcavities", *Nature Physics* 10, 394-398 (2014).

Y.X. Liu, X.W. Xu, A. Miranowicz, F. Nori, "From blockade to transparency: Controllable photon transmission through a circuit-QED system", *Phys. Rev. A* 89, 043818 (2014).

J. Dressel, K. Y. Bliokh, F. Nori, "Classical Field Approach to Quantum Weak Measurements", *Phys. Rev. Lett.* 112, 110407 (2014).

P. Zhang, Z.-L. Xiang, F. Nori, "Spin-Orbit Qubit on a Multiferroic Insulator in a Superconducting Resonator", *Phys. Rev. B* 89, 115417 (2014).

I. Georgescu, S. Ashhab, F. Nori, "Quantum Simulation", *Rev. Mod. Phys.* 86, 153 (2014).
Y.O. Averkov, V.M. Yakovenko, V.A. Yampol'skii, F. Nori, "Terahertz transition radiation of bulk and surface electromagnetic waves by an electron entering a layered superconductor", *Phys. Rev. B* 89, 094506 (2014).

L. Yu, J. Fan, S. Zhu, G. Chen, S. Jia, F. Nori, "Creating a tunable spin squeezing via a time-dependent collective atom-photon coupling", *Phys. Rev. A* 89, 023838 (2014).

Y. Zhang, L. Yu, J. -Q. Liang, G. Chen, S. Jia, F. Nori, "Quantum phases in circuit QED with a superconducting qubit array", *Scientific Reports* 4, 4083 (2014).

R.S. Akzhanov, A.V. Rozhkov, A.L. Rakhmanov, F. Nori, "Tunneling spectrum of a pinned vortex with a robust Majorana state", *Phys. Rev. B* 89, 085409 (2014).

J. Dressel, F. Nori, "Certainty in Heisenberg's uncertainty principle: Revisiting definitions for estimation errors and disturbance", *Phys. Rev. A* 89, 022106 (2014).

J.-Q. Liao, Q.-Q. Wu, F. Nori, "Entangling two macroscopic mechanical mirrors in a two-cavity optomechanical system", *Phys. Rev. A* 89, 014302 (2014).

X. Lu, L. Zhou, L.-M. Kuang, F. Nori, "Single-photon router: Coherent Control of multi-channel scattering for single-photons with quantum interferences", *Phys. Rev. A* 89, 013805 (2014).

C. Emary, N. Lambert, F. Nori, "Leggett-Garg Inequalities", *Reports on Progress in Physics* 77, 016001 (2014).

M. Tahir, F. Nori, B. Yellen, “Dynamically-tunable colloidal band-pass and band-gap filters”, *Journal of Applied Physics* 115, 134902 (2014).

K.Y. Bliokh, J. Dressel, F. Nori, “Conservation of the spin and orbital angular momenta in electromagnetism”, *New Journal of Physics* 16, 093037 (2014).

B. Peng, S.K. Ozdemir, W. Chen, F. Nori, L. Yang, “What is and what is not electromagnetically induced transparency in whispering-gallery microcavities”, *Nature Communications* 5, 5082 (2014).

B. Peng, S.K. Ozdemir, S. Rotter, H. Yilmaz, M. Liertzer, F. Monifi, C. M. Bender, F. Nori, L. Yang, “Loss-induced suppression and revival of lasing”, *Science* 346, 328-332 (2014).

K.Y. Bliokh, A.Y. Bekshaev, F. Nori, “Extraordinary momentum and spin in evanescent waves”, *Nature Communications* 5, 3300 (2014).

4.2. Conference Presentations

2020:

Gregory Smail, Tuan Trinh, Krishnandu Makhal, Da Yang, Jinsang Kim, Stephen Rand, “Theory and Observation of Magneto-Electric Field-induced Second Harmonic Generation”, Conf. on Lasers & Electro-optics (CLEO’20), San Jose, California, March 2-6, paper SW4G.2.

Da Seul Yang, Jinsang Kim “Polymer Chain Alignment Near the Semiconductor-dielectric Interface” MRS Spring Meeting, Phoenix, April 2020.

Da Seul Yang, Jinsang Kim “Alignment of Lyotropic Liquid Crystalline Conjugated Polymer via Floating Film Transfer Method” MRS Spring Meeting, Phoenix, April 2019.

2019:

(Invited) S.C. Rand, “Optically-induced Magnetization and Charge Separation for Quantum Information and Magneto-Photonics”, *Physics of Quantum Electronics (PQE’19)*, Snowbird, Utah, January 6-11, 2019.

M.T. Trinh, K. Makhal, A. Ayesheshim, and S.C. Rand, “Transient Charge Separation in Centro-symmetric Media by Magneto-optic Nonlinearities”, *Photonics West*, San Francisco, 2019.

(Invited) S.C. Rand, K. Makhal, A. Ayesheshim, and M.T. Trinh, “First Evidence of Magneto-electric Charge Separation at the Molecular Level”, *Winter Conference on Physics of Quantum Electronics (PQE-2019)*, Snowbird, January, 2019.

M.T. Trinh, K. Makhal, Da S. Yang, J. Kim, and S.C. Rand, “First Observations of Ultrafast Magneto-electric Charge Separation and Induced Molecular Rotations”, *OSA Nonlinear*

Optics Conference, Waikoloa Beach, Hawaii, July 15-19, 2019.

(Invited) G. Smail, A. Ayesheshim, K. Makhal, T. Trinh, and S.C. Rand, “Experiments and theory of second harmonic generation induced by magneto-electric rectification”, Foundations of Nonlinear Optics (FoNLO’19), Dayton, Ohio, August 6-8(2019).

(Invited) K. Makhal, G. Smail, A. Ayesheshim, T. Trinh, and S.C. Rand, “Orbital Topography by magneto-electric scattering”, Foundations of Nonlinear Optics (FoNLO’19), Dayton, Ohio, Aug. 6-8(2019).

(Invited) T. Trinh, G. Smail, A. Ayesheshim, K. Makhal, and S.C. Rand, “Magneto-electric charge separation - a new optical nonlinearity”, Foundations of Nonlinear Optics (FoNLO’19), Dayton, Ohio, August 6-8, 2019.

K. Makhal, M.T.Trinh, G. Smail, C. Spitzfaden, J. Guan, R.M. Laine, and S.C. Rand, “Probing the 3D-conjugated LUMOs of Silsesquioxanes with Light Scattering”, OSA Advanced Photonics Congress, Burlingame, California, July 29-August 1, 2019, paper NoM2B.5.

Da Seul Yang, Maciej Barlog, Jongsik Park, Kyeongwoon Chung, Apoorv Shanker, Jonathan Sun, Joonkoo Kang, Kwangyeol Lee, Mohammed Al-Hashimi, Jinsang Kim “Alignment of Lyotropic Liquid Crystalline Conjugated Polymer via Floating Film Transfer Method” MRS Spring Meeting, Phoenix, April 2019.

(Plenary) T. F. Heinz, “Seeing and Controlling Excitons in 2D Materials,” Twentieth International Conference on the Science and Applications of Carbon Nanotubes and Low Dimensional Materials NT19, Wuerzburg, Germany, 7/21-7/26/19.

T. F. Heinz, “Ultrafast Electron Dynamics in 2D Materials and Heterostructures,” Femto14 – Femtochemistry Conference – Dynamics of Complexity in Chemistry, Biology, and Physics, Shanghai, China, 7/28-8/2/19.

2018:

T. F. Heinz, “Controlling Excitons and Many-Body Interactions in 2D Semiconductors,” Physics of Quantum Electronics PQE-2018 Conference, Snowbird, UT, 1/7 – 1/12/18.

(Keynote) T. F. Heinz, “Tuning both the optical and electronic properties of atomically thin materials,” Graphene for US, New York, NY, 2/22-2/23/18.

T. F. Heinz, “Seeing and Controlling Dark and Bright excitons in 2D Materials,” Excited State Processes in Electronic and Bio Nanomaterials Conference, Santa Fe, NM, 6/4 – 6/7/18.

T. F. Heinz, “Probing and controlling excitations in transition metal dichalcogenides with magnetic fields,” 23rd International Conference on High Magnetic Fields in Semiconductor Physics (HMF-23), Toulouse, France 7/22 – 7/27/18.

(Plenary) T. F. Heinz, “Probing and controlling excitons in 2D semiconductors,” International Conference on Superlattices, Nanostructures and Nanodevices, Madrid, Spain, 7/23 – 7/27/18.

(Plenary) T. F. Heinz, “Optical properties of 2D materials and heterostructures,” IEEE 13th Nanotechnology Materials and Devices Conference (NMDC 2018), Portland, OR, 10/14 – 10/17/18.

(Invited) “Nonlinear Beam Deflection for Material Response Characterization“, Eric Van Stryland and David Hagan, Stegeman Memorial Conference, UCF, Orlando, FL March 12-13, 2018.

(Invited) David J. Hagan, Peng Zhao and Eric W. Van Stryland, “Ultrafast dynamics of nonlinear refraction.”, MRS Spring Meeting, Phoenix, AZ, (April 2018)

(Invited) “Ultrafast dynamics and spectral dependence of optical nonlinearities in doped semiconductors at Epsilon-Near-Zero”, Sepehr Benis, David Hagan, Eric Van Stryland, Metamaterials, Metadevices, and Metasystems 2018, part of SPIE Nanoscience + Engineering, paper 10719-34, SPIE San Diego, August 19-23, 2018.

(Invited) Sepehr Benis, David J. Hagan, Eric W. Van Stryland, "Measurement of the ultrafast dynamics of nonlinear refraction and absorption of highly doped semiconductors at epsilon-near-zero", SPIE Defense + Security, Ultrafast Bandgap Photonics III. Vol. 10638. International Society for Optics and Photonics, Orlando, FL, April, 2018.

(Invited) David J. Hagan and Eric W. Van Stryland, “Time-domain nonlinear refraction - toward tailorable nonlinear optical responses.” Nonlinear Optics Applications Workshop, Wroclaw, (May/June, 2018)

(Invited) David J. Hagan, Sepehr Benis, and Eric W. Van Stryland, “Enhanced Nonlinear Optical Response of Transparent Conductive Oxides at Epsilon-Near-Zero” Collaborative Conference on Materials Research (CCMR), Daejeon, Korea, (June 2018)

(Invited) Sepehr Benis, Eric W. Van Stryland, David J. Hagan, “Dynamics and spectral dependence of ultrafast optical nonlinearities in doped semiconductors at Epsilon-Near-Zero:”, PIERS 2018, Toyama, Japan, (July 2018)

(Invited) David J Hagan and Eric W. Van Stryland, “Ultrafast dynamics of nonlinear refraction.” Latin American Optics and Photonics (LAOP) Conference, Lima, Peru, (October 2018)

(Invited) David Hagan, Eric Van Stryland, “Measurement of nonlinear refraction in the time-domain”, Asia Communications and Photonics Conference (ACP) (Hangzhou, China, 26 -29 October 2018)

(Invited) D.J. Hagan, S. Benis, N. Munera-Ortiz, H-J Chang and E.W. Van Stryland, “Time-resolved ultrafast nonlinear refraction”, Photonics 2018 IIT Delhi, India, (December 2018)

S. Benis, D. Hagan, E.W. Van Stryland, "Enhancement Mechanism of Nonlinear Optical Response of Transparent Conductive Oxides at Epsilon-Near-Zero", CLEO, San Jose, California, May 13-18, 2018.

"Third-Order Nonlinear Optical Coefficients of Si and GaAs in the Near-Infrared Spectral Region", Joel Hales, San-Hui Chi, Taylor Allen, Sepehr Benis, Natalia Munera, Joseph Perry, Dale McMorro, David Hagan, Eric Van Stryland, CLEO: Applications and Technology, JTU2A. 59, San Jose, California, May 13-18, 2018.

(Plenary) Franco Nori, "Parity-time symmetric optics, extraordinary momentum, spin in evanescent waves, and quantum spin Hall effect of light", Int. Conf. on Nonlinear & Quantum Optics, Kuala Lumpur, Malaysia (February 3, 2018).

(Invited) S.C. Rand, "Stimulated Librations: confirmation of the torque mechanism of enhanced optical magnetization", Int. Conf. on Nonlinear & Quantum Optics, Kuala Lumpur, Malaysia (February 3, 2018).

J. Kim "Lyotropic Liquid Crystalline Conjugated Polymers with Directed Alignment Capability for Plastic Electronics" ACS Poly Division, 256th ACS National Meeting, August, 2018.
M.T. Trinh, K. Makhal, E.F.C.Dreyer, S.C. Rand, "Experimental Observation of Molecular Rotations Stimulated by Optical Magnetic Forces", APS March Meeting, Los Angeles, CA, March 5-9, 2018.

M.T. Trinh, K. Makhal, E.F.C. Dreyer, S.C. Rand, "Optical Magnetic Force Induces Molecular Rotations", Submitted to CLEO Meeting, San Jose, CA, May 1-18, 2018.

(Invited) M.T. Trinh, K. Makhal, S. Rand, "Generation of rotations in small molecules with magneto-electric nonlinearities", Foundations of Nonlinear Optics (FoNLO), June 19-21, 2018, Skidmore, NY, USA.

(Invited) H. Chandralalim "Micro-ring resonators for magneto-electric experimentation", Foundations of Nonlinear Optics (FoNLO), June 19-21, 2018, Skidmore, NY, USA.

(Invited) S. Rand, "Magneto-electric phenomena at the molecular level", Foundations of Nonlinear Optics (FoNLO), June 19-21, 2018, Skidmore, NY, USA.

(Invited) A. Lou and T. Marks, "Third Order and Magneto-Electric Response of Twisted Chromophores", Foundations of Nonlinear Optics (FoNLO), June 19-21, 2018, Skidmore College, Saratoga, NY.

M. T. Trinh, K. Makhal, D. Yang, J. Kim, and S. C. Rand, "Magneto-electric Charge Separation in Organic Semiconductors", Nonlinear Optics and Excitation Kinetics in Semiconductors - NOEKS 14, Sep. 23-27, 2018, Berlin, Germany

K. Makhal, M.T. Trinh, S. Rand, "Evidence of Magnetic Torque Dynamics in Optically-induced Magnetization", Frontiers in Optics, FM4B. 5. Sep 16-20, 2018, Washington, DC, USA

M.T. Trinh, K. Makhal, A. Ayesheshim, S. Rand , “Transient charge separation in centrosymmetric media by magneto-optic nonlinearities “, Photonics West (SPIE), Feb 2-7, 2019, San Francisco, USA.

F. Nori, “Quantum Simulation of Strongly correlated Systems” — ImPACT “Advanced Information Society Infrastructure Linking Quantum Artificial Brains in Quantum Network” Quantum Information Technology Workshop (Annual Review Meeting 2018) JST, Tokyo, Mar, 2018

F. Nori, “Parity-Time-Symmetric Optics, extraordinary momentum and spin in evanescent waves, and the quantum spin Hall effect of light” — International Symposium on Quantum Computing and Quantum Optics, Hangzhou, China, May, 2018

F. Nori, “Parity-Time-Symmetric Optics, extraordinary momentum and spin in evanescent waves, and the quantum spin Hall effect of light” — IWSSQC - 9th International Workshop on Solid State Quantum Computing, Hangzhou, China, May, 2018

F. Nori, “Parity-Time-Symmetric Optics, extraordinary momentum and spin in evanescent waves, and the quantum spin Hall effect of light” — Nanophotonics and Metamaterials Doctoral Summer School, ITMO University, St.Petersburg, Russia ,June, 2018

F. Nori, “Parity-Time-Symmetric Optics, extraordinary momentum and spin in evanescent waves, and the quantum spin Hall effect of light” — IEEE Photonics Society 2018 Summer Topicals, U.S.A, Hawaii, July, 2018

2017:

(Plenary) S.C. Rand, "Optical Magnetism in a New Light", PQE'17), Snowbird, Utah, USA (January 9, 2017).

S. Benis, D.J. Hagan, E.W. Van Stryland, "Cross-propagating beam-deflection measurements of third-order nonlinear optical susceptibility", SPIE Photonics West, San Francisco, CA January 28 - February 2, 2017, paper 10088-21.

T.F. Heinz, "Controlling Excitons in 2D Materials", International Winterschool on the Electronic Properties of Novel Materials, Kirchberg, Austria, March 3-11, 2017.

(Plenary) T.F. Heinz, "Seeing Electrons in 2D - Light/Matter Interactions in Atomically Thin Semiconductors", Graphene 2017, Barcelona, Spain, March 28-31, 2017.

J. Kim, “Rational Molecular Design and Engineering of Functional Polymers for Facilitated Thermal Energy and Charge transport” Air Force Research Lab, Ohio, April, 2017.

J. Kim, "Functional Organic Molecules and Conjugated Polymers for Optoelectronic and Biosensor Application" Department of Chemical & Biological Engineering, University of New Mexico, April, 2017.

J. Kim, "Rational Molecular Design and Engineering of Functional Polymers for Facilitated Thermal Energy and Charge transport" Science and Technology Innovation Forum, Korean Academy of Science and Technology, Seoul, May, 2017.

T.J. Marks, "New Directions for Twisted Chromophores". Foundations of Nonlinear Optics 2017, University of the Bahamas, Nassau, Bahamas. May, 2017.

B.C. Smith and J.F. Whitaker, "Conference on Lasers and Electro-Optics" (Optical Society of America), San Jose, CA, paper SM1J.6, May 14-19, 2017.

T.F. Heinz, "Optical Properties of Atomically Thin Two-Dimensional Materials", Conference on Lasers and Electro-Optics CLEO 2017, San Jose, CA, May 14-19, 2017.

H. Chandralalim, S. C. Rand, and X. Fan, "Refillable and Reconfigurable Dye-doped Ring Lasers", CLEO : Science and Innovations, JTh2A, May 14-19, 2017.

H. Chandralalim, S. C. Rand, and X. Fan, "Integration of Ultrafast Laser-inscribed Optical Waveguides and Renewable Ring Lasers", CLEO: Applications and Technology, AW4B. 5. May 14-19, 2017.

E.F. C. Dreyer, A.A. Fisher, and S.C. Rand, "Experimental Comparisons of P-T Symmetric Magneto-electric Interactions in Molecular Liquids", Conference on Lasers & Electro-Optics (CLEO'17), San Jose, CA May 14-19, 2017.

H. Chandralalim, S.C. Rand, and X. Fan, "Integration of renewable ring lasers and ultrashort pulse laser-inscribed optical waveguides", Conference on Lasers & Electro-Optics (CLEO'17), San Jose, CA, May 14-19, 2017.

H. Chandralalim, S.C. Rand, and X. Fan, "Refillable and configurable dye-doped polymer ring lasers", Conference on Lasers & Electro-optics (CLEO'17), San Jose, CA, May 14-19, 2017.

(Keynote) D.J. Hagan and E.W. Van Stryland, "Electronic and Nuclear Optical Nonlinearities in Organic Materials and Solvents", 14th International Conference on Frontiers of Polymers and Advanced Materials (ICFPAM), Daejeon, South Korea <http://www.icfpam2016.org/>, 2017.

(Plenary) P. Zhao, D. J. Hagan, E. W. Van Stryland, "Dispersion of extremely nondegenerate nonlinearities in semiconductors", Page(s):711 - 712 2017 IEEE Photonics Conference (IPC), Orlando, FL Oct. 1-5, 2017.

T.F. Heinz, "Light-Matter Interactions in Atomically Thin 2D Semiconducting Transition Metal Dichalcogenides", Eighth International Conference on Physics of Light-Matter Coupling in Nanostructures, Wuerzburg, Germany, July 9-14, 2017.

T.F. Heinz, "Controlling Excitons and the Valley Degree of Freedom in 2D semiconductors", Valleytronics Workshop, Cambridge, MA, August 22-23, 2017.

T.F. Heinz, "Controlling Excitons in 2D Materials", Nanophotonics of 2D Materials N2D 2017, San Sebastian, Spain, July 31-August 3, 2017.

J. Kim, "Functional Organic Molecules and Conjugated Polymers for Optoelectronic and Biosensor Application" School of Chemical Engineering, Sungkyunkwan University, August, 2017.

T.F. Heinz, "Controlling Excitons and the Valley Degree of Freedom in 2D semiconductors", Fundamental Optical Processes in Semiconductors FOPS 2017, Stevenson, WA, August 27-September 1, 2017.

(Invited) S.C. Rand, T.M. Trinh, and L. Andre, "New Methods and Materials for Laser-Cooled Solids", International Conference on Luminescence (ICL'17), Joao Pessoa (PB), Brazil, August 27 - September 1, 2017.

T.F. Heinz, "Controlling the Valley Degree of Freedom in 2D Transition Metal Dichalcogenides", International Symposium of the American Vacuum Society, Tampa, FL, October 29-November 3, 2017.

T.F. Heinz, "Seeing Electronics in 2D: Optical Spectroscopy of Atomically Thin Materials", CUI Symposium in Honour of A. Millis, Hamburg, Germany, November 9, 2017.

(Invited) Alexander J.-T. Lou, Elizabeth F. C. Dreyer, Alex A. Fisher, Stephen C. Rand, Apoorv Shanker, Jinsang Kim, and Tobin J. Marks, "Material Guidelines for Magneto-electric Interactions on the Atomic Scale", Materials Research Society, Boston, USA, November, 2017.

T.F. Heinz, "Many-body Effects in Atomically Thin Materials", MRS Fall Meeting, Boston, MA, November 27-December 1, 2017.

F. Nori, "A Single Photon Can Simultaneously Excite Two or More Atoms" Light-Matter Interactions in Cavity & Circuit QED Systems in the Light of Quantum Technology - IWQD 2017 -Interdisciplinary Workshop on Quantum Device, towards development of the quantum information device 2017, NII, Tokyo, March 6th, 2017

F. Nori, "Nano-Electronics using Quantum Circuits as Artificial Atoms on a Chip" Physics Department Colloquium, Scuola Normale Superiore, Pisa, May, 2017

F. Nori, "Nano—Electronics using Quantum Circuits as Artificial Atoms on a Chip" Physics Department Colloquium, Florida State University, Tallahassee, Florida, USA, May, 2017

F. Nori, "Nano—Electronics using Quantum Circuits as Artificial Atoms on a Chip" Nano KOREA 2017 Symposium, KINTEX, Ilsan, Korea, July, 2017

F. Nori, "Parity-Time-Symmetric Optics, extraordinary momentum and spin in evanescent waves, and the quantum spin Hall effect of light" - META'17, the 8th International Conference on Metamaterials, Photonic Crystals and Plasmonics, Songdo Convensia, Incheon - Seoul, South Korea, July, 2017

F. Nori, "Parity-Time-Symmetric Optics, extraordinary momentum and spin in evanescent waves, and the quantum spin Hall effect of light"—International Conference on Metamaterials and Nanophotonics, METANANO 2017, Vladivostok, Russia, Sep, 2017

F. Nori, The Fully Quantized Dynamical Casimir Effect – Vacuum Casimir-rabi Oscillations in Optomechanical Systems – International School and Symposium on Nanoscale Transpory and phoTonics, Kangawa, Japan, Nov, 2017

2016:

(Invited) A.A. Fisher, E.F. Dreyer, A. Chakrabarty, and S.C. Rand, "On the Origin of Intense Optical Magnetism in Natural Materials", Progress in Quantum Electronics (PQE'16), Snowbird, Utah, January 04-08, 2016.

C.D. Nie, S. Bera, J.A. Harrington, N. Taylor, R.M. Laine, E.F.C. Dreyer, S.C. Rand, S. Trembath-Reichert, "Rare-earth doped, single crystal fibers grown from ceramic and single crystal preforms", Photonics West, San Francisco, CA February 8-13, 2016.

M.J. Purcell, M. Kumar, S.C. Rand, "Holographic imaging through a scattering medium by diffuser-assisted statistical averaging", Proc. SPIE 9771, Practical Holography XXX: Materials and Applications, March 7, 2016, paper 97710F.

(Plenary) T.F. Heinz, "Atomically Thin Semiconductors and Heterostructures", Graphene Week Conference 2016, Warsaw, Poland, Jun 13-17, 2016.

T.F. Heinz, "Electronic Excitations and dynamics in 2D Semiconductors", Ultrafast Dynamics at the Nanoscale, Okinawa, Japan July 13-16, 2016.

S.C. Rand, E.F.C. Dreyer, P. Anisimov, A.A. Fisher, "Experimental Evidence of Enhancement of Optical Magnetism by Magnetic Torque", 19th Conference on Dynamical Processes in Excited States of Solids (DPC'16), July 17-22, 2016.

(Plenary) T.F. Heinz, "Seeing electrons in 2D - light/matter interactions in atomically thin semiconductors", International Conference on the Physics of Semiconductors ICPS 2016, Beijing, China, July 31 - August 05, 2016.

(Plenary) T.F. Heinz, "Two-Dimensional Semiconductors: The Counterpart to Graphene", Sixteen International Conference on the Science and Application of Nanotubes NT 16, Vienna, Austria, August 07-13, 2016.

A. Lou, "Third Order NLO Response in Twisted Chromophores", Foundations of Nonlinear Optics (FoNLO 2016), Medford, MA August 09-11, 2016.

B.C. Smith, J.F. Whitaker and S.C. Rand, "The Steering of THz pulses using thin emitters excited by tilted optical pulse-fronts", OSA Annual Meeting, Frontiers in Optics (FiO'16), Rochester, NY, October 17-21, 2016, paper FF3F.4.

F. Nori, "Parity-time-symmetric microcavities and extraordinary properties of light including the Quantum spin Hall effect of light", The 4th International Workshop on Frontiers in Quantum Optics and Quantum Information: Optomechanics meets circuit QED, Beijing, China, June 16th, 2016

F. Nori, "Parity-Time-Symmetric Optics, extraordinary spin in evanescent waves, and the quantum spin Hall effect of light", ITAMP and Physics Department Colloquium, Harvard University, Cambridge, MA, USA, September, 2016

F. Nori, "Electron Vortex Beams", ITAMP and Physics Department, Harvard University, Cambridge, MA, USA, September, 2016

F. Nori, "Parity-Time-Symmetric Optics, extraordinary spin in evanescent waves, and the quantum spin Hall effect of light", Physics Department, MIT, Cambridge, MA, USA, September, 2016

F. Nori, "Nano-Electronics using Quantum Circuits as Artificial Atoms on a Chip" Physics Department Colloquium, EPFL, Lausanne, Switzerland, October, 2016

F. Nori, "Parity-Time-Symmetric Optics, extraordinary spin in evanescent waves, and the quantum spin Hall effect of light", APPC-AIP Joint 13TH Asia-Pacific Physics Conference and 22nd Australian Institute of Physics Congress, Brisbane, Australia, Dec. 8, 2016

F. Nori, "Nano-Electronics using Quantum Circuits as Artificial Atoms on a Chip", 8th international workshop on solid-state quantum computing, and mini-school on quantum information science, University of Taiwan, Dec. 11th, 2016

F. Nori, "An Introduction to Parity-time-Symmetric Optics", 8th international workshop on solid-state quantum computing, and mini-school on quantum information science, University of Taiwan, Dec. 11th, 2016

F. Nori, "Parity-Time-Symmetric Optics, extraordinary spin in evanescent waves, and the quantum spin Hall effect of light" 8th international workshop on solid-state quantum computing, and mini-school on quantum information science, University of Taiwan, Dec. 12th, 2016

2015:

T.J. Marks, Light-Matter Interactions, Pacificchem, Honolulu HI, USA December 2015.

T.J. Marks, Light-Matter Interactions, International Conference on Transparent Conductive Materials, Tsukuba, Japan, October 2015.

T.F. Heinz, "Optical Properties of 2D Semiconductors and Heterostructures," Laser Science/FiO Meeting, San Jose, California, USA October 19-22, 2015.

A.A. Fisher, A. Chakrabarty, E.F.C. Dreyer, and S.C. Rand, "Depolarizing Molecular Rotations in Magneto-electric Light Scattering", Frontiers in Optics (FiO'15), San Jose, California, USA (October 18-22, 2015, paper FW4A5).

A. Chakrabarty, C. Zhang, A.A. Fisher, E.F.C. Dreyer, Q. Li, L.J. Guo, S.C. Rand, "Nonlinear Magnetic Scattering from Polymer Micro-ring Resonators", Frontiers in Optics (FiO15), San Jose, California, USA (October 18-22, 2015, paper FW3E5).

(Invited) J. Kim "Functional Organic Molecules and Conjugated Polymers for Optoelectronic and Biosensor Application" Department of Chemistry, Florida International University, Miami, Florida, USA October 2015.

T.J. Marks, "Light-Matter Interactions", Luigi Sacconi Medal Address, Italian Chemical Society, Camerino, Italy, September 2015.

Lou, Alexander J.-T. Exceptional Nonlinear Optical Response in Twisted Chromophores. Presented at Foundations of Nonlinear Optics, Lehigh University Department of Physics, Bethlehem, Pennsylvania, USA, August 4-5, 2015.

(Invited) J. Kim "Functional Organic Molecules and Conjugated Polymers for Optoelectronic and Biosensor Application" Department of Organic and Nano System Engineering, Konkuk University, Seoul, South Korea, August 2015.

(Invited) J. Kim "Functional Organic Molecules and Conjugated Polymers for Optoelectronic and Biosensor Application" Gwangju Institute of Science and Technology, Department of Materials Science and Engineering, Gwangju, South Korea, August 2015.

(Invited) J. Kim "Functional Organic Molecules and Conjugated Polymers for Optoelectronic and Biosensor Application" Korea Institute of Industrial Technology, Cheonan, South Korea, August 2015.

(Plenary) T.F. Heinz, "2-Dimensional Materials: Graphene and Beyond," Conference on Lasers and Electrooptics CLEO, San Jose, CA, 05/11–05/15/15.

T.F. Heinz, "Optical Properties of Atomically Thin Materials," Optics of Surfaces and Interfaces (OSI), Austin, Texas, USA June 29 - July 07, 2015.

(Plenary) T.F. Heinz, "2-Dimensional Materials: Graphene and Beyond," Plenary Talk, Conference on Lasers and Electrooptics CLEO, San Jose, California, USA May 11-15, 2015.

A. Chakrabarty, A.A. Fisher, E.F.C. Dreyer, and S.C. Rand, "Four-fold enhancement of Transverse Optical Magnetism in Unstructured Solids", Quantum Electronics & Laser Spectroscopy (QELS '15), San Jose, California, USA (May 10-15, 2015, paper FW3D4).

T.F. Heinz, "Optical Response of Graphene: From the THz to the UV," Spring Meeting, Materials Research Society, San Francisco, CA April 06-10, 2015.

(Invited) J. Kim "Functional Conjugated Polymers for Biosensor and Optoelectronic Applications" Dept, of Chemistry and Chemical Biology, University of Windsor, Canada, April 2015.

T.J. Marks, Light-Matter Interactions, Spring ACS meeting, Denver, CO, USA March 2015.

T.J. Marks, Light-Matter Interactions, Spring ACS meeting, San Diego, CA, USA March 2015.

T.F. Heinz, "Optical Spectroscopy of Atomically Thin Semiconductors," Conference on Physics of Quantum Electronics, Snowbird, Utah, USA January 04-08, 2015.

(Invited) J. Kim "Functional Conjugated Polymers for Biosensor and Optoelectronic Applications" Hanwha Advanced Materials, Korea, January 2015.

2014:

T.J. Marks, Light-Matter Interactions, Gordon Research Conference on Solar Fuels, Ventura, CA, January 2014.

(Invited) A.A. Fisher, E. Cloos, B. Smith, A. Chakrabarthy, J. Whitaker and S.C. Rand, "Intense Magnetic Optical Nonlinearities - the Emerging Story", International Conference on Luminescence, Wroclaw, Poland, July 13-18 (2014).

(Invited) F. Nori, (1) *Majorana fermions in pinned vortices*; (2) *Manipulating and probing Majorana fermions using superconducting circuits*; and (3) *Controlling a nanowire spinorbit qubit via electric –dipole spin resonance*, APS March meeting, Denver, Colorado, USA (2014/Mar.)

(Keynote) F. Nori, *Recent results on quantum hybrid circuits and photonics*, Interdisciplinary Workshop on Quantum Device-towards operation of the quantum information and the quantum computer-2014, NII and Okayama University, Tokyo, Japan (2014/Mar.)

(Invited) F. Nori, *Quantum Circuits as Artificial Atoms on a Chip*, Center for Quantum Measurement Seminar, Korea Research Institute of Standards and Science (KRISS), Daejeon, Korea (2014/Jul.)

(Invited) F. Nori, *Quantum Circuits as Artificial Atoms on a Chip: a pedagogical introduction*, Nano Korea 2014 Symposium, Seoul, Korea (2014/Jul.)

(Invited) F. Nori, *Quantum Circuits as Artificial Atoms on a Chip*, KIAS seminar, Seoul, Korea (2014/Jul.)

(Plenary) F. Nori, *Quantum Circuits as Artificial Atoms on a Chip: A Pedagogical Introduction*, 32nd International Conference on the Physics of Semiconductors (ICPS 2014), The Austin Convention Center, Austin, Texas, USA (2014/Aug.)

(Invited) F. Nori, *Electron vortex beams in a magnetic field: A new twist on Landau levels and Aharonov-Bohm states*, Fujihara Seminar: Real-time Dynamics of Physical Phenomena and Manipulation by External Fields, Grand Hotel New Oji, Hokkaido (2014/Sep.)

(Invited) F. Nori, *Quantum Circuits as Artificial Atoms on a Chip*, Symposium "Frontiers of Theoretical Science – MATTER, LIFE and COSMOS - ", Kavli IPMU, The University of Tokyo (Kashiwa campus) (2014/Nov.)

(Keynote) F. Nori, *Electron vortex beams in a magnetic field: A new twist on Landau levels and Aharonov-Bohm states*, Asia-Pacific Workshops and Conferences on Quantum Information Science 2014, National Cheng Kung University, Tainan, Taiwan (2014/Dec.)

2013:

A.A. Fisher, E.F. Cloos, W.M. Fisher, and S.C. Rand, "Induced Magnetic Scattering in Non-Magnetic Solids", OSA Topical Meeting on Nonlinear Optics, Kohala Coast, Hawaii, USA, July 21-26, 2013, Postdeadline paper PTh3A.7.

E.F. Cloos, A.A. Fisher, W.M. Fisher, and S.C. Rand, "Experiments and Analysis of Second-order Magnetization in Centrosymmetric GGG Crystals", Frontiers in Optics, Orlando, Florida, USA, October 6-10, 2013, paper LTu1H.1.

T.J. Marks, Light-Matter Interactions, International Conference on Transparent Conductive Materials, Chania, Greece, October 2013.

4.3. Seminars & Colloquia

2019:

S.C. Rand, "Laser-induced charge separation – the "optical capacitor" effect", Dept. of Physics Colloquium, University of Ottawa, March 6, 2019.

T. F. Heinz, "Excitons in 2D Materials," International Workshop on Spin and Valley Effects in 2D Materials, Daejeon, South Korea, 5/20-5/24/19.

T. F. Heinz, "Optical Properties of 2D Semiconductors and Heterostructures," Winter School on 2D Materials, Rehovot, Israel, 1/14-1/17/19.

T. F. Heinz, "Quantum Emitters in 2D Semiconductors," NSF Workshop on Enabling Quantum Leap, Philadelphia, PA, 9/20/19.

T. F. Heinz, Plenary Talk: "Seeing and Controlling Excitons in 2D Materials," Center for Integrated Nanotechnologies Annual Meeting, Santa Fe, NM, 9/22-9/24/19.

2018:

J. Kim, "Functional Organic Molecules and Polymers for Plastic Electronics and Optical Sensors" Department of Chemical Engineering, University of Akron, Ohio, April 2018.

T. F. Heinz, "New Quantum Effects in 2D Materials," DoD Planning Meeting on Materials for Quantum Applications, Arlington, VA, 8/14 – 8/15/18.

2017:

J. Kim "Functional Organic Molecules and Conjugated Polymers for Optoelectronic and Biosensor Application" School of Chemical Engineering, Sungkyunkwan University, August 2017.

J. Kim "Rational Molecular Design and Engineering of Functional Polymers for Facilitated Thermal Energy and Charge transport" Science and Technology Innovation Forum, Korean Academy of Science and Technology, Seoul, May 2017.

J. Kim "Rational Molecular Design and Engineering of Functional Polymers for Facilitated Thermal Energy and Charge transport" Air Force Research Lab, Ohio, April 2017.

J. Kim "Functional Organic Molecules and Conjugated Polymers for Optoelectronic and Biosensor Application" Department of Chemical & Biological Engineering, University of New Mexico, April 2017.

T. F. Heinz, "Controlling Excitons and the Valley Degree of Freedom in 2D semiconductors," Valleytronics Workshop, Cambridge, MA, 8/22-8/23/17.

T. F. Heinz, "Seeing Electronics in 2D: Optical Spectroscopy of Atomically Thin Materials," CUI Symposium in Honour of A. Millis, Hamburg, Germany, 11/9/17.

2016:

S.C. Rand, "A New Twist on Electromagnetism for Energy Conversion", Dept. of Physics, Case Western Reserve University, Feb. 4, 2016.

S.C. Rand, "Magnetism at optical frequencies in Natural Materials", Dept. of Physics, Central Michigan University, Feb.16, 2016.

T. F. Heinz, "Seeing Electrons in 2D - Light/matter Interactions in Atomically Thin Semiconductors," Workshop on Nanoscale Matter, Venice, Italy, 9/18-9/23/16.

T. F. Heinz, "Atomically Thin Semiconductors and Heterostructures," EU Graphene Flagship – US NSF Workshop - 2D Materials, Heterostructures and Devices, Manchester, UK, 10/10-10/12/16.

T. F. Heinz, "Controlling Excitons in 2D Materials," International Winterschool on the Electronic Properties of Novel Materials, Kirchberg, Austria, 3/4 - 3/11/17.

T. F. Heinz, “Two-dimensional materials - Graphene and Beyond,” Physics Colloquium, Harvard University, Cambridge, MA, 4/11/16.

2015:

T.F. Heinz, “Optical Spectroscopy of Atomically Thin Semiconductors,” Conference on Physics of Quantum Electronics, Snowbird, UT, 01/04–01/08/15.

T.F. Heinz, “Seeing Electrons in 2-Dimensions: Optical Spectroscopy of Atomically Thin Semiconductors,” Physics Colloquium, University of Central Florida, Orlando, FL, 01/15/15.

T.F. Heinz, “Atomically Thin 2D Materials,” Materials Directorate, Air Force Research Laboratory, Dayton, OH, 01/19/15.

T.F. Heinz, “Seeing Electrons in 2-Dimensions: Optical Spectroscopy of Atomically Thin Semiconductors,” Physics Colloquium, Carnegie Mellon University, Pittsburgh, PA, 01/26/15.

A. Chernikov and T.F. Heinz, “Excitonic Effects in 2-Dimensional Semiconductors,” International Winter School on the Electronic Properties of Novel Materials, Kirchberg, Austria, 03/08–03/14/15.

(Plenary) T.F. Heinz, “2-Dimensional Materials: Graphene and Beyond,” Workshop on Nanotube Optics and Spectroscopy, Kloster Banz, Germany, 06/01–06/04/15.

T.F. Heinz, “Optical Properties of Atomically Thin Materials,” Optics of Surfaces and Interfaces (OSI), Austin, TX, 06/29–07/03/15.

T.F. Heinz, “Optical Properties of Atomically Thin Semiconductor Layers and Heterostructures,” Fundamental Optical Properties of Semiconductors, Breckenridge, CO, 08/03–08/07/15.

T.F. Heinz, “Atomically Thin Two-Dimensional Materials - Graphene and Beyond,” Material Science and Engineering Colloquium, Stanford University, 10/02/15.

T.F. Heinz, “Optical Properties of 2D Semiconductors and Heterostructures,” Laser Science/FiO Meeting, San Jose, CA, 10/19-10/22/15.

2014:

S.C. Rand, “Optical Magnetism: An Anecdote on Discovery in the 21st Century”, Distinguished Speaker at the Institute of IIT Kharagpur, India, January, 2014.

S.C. Rand, “Optical Magnetism: An Anecdote on Discovery in the 21st Century”, Bose National Center for Basic Sciences, Kolkatta, India, January 2014.

S.C. Rand, “New Science for Solar Energy?”, IIT Delhi, India, January 2014.

S.C. Rand, “Optical Magnetism: Sustained Science for Sustainable Energy”, Amity University, Haryana, India, February, 2014.

S.C. Rand, “Sustainable Energy from Optical Magnetism?”, University of Canterbury, Christchurch, NZ, April 4, 2014

S.C. Rand, “Optical Magnetism for Solar Energy?”, RIKEN, Tokyo, Japan

S.C. Rand, “Sustainable Solar Energy with Optical Capacitors?”, University of Michigan Sustainability Seminar

5. People Supported

Amy Brooks, Administrative Assistant
Brad Smith, Graduate Student Research Assistant, University of Michigan
Dr. John Whitaker, Research Scientist, University of Michigan
Gregory Smail, Graduate Student Research Assistant, University of Michigan
Cameron Spitzfaden, Graduate Student Research Assistant, University of Michigan
Alex Fisher, Graduate Student Research Assistant, University of Michigan
Theresa Chick, M. Eng. Graduate Student, University of Michigan
Elizabeth F.C. Dreyer, Graduate Student Research Assistant, University of Michigan
Dr. Hengky Chadrahalim, Post Doctoral Fellow, University of Michigan
Dr. Ayan Chakrabarty, Post Doctoral Fellow, University of Michigan
Dr. A. Ayesheshim, Post Doctoral Fellow, University of Michigan
Dr. Tuan Trinh, Post Doctoral Fellow, University of Michigan
Dr. Krishnan Makhhal, Post Doctoral Fellow, University of Michigan
Dr. Alex Salkeld, Post Doctoral Fellow, University of Michigan
Elyse Barre, Graduate Student Research Assistant, Stanford University
Dr. Xiaoxiao Zhang, Post Doctoral Fellow, Stanford University
Dr. Lutz Waldecker, Post Doctoral Fellow, Stanford (von Humboldt Fellow)
Professor David Hagan, Dean of College of Optics, University of Central Florida
Sepehr Benis, Graduate Student Research Assistant, University of Central Florida
Sanas Faryadras, Graduate Student Research Assistant, University of Central Florida
Alexander Lou, Graduate Student Research Assistant, Northwestern University
Dr. Alexander Dudnik, Post Doctoral Fellow, Northwestern University
Professor Mark Ratner, Northwestern University
Dr. Weigang Zhu, Post Doctoral Fellow, Northwestern University
Dr. Apoorv Shankar, Ph.D. University of Michigan
Dr. Seong Jun Yoon, Post Doctoral Fellow, University of Michigan
Da Seul Yang, Graduate Student Research Assistant, University of Michigan
Dr. Konstantin Bliokh, Research Scientist, RIKEN, Japan

6. Visitors & Collaborators

Dr. Petr Anisimov, Los Alamos National Laboratory
Professor Sahin Ozdemir, Penn State University, USA
Professor Lan Yang, Washington University, St. Louis, Missouri
Professor Jagdish Luthra, Amity University, Haryana, India
Dr. Peng Chen, Department of Chemistry, University of Tennessee, Knoxville, Tennessee
Professor Vasudevan Lakshminarayanan, University of Waterloo, Waterloo, Canada
Dr. Sushmita Biswas, AFRL, Wright-Patterson AFB, Dayton, Ohio
Dr. Michael Gross, Johns Hopkins University Applied Physics Laboratory (APL), Laurel MD
Prof. Swapan Pati, Jawaharla Nehru Center for Advanced Scientific Research, Jakkur, Bangalore, India
Professor Prasanta Datta, Dept. of Physics, IITKP, Kharagpur, India